Development of hydrogel dressings as delivery platforms for sustained and controlled delivery of miRNA for the treatment of diabetic foot ulcers

José Antonio Durán Mota

UNIVERSITAT RAMON LLULL

DOCTORAL THESIS

Title	Development of hydrogel dressings as delivery platforms for sustained and controlled delivery of miRNAs for the treatment of diabetic foot ulcers
Presented by	José Antonio Durán Mota
Centre	IQS School of Engineering
Department	Bioengineering
Directed by	Dr. Salvador Borrós Gómez Dr. Nuria Oliva Jorge

This page is intentionally left blank

A mi familia

This page is intentionally left blank

Once I had a dream. And this is it.

Nightwish

This page is intentionally left blank

Acknowledgements

Escriure els agraïments és potser una de les parts més importants de la tesi per tot el que comporta. No tan sols es tracta de donar les gràcies a les persones que han estat a prop, sinó també reconèixer els qui han aportat una peça al científic i, sobretot, a la persona en què un es converteix després d'aquest intens viatge anomenat doctorat. Res hagués sigut possible sense tots vosaltres.

Primerament, i seguint amb el tema de fer les coses possibles, m'agradaria començar amb tu Salvador. Gràcies per donar-me la oportunitat d'haver pogut fer el doctorat a IQS i haver confiat en mi durant aquest projecte. Acadèmicament, he aprés moltíssim i no tan sols sobre temes relacionats amb la meva tesi pròpiament sinó també sobre ciència general i com fer que tingui un impacte a la societat. En la part personal, m'he sentit també molt acompanyat quan algunes reunions desemboquen en temes més socials, polítics o personals. En particular, acabo un doctorat amb molta més confiança personal que quan vaig començar i penso que és un punt molt important a reconèixer. Ha sigut un honor poder treballar amb tu aquests anys.

La següent persona que m'agradaria anomenar ets tu Núria. Durant el doctorat he tingut la sort de viure i compartir la teva evolució fins i tot muntant un laboratori nou en un edifici que encara no estava ni tan sols acabat. També acadèmicament he pogut veure més a prop la part més dura de la investigació, lluitar pels projectes i el seu finançament. He aprés també moltes tècniques i altres habilitats que mai havia utilitzat i que segur seran important com a futur bioenginyer. També, he de remarcar el fet que no és fàcil viure per primer cop en un país estranger enmig d'una pandèmia i has sigut una de les persones que més m'ha fet sentir-me com a casa, sempre prenent les adversitats amb un somriure i un cafè.

En general, i per tancar els agraïments als directors de tesi, m'agradaria dir que tenir dos supervisors ha sigut increïblement constructiu, tenint dos punts de vistes, dues persones diferents i en diferents nivells dins la carrera acadèmica. Amb el vostre amor i entusiasme pel que feu és impossible no voler continuar pel camí de la ciència. Per això i per més, moltes gràcies al papa i a la mama de l'acadèmia.

Next, I would like to thank you, Ben Almquist, to trust me and having me in your lab and as a collaborator in an amazing project. I've really enjoyed my time at Imperial College London

and I've learnt lots of things from you. Your interest and love for science is contagious and I'm sure I've brought a part of it with me to Barcelona. Thanks also to Mara. I'm sure you'll have a brilliant career and I'm really looking forward to finishing that incredible paper.

M'agradaria també donar les gràcies a la Júlia Quintanas, que sense el seu esforç i dedicació hagués sigut més complicat avançar en el projecte. Va ser un plaer fer-te de mentor i la teva simpatia i interès va fer tot aquest procés realment fàcil.

El treball al laboratori pot arribar a ser difícil molt sovint i l'obtenció de resultats negatius no ajuda. Per sort, aquests anys he estat envoltant d'una molt bona família anomenada GEMAT. Robert, recordo que vas ser la primera persona en ajudar-me a trobar el material de laboratori, utilitzar els equips etc. De veritat que he gaudit moltíssim compartint diferents auxiliaries amb algú tan atent i curiós i amb un perfil més enfocat a la enginyeria. Espero seguir de prop la teva trajectòria perquè estic segur serà increïble. A la cultura popular hi ha moltes parelles carismàtiques, però el duo Robert-Joan és possiblement del meus favorits. Joan moltes gràcies per la teva ajuda, donant sempre un cop de realitat súper crític, però necessari gràcies al qual molts hem millorat feina, presentacions i actituds. Potser no ho sembla, però m'emporto moltíssim de vosaltres. Firmat: el *cheerleader* de Tractivus.

Tot i no haver coincidit massa temps, recordo que una de les primeres converses que vaig tenir va ser amb el Peri, que justament es doctorava la setmana que jo començava. El teu "ja veuràs noi que parpelleges i ja t'estàs doctorant" ha cobrat molt de sentit últimament. Anna Mas, gràcies per tots els consells i per ser la persona que mantenia a ratlla als altres dos tocats de l'ala del triumvirat. Ha estat també un plaer veure la teva evolució després del doctorat. Com vas poder escriure una tesi des de la saleta?

Potser perquè vam començar gairebé de la mà o perquè compartim molts hobbies, aquest camí ha sigut realment especial fer-ho amb tu Patricia. Encara segueixo admirant el teu treball com a restauradora que és increïblement interessant pels que ens dediquem més a altres branques. Gràcies per, malgrat estar a prop dels trenta, treure sempre els nens petits que tenim a dins.

Laura i Alba, una altra parella carismàtica. De veritat que sense vosaltres començant els matins amb humor i energia tot hagués anat costa amunt des del primer moment. Potser no tenim l'humor més intel·ligent, però ha sigut molt necessari. Mireia, gràcies a tu també per

baixar de tant en tant i contagiar-nos amb bon rotllo i donar forces per continuar treballant. Cris García, mi paisana manchega, gracias por compartir siempre tu amor por la ciencia y cómo comunicarlo correctamente. No creo que haya nadie que no esté enamorado de tus dibujos y forma de ser. Coral, qué buena alumna y qué buena compañera. Gracias por tu paciencia, esfuerzo y la disposición a ayudar siempre que ha sido necesario. Roberta, me ha gustado mucho compartir también este viaje contigo, aunque tengamos que hacer horas extra en el gimnasio por tus bizcochos. Gracias también a ti Oiane, fue divertido inaugurar el CTPTI y trabajar juntos durante los primeros días de trabajo durante la pandemia.

Germán i Tito, més parelles carismàtiques. Ha sigut un plaer compartir laboratori, saleta i alguna que altra festa amb vosaltres. Heu sigut peça fonamental del grup. Pol, gràcies per la teva ajuda i consells. Parlar sobre química amb tu es un altre nivell. Mario, el teu punt de vista ha estat sempre interessant i necessari, realment he aprés moltíssimes coses a nivell professional i personal. Núria Puigmal, moltes gràcies també per la teva dedicació i els consells donats, sobretot amb els fibroblasts i pell en general. La teva tendresa ens captiva a tots. Gràcies i ànims també a tots els que esteu començant, Laura, Mònica i Glòria. Va ser un plaer ser el vostre auxiliar.

Voldria també agrair al Gabriel Martínez, que compartint classe d'anglès abans del doctorat em va proposar "i si mires a IQS per fer el doctorat? Segur que hi ha alguna cosa interessant". Tota la raó.

Marta Guerra, Benjamí i Martí, gràcies per tota la ajuda que ens heu donat, que ha sigut molta. És increïble el que esteu aconseguint i de veritat espero estar molt a prop per veure el vostre futur que sense dubte serà brillant.

Si la paraula "paciència" es pogués personificar segurament donaria com a resultat a la Núria Agulló i la Marina. Vau sortir del vostre metre quadrat de despatx per trobar-vos amb una colla de bojos. Moltes gràcies per l'ajuda rebuda sempre amb una rapidesa tremenda i per aguantar-nos a diari. Sou un engranatge indispensable.

Un dels moments més durs del doctorat sense dubte va ser acomiadar-nos de Sagetis. Moltíssimes gràcies a tots vosaltres perquè la majoria ens vau formar en cultius i moltes altres tècniques molt necessàries al grup. Tenir-vos sempre present al laboratori és un dels records més estimats que, estic segur, molts ens emportarem del doctorat.

I would also like to thank my family at Imperial College London. Mike, Sihao, Kostas, Francesco, Mag, Grace and John. I've felt really lucky to share lots of hours with you in and out of the office. Also, rehearsing in a rock band with some of you has been incredibly special for me. Many thanks to Sharad, Olivier, Miguel and the rest of people in core facilities for your trainings and patience.

Per anar acabant, m'agradaria incloure en els agraïments a l'IQS i el conjunt dels seus treballadors, ja que tots formen una peça indispensable que dona sentit al conjunt i sense els quals tot això no hagués estat possible.

Finalment, gràcies a la família per l'amor que he rebut sempre i pel vostre suport durant aquests anys, des de la terra i des del cel.

Abstract

Diabetic foot ulcers (DFUs) stand out as one of the most challenging complications of diabetes. Current treatments are generally focused on the hydration of the wound and the avoidance of infections, ineffectively closing the wound and only delaying a limb amputation in numerous cases. In the recent years, it was discovered that dysregulation of several micro-RNA segments (miRNAs) in diabetic fibroblasts affects cell functions of paramount importance in wound healing such as proliferation. Specifically, the overexpression of two miRNAs was found to be widely involved. In this sense, the inhibition of these problematic miRNAs raises as an interesting approach to accelerate proliferation of diabetic fibroblasts aiming to the DFUs closure, preventing amputations and improving the patient's quality of life.

The technology developed in the present thesis consists of an injectable hydrogel-based wound dressing doped with polyplexes to locally deliver genetic material to human dermal fibroblasts in a sustained manner over time. The development of the functional delivery platform is described in different parts. First, a new formulation of poly(β-amino esters)s (PBAE) polyplexes named C6RH were optimized to transfect human dermal fibroblasts showing unprecedented efficiencies for this type of primary cells. Next, several hydrogel formulations were explored based on thiolated 4-armed polyethylene glycol (PEG) crosslinked with thiol-reactive hydrophilic PBAEs. Hence, using PBAEs in both the hydrogel and the polyplexes might increase the stability of the particles. Different formulations were obtained tuning the PEG/PBAE ratio and the number of thiol-reactive groups per chain. The hydrogels prepared were doped with the C6RH polyplexes afterwards. This inclusion showed a divergent behaviour in the degradation of the hydrogels resulting in different polyplexes' release profiles. Human fibroblasts were transfected *in vitro* using the completed platform and showing a successful efficiency.

Finally, the polyplexes were re-optimized to deliver therapeutic miRNAs to fibroblasts isolated from diabetic patients' ulcers. The transfection of the miRNA inhibitors resulted in an increase of the proliferation and restoration of the altered expression of different genes involved in wound healing. Overall, the technology developed herein enables the development of novel gene therapies for the treatment of diabetic wounds. Moreover, the high transfection efficiencies together with the easiness of tunability of the polyplexes open the possibility for their use in other applications with one generalizable approach.

This page is intentionally left blank

Resumen

Las úlceras de pie diabético (UPDs) destacan como una de las complicaciones más desafiantes de la diabetes. Los tratamientos actuales están centrados en hidratar la herida y prevenir infecciones, cerrando la herida de manera ineficaz y solo retrasando la amputación de extremidades en numerosos casos. En los últimos años, se descubrió que la desregulación de varios segmentos de micro-ARN (miARNs) en los fibroblastos diabéticos están relacionados con funciones importantes en la cicatrización de heridas como la proliferación. Específicamente, se encontró que la sobreexpresión de dos miARNs estaba especialmente involucrada. Así, la inhibición de estos miARN problemáticos surge como un enfoque interesante para acelerar la proliferación de los fibroblastos con el objetivo de cerrar las UPDs, prevenir amputaciones y mejorar la calidad de vida del paciente.

La tecnología desarrollada en la tesis consiste en un apósito inyectable a base de hidrogel dopado con poliplejos para entregar localmente material genético a fibroblastos de manera sostenida. El desarrollo de la plataforma se realiza en diferentes partes. Primero, se optimizó una nueva formulación de poliplejos de poli(β-aminoésteres) (PBAE) denominada C6RH para transfectar fibroblastos de la dermis, mostrando eficiencias sin precedentes para este tipo de células primarias. A continuación, se exploraron varios hidrogeles basados en polietilenglicol (PEG) de 4 brazos tiolado reticulado con PBAEs hidrofílicos que reaccionan con tioles. Así, el uso de PBAE tanto en el hidrogel como en los poliplejos podría aumentar la estabilidad de las partículas. Se obtuvieron diferentes formulaciones ajustando la relación PEG/PBAE y el número de grupos reactivos por cadena. Los hidrogeles preparados se doparon con los poliplejos C6RH después. Esto mostró un comportamiento divergente en la degradación dando como resultado diferentes perfiles de liberación. Los fibroblastos se transfectaron *in vitro* usando las plataformas completas mostrando una eficacia exitosa.

Finalmente, los poliplejos se re-optimizaron para administrar miARN terapéuticos a fibroblastos aislados de úlceras de pacientes diabéticos. La transfección de los inhibidores de miARN resultó en un aumento de la proliferación y restauración de la expresión alterada de diferentes genes implicados en la cicatrización de heridas. En general, la tecnología desarrollada permite el nacimiento de nuevas terapias génicas para el tratamiento de heridas diabéticas. Además, las altas eficiencias de transfección junto con la facilidad de modificación de los poliplejos abren la posibilidad de su uso en otras aplicaciones siguiendo este enfoque generalizable.

This page is intentionally left blank

Resum

Les úlceres de peu diabètic (UPDs) destaquen com una de les complicacions més desafiants de la diabetis. Els tractaments actuals estan centrats en hidratar la ferida i prevenir infeccions, tancant la ferida de manera ineficaç i només endarrerint l'amputació d'extremitats en nombrosos casos. En els darrers anys, es va descobrir que la desregulació de diversos segments de microARN (miARNs) en els fibroblasts diabètics estan relacionats amb funcions importants en la cicatrització de ferides com la proliferació. Específicament, es va trobar que la sobreexpressió de dos miARNs estava especialment involucrada. Així, la inhibició d'aquests miARN problemàtics sorgeix com un enfocament interessant per accelerar la proliferació dels fibroblasts amb l'objectiu de tancar les UPDs, prevenir amputacions i millorar la qualitat de vida del pacient.

La tecnologia desenvolupada en la tesi consisteix en un apòsit injectable a base d'hidrogel dopat amb poliplexos per lliurar localment material genètic a fibroblasts de manera sostinguda. El desenvolupament de la plataforma es realitza en diferents parts. Primer, es va optimitzar una nova formulació de poliplexos de poli(β-aminoèsters) (PBAE) anomenada C6RH per transfectar fibroblasts de la dermis, mostrant eficiències sense precedents per a aquest tipus de cèl·lules primàries. A continuació, es van explorar diversos hidrogels basats en polietilenglicol (PEG) de 4 braços tiolat reticulat amb PBAEs hidrofílics que reaccionen amb tiols. Així, l'ús de PBAE tant a l'hidrogel com als poliplexos podria augmentar l'estabilitat de les partícules. S'obtingueren diferents formulacions ajustant la relació PEG/PBAE i el nombre de grups reactius per cadena. Els hidrogels preparats es van dopar amb els poliplexos C6RH després. Això va mostrar un comportament divergent a la degradació donant com a resultat diferents perfils d'alliberament. Els fibroblasts es van transfectar *in vitro* usant les plataformes completes mostrant una eficàcia exitosa.

Finalment, els poliplexos es van re-optimitzar per administrar miARN terapèutics a fibroblasts aïllats d'úlceres de pacients diabètics. La transfecció dels inhibidors de miARN va resultar en un augment de la proliferació i la restauració de l'expressió alterada de diferents gens implicats en la cicatrització de ferides. En general, la tecnologia desenvolupada permet el naixement de noves teràpies gèniques pel tractament de ferides diabètiques. A més, les altes eficiències de transfecció juntament amb la facilitat de modificació dels poliplexos obren la possibilitat del seu ús en altres aplicacions seguint aquest enfocament generalitzable.

This page is intentionally left blank

Table of Contents

This page is intentionally left blank

Index of Figures

This page is intentionally left blank

Index of Schemes

This page is intentionally left blank

Index of Tables

This page is intentionally left blank

Index of Equations

This page is intentionally left blank

List of Abbreviations

AcONa	Sodium acetate buffer
AKT	Protein kinase B
ANOVA	Analysis of variance
AGO2	Protein argonaute-2
AU	Arbitrary unit
BAD	BCL2 associated agonist of cell death
Cys	Cysteine
DCC	*N,N'*-Dicyclohexylcarbodiimide
DFU	Diabetic Foot Ulcer
DMAP	4-Dimethylaminopyridine
DMEM	Dulbecco's Modified Eagle Medium
DMSO	Dimethyl sulfoxide
DNA	Deoxyribonucleic acid
DOPC	1,2-Dioleoyl-sn-glycero-3-phosphocholine
DOPE	1,2-dioleoyl-sn-glycero-3-phosphoethanolamine
DOTAP	Dioleoyl-3-trimethylammonium propane
DOTMA	1,2-di-O-octadecenyl-3-trimethylammonium propane
ECM	Extracellular matrix
EDTA	Ethylenediaminetetraacetic acid
ELISA	Enzyme-Linked Immunosorbent Assay
ERK	Extracellular signal-regulated kinase
FACS	Fluorescent Activated Cell Sorter
FBS	Fetal Bovine Serum
FDA	Food and Drug Administration
FITC	Fluorescein isothiocyanate
FLUC	Firefly luciferase reporter
FRET	Fluorescence resonance energy transfer
GFP	Green fluorescent protein
GRB2	Growth factor receptor-bound protein 2
GSK3B	Glycogen Synthase Kinase 3 Beta
H	Histidine
HA	Hyaluronic acid
HCl	Hydrochloric acid

HDF	Human dermal fibroblasts
His	Histidine
HPLC-MS	High performance liquid chromatography – mass spectrometry
HSD	Honestly-significant-difference
IGF-1	Insulin-like growth factor 1
IRS1	Insulin receptor substrate 1
IRS2	Insulin receptor substrate 2
KRAS	Kirsten rat sarcoma virus protein
LUC	Luciferase
LVR	Linear viscoelastic region
MAPK	Mitogen-activated protein kinase
MEK	Mitogen-activated protein kinase kinase
miR	Micro-ribonucleic acid
miRNA	Micro-ribonucleic acid
MMP	Matrix metallopeptidase
mRNA	Messenger ribonucleic acid
mTOR	Mammalian target of rapamycin
ncRNA	Non-coding ribonucleic acid
NMR	Nuclear magnetic resonance
OCT	Optimal cutting temperature compound
OM-PBAE	Oligopeptide-modified poly(β-amino ester)s
p70S6	Ribosomal protein S6 kinase beta-1
PACT	Protein activator of interferon induced protein kinase EIF2AK2
PBAE	Poly(β-amino ester)s
PBS	Phosphate buffered saline
PCR	Polymerase chain reaction
PDGF	Platelet-derived growth factor
PDK	Pyruvate dehydrogenase kinase
PEG	Polyethylene glycol
PEI	Polyethyleneimine
pFLUC	Firefly luciferase reporter plasmid
pGFP	Green fluorescent protein plasmid
PI3K	Phosphoinositide 3-kinases
PIP3	Phosphatidylinositol (3,4,5)-trisphosphate
PLGA	Poly(lactic-co-glycolic acid)

PVA	Polyvinyl alcohol
R	Arginine
RAF	Rapidly Accelerated Fibrosarcoma serine/threonine-protein kinase
RISC	Ribonucleic acid-induced silencing complex
RLU	Relative luminescence units
RNA	Ribonucleic acid
RNAa	Ribonucleic acid activation
RNAi	Ribonucleic acid interference
RPS6KB1	Ribosomal protein S6 kinase beta-1
RT-qPCR	Reverse transcription quantitative real-time PCR
SAOS	Small-amplitude oscillatory shear
saRNA	Small activating ribonucleic acid
SEM	Scanning Electron Microscopy
siRNA	Small interfering ribonucleic acid
SOS	Son of sevenless protein
SPDP	3-(2-pyridyldithio)propanoic acid
T	Thiopyridyl group
TFA	Trifluoroacetic acid
TRBP	Transactivation response element RNA-binding protein
UTR	Untranslated region
UV-Vis	Ultraviolet–visible spectroscopy
VEGF	Vascular endothelial growth factor

This page is intentionally left blank

Chapter 0: Motivations and aims

This page is intentionally left blank

Motivations and aims

0.1. Introduction

Skin is the largest organ of the human body. It is a complex system structured by layers that are composed by different configurations of cells and tissues, principally acting as protection from external factors. Typically, these layers are classified into epidermis, dermis and subcutaneous tissue, from the outermost to the innermost[1]. Each of them presents specific chemical and biological characteristics that change gradually throughout the system, but still contribute together to develop different functions as one whole. Skin protects internal organs, muscles, bones and other tissues from external harmful agents such as pathogens, chemical substances and even physical injuries. Beyond protection, skin is also responsible for sensation, thermoregulation of the body, synthesis of collagen and its own regeneration and healing among others[1,2]. Unfortunately, there are different pathologies that affect skin and can compromise the correct development of these functions. Impaired wound healing is among the most critical skin conditions, and is exacerbated by other factors such as obesity, ischemia or diabetes, shown to further delay the wound healing processes, leading to a chronic wound[3]. Only in the United States, over 2% of the total population suffers from chronic wounds. Due to lengthy and ineffective treatments, chronic wounds have a tremendous impact on healthcare systems worldwide. For example, in 2014, the average annual cost for wound care reached $2.8 billion[4]. Diabetic foot ulcers (DFUs) – one of the main complications of diabetes – are one of the most problematic types of chronic wounds. One in four diabetic patients will develop DFUs, which alone are responsible for about 1% of the total healthcare budget in most developed countries[5]. Moreover, they are the leading cause of non-traumatic amputation worldwide, and have lower 5-year survival rates than breast or prostate cancer[6]. Even more alarming, there is no glimpse of a cure for these wounds in a short period of time. Currently, solutions lie in minimising the complications of these wounds, such as applying antibiotic dressings to prevent infection, and performing painful mechanical debridement to remove necrotic tissue. When these therapies no longer work, amputation becomes the course of action[7–10].

The normal wound healing is a complex biological process that occurs as a cellular response to injury and involves activation of several cellular types and release of different growth factors such as platelet-derived growth factors (PDGF) or vascular endothelial growth factors

(VEGF), among others, as well as specific cytokines that are needed to coordinate and drive the repair of injured tissue. In the case of DFUs, there is an insufficient production of growth factors, a prolonged inflammation stage, an impaired neovascularisation and a decreased synthesis of collagen. Interestingly, several studies show that the expression of many genes is dysregulated (upregulated or downregulated) during chronic wound healing, compared to normal wound healing. These genes produce an altered protein expression profile in the cells present in the diabetic ulcer that renders these cells unresponsive to growth factors[11,12]. Hence, the use of the current growth factor therapies to treat DFUs has proven to be inefficient[13]. For these reasons, a molecular approach is needed to restore gene and protein expression of cells in the wound re-establishing healthy cell homeostasis.

In this sense, strong evidence suggests that microRNAs (miRNAs) play a key role in the biochemical alterations of signalling networks in the local microenvironment of DFUs. miRNAs are non-coding RNA molecules containing about 20-25 nucleotides that elicit RNA silencing and post-transcriptional regulation of gene expression via base-pairing with complementary sequences within messenger RNA (mRNA) molecules. Recently, the expression signature of a specific set of miRNAs has been discovered to be dysregulated in the progression of diabetes miellitus[14]. Specifically, two of them have been identified to clearly play a decisive role on the proliferation of fibroblasts, the cells in the dermis layer that are present throughout different stages of the wound healing process (unpublished data from collaborator Dr. Almquist). Hence, combinatorial therapies based on these miRNAs raise as a promising approach to restore cell homeostasis, promoting DFU healing. This approach can also be extrapolated to other types of impaired wound healing with different miRNA dysregulation.

On the basis of these developments and considerations, gene therapy stands out as an interesting strategy to tackle diabetic foot ulcers via the delivery of these specific miRNA mimics or inhibitors to the wound site to restore a natural expression profile. Broadly, gene therapy consists in the transference of genetic material to a patient in order to treat a disease. This approach is gaining momentum after the approval of several gene therapy-based products[15] and mRNA-based vaccines to treat COVID-19, opening a viable path to the clinical translation of new gene therapies. However, the delivery of nucleic acids presents some challenges. For example, when in contact with physiological fluids, they are susceptible to degradation and clearance from the body. Moreover, they cannot be readily transported through cytoplasmatic membranes to reach their target locations (cytosol for RNA and nucleus for DNA)[16]. Therefore, the use of vehicles that protect and deliver the genetic material

inside the cell is key to the development of successful gene therapies. Despite advances in the last decade, an optimal delivery system is still not available[16,17]. Viral vectors are capable of a sustained transgene expression, owing to their high transduction efficiency, but they cause high immunogenicity and inherent safety risks[18]. In contrast, non-viral vectors show lower transfection efficiencies, but are usually low cost and safer, and present better loading capacities for both DNA and RNA. Two major groups are found inside this family, lipoplexes and polyplexes. They are generally formed by cationic lipids or polymers, respectively, that present the ability to bind to negatively charged oligonucleotides forming discrete nanoscaled particles. Both present different advantages that make them suitable for specific applications, and their main challenge is the optimisation of their structure to find an equilibrium between key parameters, such as transfection efficiency, stability and cytotoxicity. Specifically, synthetic cationic polymers are found to be easier to modify thus facilitating the tuning of these polyplexes to meet the optimal balance of the parameters mentioned above[19,20]. Positive polyplexes bind to the cell membrane and enter the cytoplasm via endosomal transport. Transfection efficiencies can be improved by the conjugation of endosomolytic moieties that facilitate endosomal escape[21]. In addition, an increase in the specificity of the delivery is possible through conjugation of these vectors with targeting moieties. In particular, the Materials Engineering Group at the Institut Químic de Sarrià has worked for years on a class of polyplexes made of cationic polymers known as poly(β-amino ester)s (PBAE)s. These polymers are synthesized by Michael addition, forming a chain by reacting amines with acrylate-ended molecules. Selecting specific amine-bearing molecules, polyplexes' properties are tuned to include additional features of interest such as the control over the polarity or the inclusion of a reactive moiety. Moreover, the acrylates at both ends of the chains can be further modified with oligopeptides to increase the stability, improve the encapsulation efficiency of oligonucleotides and to boost the transfection without compromising the cytotoxicity and enhancing the biocompatibility in comparison to chemical cappings[22–25].

Wound healing is a dynamic process involving four overlapping stages known as haemostasis, inflammation, proliferation and maturation[26,27]. Each of these phases is characterized by specific actuators and specificities. Thus, it is clear that nanoparticles dosage must be sustained and controlled over time to ensure adequate levels and duration of transgene expression. Biomaterials present themselves as ideal candidates for this task, as they can act as drug depots and enable sustained release over time[28–30]. Hydrogels in particular are highly biocompatible materials[31–33] composed mostly of water, which is thought to provide a warm and moist environment to help wound healing progress in a successful

manner[34]. Hydrogels are formed by hydrophilic polymers, such as hyaluronic acid (HA), polyacrylates, polyvinyl alcohol (PVA) or polyethylene glycol (PEG)[35]. The formation can occur by physical entangling or by chemical bonding of these chains. The physicochemical properties of these materials allow them to absorb up to 90% of water or fluids, providing high flexibility, porosity and a soft structure similar to human tissues. In fact, solid, semi-solid or liquid hydrogels are obtained by controlling these properties together with the crosslinking rate[36]. Synthetic hydrogels can be modified to obtain formulations that present low immunogenicity, biodegradability, biocompatibility or that forms *in situ* adapting a certain form, vitally important features for wound healing applications[37]. Additionally, their capability to incorporate drugs and their ease of usage and handling along with the previously mentioned characteristics have allowed their entry into the medical market as commercial products[38].

In the present thesis, the development of a new platform to treat diabetic foot ulcers is described (**figure 0.1**). Specifically, the new wound dressing consists of an injectable hydrogel formed by crosslinking thiolated 4-arm PEG molecules using thiol-reactive PBAE polymers *via* disulphide bonding. This material contains polyplexes made of a PBAE formulation that efficiently transfect fibroblasts from the human dermis and are released in a sustained manner over time as the hydrogel degrades. Moreover, we hypothesize that using PBAE polymers both as a component of the hydrogel and the polyplexes can increase the stability of these particles during the release time frame. Additionally, PEG is known to be biocompatible and biodegradable. Equally importantly, PEG presents low immunogenicity and antifouling properties, limiting bacterial approach to the tissue surface, minimising the risk of wound infection. Polyplexes are loaded with miRNA mimics or inhibitors, aimed to correct the defective protein expression linked to low proliferation in diabetic fibroblasts. We hypothesise that restoring miRNA expression in diabetic fibroblasts will enhanced wound healing of DFUs, ultimately decreasing the hospital admissions and improving the quality of life of the patients. To accomplish the purpose of the present work, the following objectives were previously defined:

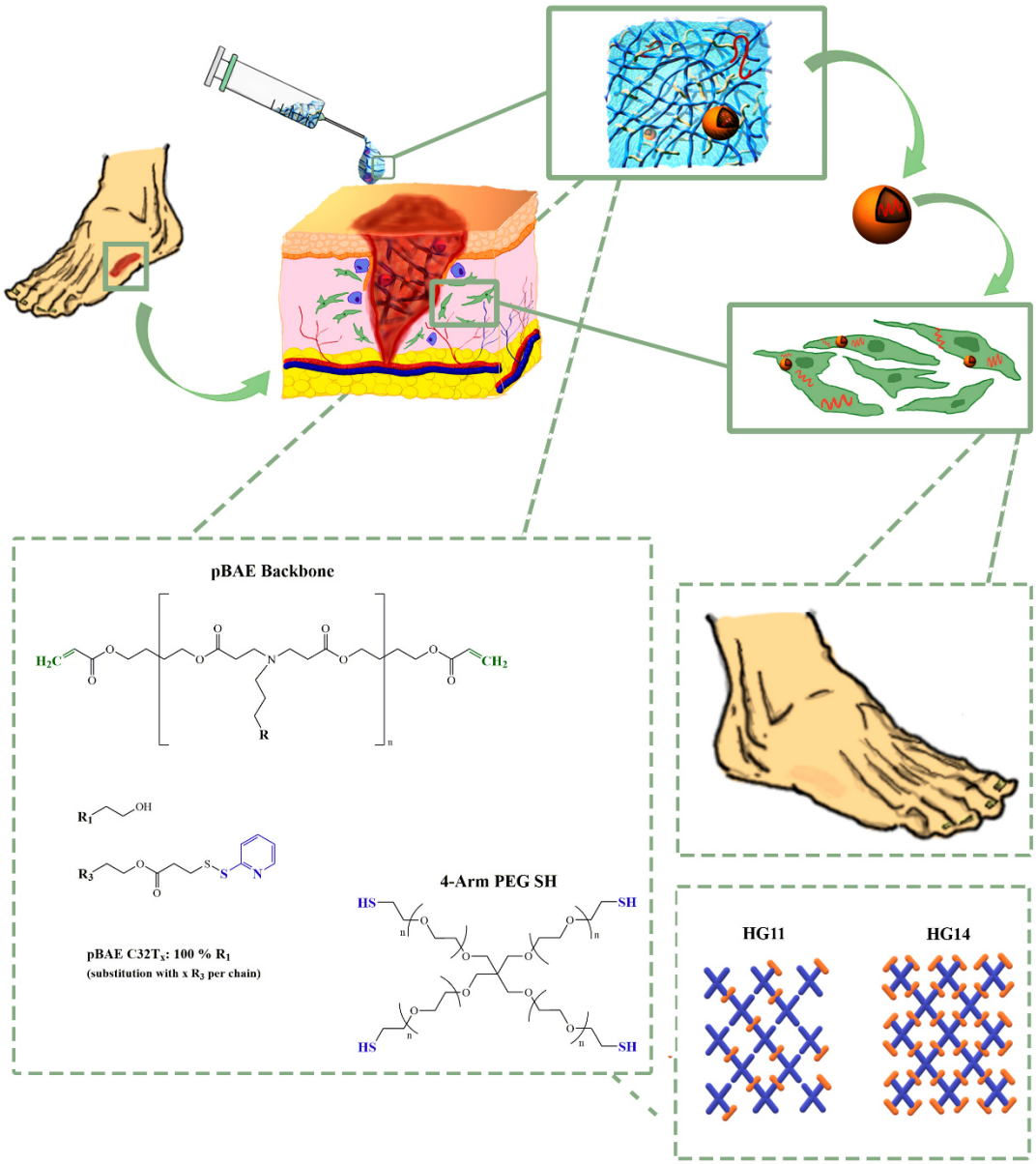

Figure 0.1. Schematic diagram of the composite PEG-PBAE hydrogel-based wound dressing designed herein for the treatment of diabetic foot ulcers. Human dermal fibroblasts from the ulcer are transfected using miRNA-loaded PBAE polyplexes to induce fibroblasts proliferation aiming to completely close the wound.

1) Design and preparation of a hydrogel-based platform for the sustained delivery of polynucleotide-loaded polyplexes to human dermal fibroblasts.

1.1.) Optimization of a new formulation of PBAE polyplexes tuned to effectively cross the plasmatic membrane and escape the endosome to deliver different nucleic acids to human dermal fibroblast (HDFs) efficiently.

1.2.) Development and characterization of a PBAE-PEG hydrogel-based wound dressing that degrades over time and study of the cytotoxicity of its degradation products.

1.3.) Incorporation of PBAE polyplexes into the hydrogel matrix. Study of the release kinetics and stability of the nanoparticles released.

1.4.) Transfection of HDFs using the platform designed.

2) Re-optimization of the PBAE polyplexes to contain the specific miRNA segments to restore a normal proliferation of diabetic fibroblasts.

2.1.) Transfection of diabetic fibroblasts obtained from diabetic foot ulcers using specific miRNA mimics and inhibitors involved in the proliferation of these cells.

2.2.) Study and understand the effects of the transfection of the different miRNA in the proliferation of healthy and diabetic fibroblasts and their implication in selected diabetes-related genes.

0.2. Contents of the dissertation

The objectives previously defined are tackled throughout the thesis in the order shown above and encompassed within different chapters as follows:

In Chapter 1, a new formulation of oligopeptide-ended PBAE polymers is optimized to transfect human dermal fibroblasts. This last decade has witnessed the appearance of a wide variety of new cationic polymers. Among them, PBAEs have shown tremendous potential as non-viral polynucleotide delivery vectors[39–41]. However, their use have been mainly focused on cancer and immortalized cell lines[23–25,40]. HDFs are difficult-to-transfect cells[42] highly involved in the vast majority of wound healing stages[9,43]. For further use of the material as a therapeutic wound healing platform, an efficient transfection of HDFs must be achieved. Hence, different DNA and RNA-loaded PBAE nanoparticles are also tested in the chapter to study the effects of their formulation on their ability to cross the cytoplasmic (RNA) or the nuclear (DNA) membranes.

Chapter 2 shows the development of the wound dressing hydrogel matrix. Hydrogels are three-dimensional, hydrophilic, polymeric networks with the ability to store water or biological fluids thus resembling natural tissues, conferring them high biocompatibility. Physicochemical properties of macromolecules that form hydrogels dictate their degradation mode and kinetics, allowing for control over cargo release. This new hydrogel formulation is formed by crosslinking thiolated 4-arm PEG using hydrophilic PBAEs modified to incorporate thiol-reactive groups. The hydrogel matrix can be formed both physically and chemically depending on the number of thiol-reactive groups and using different molecule ratios. Thus, several formulations can be obtained showing different properties such as swelling and degradation behaviours, with implication in the cytotoxicity of the degradation by-products. Moreover, these results can be compared to understand the release of nanoparticles and the specific window of time when it occurs. Hence, this opens the possibility for the preparation of improved smart hydrogel formulations with sustained deliveries adapted to the application desired and facilitating a rapid translation to *in vivo* experiments.

The incorporation of the polyplexes optimized in Chapter 1 inside the hydrogels developed in Chapter 2 is shown and discussed in Chapter 3. The correct doping of the hydrogel using the nanoparticles is studied by fluorescently tagging the polymers and the nucleic acids forming the polyplexes and imaging using confocal microscopy. We hypothesize that the use of

PBAEs in both components can improve stability of these polyplexes inside the hydrogel and facilitate control over transfection. Then, the release of these polyplexes from the hydrogel is studied over time by fluorescence tracking. Finally, HDFs are transfected using the polyplex-loaded hydrogels.

Chapter 4 focuses on the delivery of therapeutic miRNAs using the platform designed in the previous chapters. For that, the polyplexes in Chapter 1 are optimized to encapsulate selected miRNAs and the proliferation of healthy and diabetic fibroblasts are studied after transfection using these nanoparticles. Finally, the expression of different genes affected by these miRNAs is studied after the transfections to understand their role.

As a summary, miRNA-based therapies are challenging for their susceptibility to enzymatic degradation and hence, there is a need to engineer vehicles for optimal cell transfection. Moreover, miRNA activity in the cells is limited to 8 to 12 hours in vivo, drastically reducing its efficacy and making it necessary to deliver these molecules over time using a hydrogel-based delivery platform. Hence, in this work, a delivery system capable of achieving controlled and sustained release of miRNA-loaded nanoparticles is designed to guarantee efficient cell transfection and prolonged activity over longer periods of time. The platform developed herein can be used to deliver miRNA combinations to a wide range of primary cells from tissues, increasing its impact across medical problems with one generalizable approach.

0.3. References

(1) Kolarsick, P. A. J.; Kolarsick, M. A.; Goodwin, C. Anatomy and Physiology of the Skin. *J. Dermatol. Nurses. Assoc.* **2011**, *3* (4), 203–213. https://doi.org/10.1097/JDN.0b013e3182274a98.

(2) *Skin Aging & Cancer: Ambient UV-R Exposure*; Dwivedi, A., Agarwal, N., Ray, L., Tripathi, A. K., Eds.; Springer Singapore: Singapore, **2019**. https://doi.org/10.1007/978-981-13-2541-0.

(3) Guo, S.; DiPietro, L. A. Critical Review in Oral Biology & Medicine: Factors Affecting Wound Healing. *J. Dent. Res.* **2010**, *89* (3), 219–229. https://doi.org/10.1177/0022034509359125.

(4) Sen, C. K. Human Wounds and Its Burden: An Updated Compendium of Estimates. *Adv. Wound Care* **2019**, *8* (2), 39–48. https://doi.org/10.1089/wound.2019.0946.

(5) Singh, N.; Armstrong, D. G.; Lipsky, B. A. Preventing Foot Ulcers. *J. Am. Med. Assoc.* **2005**, *293* (2), 94–96. https://doi.org/10.1001/jama.293.2.217.

(6) *International Diabetes Federation. IDF Diabetes Atlas*, 7th ed.; Cavan, D., da Rocha Fernandes, J., Makaroff, L., Ogurtsova, K., Webber, S., Eds.; International Diabetes Federation: Brussels, **2015**.

(7) Eming, S. A.; Martin, P.; Tomic-Canic, M. Wound Repair and Regeneration: Mechanisms, Signaling, and Translation. *Sci. Transl. Med.* **2014**, *6* (265), 265sr6. https://doi.org/10.1126/scitranslmed.3009337.

(8) Broughton, G.; Janis, J. E.; Attinger, C. E. Wound Healing: An Overview. *Plast. Reconstr. Surg.* **2006**, *117* (SUPPLEMENT), 1e-S-32e-S. https://doi.org/10.1097/01.prs.0000222562.60260.f9.

(9) Morton, L. M.; Phillips, T. J. Wound Healing and Treating Wounds. *J. Am. Acad. Dermatol.* **2016**, *74* (4), 589–605. https://doi.org/10.1016/j.jaad.2015.08.068.

(10) Han, G.; Ceilley, R. Chronic Wound Healing: A Review of Current Management and Treatments. *Adv. Ther.* **2017**, *34* (3), 599–610. https://doi.org/10.1007/s12325-017-0478-y.

(11) Barrientos, S.; Stojadinovic, O.; Golinko, M. S.; Brem, H.; Tomic-Canic, M. PERSPECTIVE ARTICLE: Growth Factors and Cytokines in Wound Healing. *Wound Repair Regen.* **2008**, *16* (5), 585–601. https://doi.org/10.1111/j.1524-475X.2008.00410.x.

(12) Barrientos, S.; Brem, H.; Stojadinovic, O.; Tomic-Canic, M. Clinical Application of Growth Factors and Cytokines in Wound Healing. *Wound Repair Regen.* **2014**, *22* (5),

569. https://doi.org/10.1111/wrr.12205.

(13) Loots, M. A. M.; Kenter, S. B.; Au, F. L.; Van Galen, W. J. M.; Middelkoop, E.; Bos, J. D.; Mekkes, J. R. Fibroblasts Derived from Chronic Diabetic Ulcers Differ in Their Response to Stimulation with EGF, IGF-I, BFGF and PDGF-AB Compared to Controls. *Eur. J. Cell Biol.* **2002**, *81* (3), 153–160. https://doi.org/10.1078/0171-9335-00228.

(14) Kim, M.; Zhang, X. The Profiling and Role of MiRNAs in Diabetes Mellitus. *J. Diabetes Clin. Res.* **2019**, *1* (1), 5–23. https://doi.org/10.33696/diabetes.1.003.

(15) Anguela, X. M.; High, K. A. Entering the Modern Era of Gene Therapy. *Annu. Rev. Med.* **2019**, *70* (1), 273–288. https://doi.org/10.1146/annurev-med-012017-043332.

(16) Khalil, I. A.; Sato, Y.; Harashima, H. Recent Advances in the Targeting of Systemically Administered Non-Viral Gene Delivery Systems. *Expert Opin. Drug Deliv.* **2019**, *16* (10), 1037–1050. https://doi.org/10.1080/17425247.2019.1656196.

(17) Nayerossadat, N.; Ali, P.; Maedeh, T. Viral and Nonviral Delivery Systems for Gene Delivery. *Adv. Biomed. Res.* **2012**, *1* (2), 27–37. https://doi.org/10.4103/2277-9175.98152.

(18) Hirsch, T.; Spielmann, M.; Yao, F.; Eriksson, E. Gene Therapy in Cutaneous Wound Healing. *Front. Biosci.* **2007**, *12* (7), 2507–2518. https://doi.org/10.2741/2251.

(19) Wu, P.; Chen, H.; Jin, R.; Weng, T.; Ho, J. K.; You, C.; Zhang, L.; Wang, X.; Han, C. Non-Viral Gene Delivery Systems for Tissue Repair and Regeneration. *J. Transl. Med.* **2018**, *16* (1), 29–48. https://doi.org/10.1186/s12967-018-1402-1.

(20) Aggarwal, R.; Targhotra, M.; Kumar, B.; Sahoo, P. .; Chauhan, M. K. Polyplex: A Promising Gene Delivery System. *Int. J. Pharm. Sci. Nanotechnol.* **2019**, *12* (6), 4681–4686. https://doi.org/10.37285//ijpsn.2019.12.6.1.

(21) Ahmad, A.; Khan, J. M.; Haque, S. Strategies in the Design of Endosomolytic Agents for Facilitating Endosomal Escape in Nanoparticles. *Biochimie* **2019**, *160*, 61–75. https://doi.org/10.1016/j.biochi.2019.02.012.

(22) Fornaguera, C.; Guerra-Rebollo, M.; Ángel Lázaro, M.; Castells-Sala, C.; Meca-Cortés, O.; Ramos-Pérez, V.; Cascante, A.; Rubio, N.; Blanco, J.; Borrós, S. MRNA Delivery System for Targeting Antigen-Presenting Cells In Vivo. *Adv. Healthc. Mater.* **2018**, *7* (17), 1–11. https://doi.org/10.1002/adhm.201800335.

(23) Dosta, P.; Ramos, V.; Borrós, S. Stable and Efficient Generation of Poly(β-Amino Ester)s for RNAi Delivery. *Mol. Syst. Des. Eng.* **2018**, *3* (4), 677–689. https://doi.org/10.1039/c8me00006a.

(24) Segovia, N.; Dosta, P.; Cascante, A.; Ramos, V.; Borrós, S. Oligopeptide-Terminated Poly(ß-Amino Ester)s for Highly Efficient Gene Delivery and Intracellular Localization.

Acta Biomater. **2014**, *10* (5), 2147–2158. https://doi.org/10.1016/j.actbio.2013.12.054.

(25) Dosta, P.; Segovia, N.; Cascante, A.; Ramos, V.; Borrós, S. Surface Charge Tunability as a Powerful Strategy to Control Electrostatic Interaction for High Efficiency Silencing, Using Tailored Oligopeptide-Modified Poly(Beta-Amino Ester)s (PBAEs). *Acta Biomater.* **2015**, *20*, 82–93. https://doi.org/10.1016/j.actbio.2015.03.029.

(26) Boateng, J. S.; Matthews, K. H.; Stevens, H. N. E.; Eccleston, G. M. Wound Healing Dressings and Drug Delivery Systems: A Review. *J. Pharm. Sci.* **2008**, *97* (8), 2892–2923. https://doi.org/10.1002/jps.21210.

(27) Boateng, J.; Catanzano, O. Advanced Therapeutic Dressings for Effective Wound Healing - A Review. *J. Pharm. Sci.* **2015**, *104* (11), 3653. https://doi.org/10.1002/jps.24610.

(28) Hu, Y.; Hu, S.; Zhang, S.; Dong, S.; Hu, J.; Kang, L.; Yang, X. A Double-Layer Hydrogel Based on Alginate-Carboxymethyl Cellulose and Synthetic Polymer as Sustained Drug Delivery System. *Sci. Rep.* **2021**, *11* (1), 1–14. https://doi.org/10.1038/s41598-021-88503-1.

(29) Alinavaz, S.; Mahdavinia, G. R.; Jafari, H.; Hazrati, M.; Akbari, A. Hydroxyapatite (HA)-Based Hybrid Bionanocomposite Hydrogels: Ciprofloxacin Delivery, Release Kinetics and Antibacterial Activity. *J. Mol. Struct.* **2021**, *1225*, 129095. https://doi.org/10.1016/j.molstruc.2020.129095.

(30) Xiao, Z.; Zheng, X.; An, Y.; Wang, K.; Zhang, J.; He, H.; Wu, J. Zwitterionic Hydrogel for Sustained Release of Growth Factors to Enhance Wound Healing. *Biomater. Sci.* **2021**, *9* (3), 882–891. https://doi.org/10.1039/d0bm01608j.

(31) Jones, A.; Vaughan, D. Hydrogel Dressings in the Management of a Variety of Wound Types: A Review. *J. Orthop. Nurs.* **2005**, *9* (SUPPL. 1), S1–S11. https://doi.org/10.1016/S1361-3111(05)80001-9.

(32) Koehler, J.; Brandl, F. P.; Goepferich, A. M. Hydrogel Wound Dressings for Bioactive Treatment of Acute and Chronic Wounds. *Eur. Polym. J.* **2018**, *100*, 1–11. https://doi.org/10.1016/j.eurpolymj.2017.12.046.

(33) Kamoun, E. A.; Kenawy, E. R. S.; Chen, X. A Review on Polymeric Hydrogel Membranes for Wound Dressing Applications: PVA-Based Hydrogel Dressings. *J. Adv. Res.* **2017**, *8* (3), 217–233. https://doi.org/10.1016/j.jare.2017.01.005.

(34) Sharman, D. Moist Wound Healing: A Review of Evidence, Application and Outcome. *Diabet. Foot J.* **2003**, *6* (3), 112-116 3p.

(35) Jeong, K. H.; Park, D.; Lee, Y. C. Polymer-Based Hydrogel Scaffolds for Skin Tissue Engineering Applications: A Mini-Review. *J. Polym. Res.* **2017**, *24* (7).

https://doi.org/10.1007/s10965-017-1278-4.

(36) da Silva, L. P.; Reis, R. L.; Correlo, V. M.; Marques, A. P. Hydrogel-Based Strategies to Advance Therapies for Chronic Skin Wounds. *Annu. Rev. Biomed. Eng.* **2019**, *21* (1), 145–169. https://doi.org/10.1146/annurev-bioeng-060418-052422.

(37) Jones, V.; Grey, J. E.; Harding, K. G. Wound Dressings. *BMJ* **2006**, *332* (7544), 777–780. https://doi.org/10.1136/bmj.332.7544.777.

(38) Cascone, S.; Lamberti, G. Hydrogel-Based Commercial Products for Biomedical Applications: A Review. *Int. J. Pharm.* **2020**, *573*, 118803–118821. https://doi.org/10.1016/j.ijpharm.2019.118803.

(39) Kozielski, K. L.; Tzeng, S. Y.; Hurtado De Mendoza, B. A.; Green, J. J. Bioreducible Cationic Polymer-Based Nanoparticles for Efficient and Environmentally Triggered Cytoplasmic SiRNA Delivery to Primary Human Brain Cancer Cells. *ACS Nano* **2014**, *8* (4), 3232–3241. https://doi.org/10.1021/nn500704t.

(40) Segovia, N.; Pont, M.; Oliva, N.; Ramos, V.; Borrós, S.; Artzi, N. Hydrogel Doped with Nanoparticles for Local Sustained Release of SiRNA in Breast Cancer. *Adv. Healthc. Mater.* **2015**, *4* (2), 271–280. https://doi.org/10.1002/adhm.201400235.

(41) Karlsson, J.; Rhodes, K. R.; Green, J. J.; Tzeng, S. Y. Poly(Beta-Amino Ester)s as Gene Delivery Vehicles: Challenges and Opportunities. *Expert Opin. Drug Deliv.* **2020**, *17* (10), 1395–1410. https://doi.org/10.1080/17425247.2020.1796628.

(42) Gresch, O.; Altrogge, L. Transfection of Difficult-to-Transfect Primary Mammalian Cells. *Methods in Molecular Biology*; **2012**; Vol. 801, pp 65–74. https://doi.org/10.1007/978-1-61779-352-3_5.

(43) Schreml, S.; Szeimies, R.-M.; Prantl, L.; Landthaler, M.; Babilas, P. Wound Healing in the 21st Century. *J. Am. Acad. Dermatol.* **2010**, *63* (5), 866–881. https://doi.org/10.1016/j.jaad.2009.10.048.

Chapter 1: Oligopeptide-Modified Poly(β-Amino Ester)s for Transfection of Human Dermal Fibroblasts

This page is intentionally left blank

Oligopeptide-Modified Poly(β-Amino Ester)s for Transfection of Human Dermal Fibroblasts

The polyplex-forming PBAE formulation C6RH is presented and optimized in the present chapter to deliver mRNA and other nucleic acids to human dermal fibroblasts, a difficult-to-transfect primary cell line.

This formulation appeared as an attractive option to be used as a transfection agent of primary cells from skin due to its hydrophilicity/hydrophobicity balance and its capability to escape the endosome after internalization. The synthesis and characterization of this PBAE polymers and the polyplexes formation are discussed first. Human dermal fibroblasts are then transfected using the C6RH nanoparticles and compared to other well-known formulations from our group.

1.1. Introduction

The use of polynucleotides to tackle diseases with a genetic or epigenetic component is a relatively new approach that is gaining momentum in the field of tissue regeneration[1]. Polynucleotides that are commonly used include plasmids containing transgenes, oligonucleotides or DNAzymes in the DNA family and mRNA, small interfering RNA (siRNAs) and miRNAs in the RNA one. Nucleic acids can be used to bind a receptor and inhibit signal transduction, to promote degradation of a gene or inhibition of translation or to make the host cells express a protein or antigen of interest[2–4]. However, the efficient use of these macromolecules as therapeutics is hampered by a rapid clearance from the body via glomerular filtration by the kidneys, their susceptibility to nuclease degradation, their strong immunogenicity and the difficulty to cross hydrophobic cell membranes that present the same negative net charge as nucleic acids[5,6]. Hence, the use of a vehicle that protects the cargo, evades the immune system and delivers nucleic acids into the cytoplasm (or even into the nucleus) is of paramount importance. Amongst the existing families of polynucleotide carriers for biomedical applications (discussed later in this chapter), cationic polymers stand out due to the many advantages they present in comparison to the rest (i.e., liposomes or viruses)[7–9]. These have shown low cytotoxicity and immunogenicity, high loading capacity, no risk of DNA integration, easily scalable production and tuneability to increase the delivery efficiency.

In the following sections, a general glimpse on these basics above mentioned are reviewed more profoundly in order to contextualize and facilitate the understanding of the technology developed in the present thesis.

1.1.1. Gene delivery for biomedical applications

Gene therapy is an emerging form of treatment that comprises the delivery of polynucleotides to a patient *in vivo* or *ex vivo* in order to correct defective gene expression. This can be done by increasing or decreasing the expression of a gene or directly editing the original DNA copies from the host[10–12]. However, the latter is out of the scope of the present dissertation and this section will only cover the use of nucleic acids to transiently control the level of gene expression. Generally, we can classify these nucleic acids in two families depending on whether the structure of their chain is DNA or RNA-based.

1.1.1.1. DNA-based therapeutics

The wide variety of different therapeutic strategies using DNA-based polynucleotides has made them an attractive approach to treat genetic defects. Moreover, DNA superior stability compared to RNA facilitates the handling and manipulation.

Plasmids, one of the most popular macromolecules in this category, are double-stranded DNA constructs, generally presenting a circular form and encoding for specific proteins. The main use of plasmids is making a host cell produce a therapeutic protein or increase protein expression when there is an abnormal underexpression of a gene. For that, the plasmid must be internalized inside the cells and reach the nucleus to make use of the transcription and translation machinery that will produce the desired proteins[3]. In contrast, gene expression can also be silenced using DNA segments known as antigene oligonucleotides. These are single-stranded DNA segments formed by up to 50 nucleotides that are complementary to a target gene. By Hoogsteen hydrogen bonding, the antigene oligonucleotide forms a triplex with the gene inside the nucleus, inhibiting the translation and transcription processes. Additionally, oligonucleotides can also be engineered to bind mRNA or pre-mRNA chains through Watson-Crick hydrogen-bonding interactions, known as antisense oligonucleotides. These oligonucleotides silence the expression of genes, and hence are typically used to modulate the expression of an overexpressed gene[3,13,14]. Other oligonucleotides used to silence gene expression include DNAzymes and aptamers. DNAzymes present strong catalytic activity, cleaving the complementary mRNA strain upon hybridisation and interrupting the translation process. Aptamers, in contrast, work by interacting with proteins, inhibiting molecular functions and pathways involved in disease[3,13,14].

Despite the variety of DNA-based therapeutics, the expression of a protein of interest is limited to the use of plasmids. The main disadvantage of plasmids is that they have to reach the

nucleus of cells, where they then have to use the cell's machinery to be transcribed. Crossing the nuclear membrane is challenging, and is often during cell mitosis that plasmids in the cytoplasm may be incorporated into the dividing nucleus and be transcribed in daughter cells[15]. Needless to say, this is a highly inefficient process, leading to very low transfection efficiencies. Alternatively, viral machinery can be used to reach the nucleus, with their own limitations, highlighted later in this chapter.

1.1.1.2. RNA-based therapeutics

RNA-based technologies are generally focused on two functions: 1) promoting the expression of a therapeutic protein or a target protein that is abnormally underexpressed or 2) silencing a protein expression via interference with mRNA expression[4,16,17].

The easiest strategy to replace dysfunctional or absent gene function or to express a protein that has therapeutic properties is by transfection using coding mRNAs. Theoretically, any disease in which an additional expression of a protein is needed could be treated using these technologies, but as it will be discussed later, efficient cell delivery is the limiting factor. Some RNA segments can also regulate the gene expression at a post-transcriptional level. This repression or activation of genes occurs by using non-coding RNAs (ncRNAs) of around 25 nucleotides that target specific mRNAs. The biological process by which suppression of expression occurs is named RNA interference (RNAi)[12,16,18–20]. In contrast, the activation of genes is called RNA activation (RNAa)[17]. RNAi is carried through by small interfering RNAs (siRNAs) and microRNAs (miRNAs), both following a similar mechanism directed to the degradation of target mRNAs[20,21]. The main difference of these RNAs is the specificity and origin. siRNAs are synthetic, exogenous sequences designed to bind only one target mRNA, while miRNAs are endogenous and can present different targets due to their imperfect pairing[22]. Interestingly, miRNAs can also participate in RNAa, activating the expression of genes instead of silencing them. Lastly, a class of RNAs named small activating RNAs (saRNAs), can only participate in RNAa. Thus, saRNAs structure is similar to siRNAs, but work oppositely[23]. The mechanism followed by RNAa is still not fully known, but just like RNAi, proteins from the Argonaute family play an important role[23,24]. Further insights about how miRNAs work will be covered in Chapter 4.

The main advantage of using RNA-based therapies, as opposed to DNA, is the fact that RNA segments only need to reach the cytoplasm to perform their function, simplifying the process and increasing the efficiency of the therapy. Additionally, this activity is not permanent,

meaning that the treatment can be stopped or modified if needed only by controlling the administration. In terms of safety, RNAs are unable to integrate into the patient's genome, hence making them safer than DNA. Unfortunately, both DNA and RNA are susceptible to enzymatic degradation and clearance from the body and they can both trigger an immune response. Since they present a negative net charge like the cell membrane, they are unable to cross it to reach cytoplasm, hampering the efficacy of these therapies. For these reasons, a vehicle that can protect the polynucleotides, evade the body's immune system and deliver them into the cells is key to improve the efficacy of treatments.

1.1.2. Vectors for local delivery of genes

The major goal to ensure the success of polynucleotide-based therapies is the efficient protection and delivery of the cargo using specific vectors. These therapies can be administered locally or systematically. When administered intravenously, a targeting moiety is often required to reach the organ or tissue that needs the treatment. Apart from the administration route, these vehicles are grouped into two general groups depending on their nature, viral and non-viral vectors (**Figure 1.1.**).

1.1.2.1. Viral vectors

Viruses have the major advantage of high transfection efficiencies and cell specificity, gained over thousands of years of evolution. However, viruses act in a pathogenic manner, replicating and delivering their genetic information to targeted cells. The generation of replication-defective viral vectors is, indeed, the cornerstone of the viral delivery vehicles in gene therapy[25,26]. Additionally, these viruses must be also engineered to replace their viral genome with therapeutic polynucleotides. The viral genome can be integrated into the DNA of the host cell to achieve a prolonged expression, or be delivered into the nucleus to remain episomal. Depending on the desired performance, the viral vectors that are commonly used are adeno-associated viruses and retroviruses or vectors based on adenoviruses and herpes simplex virus type 1, respectively[27–29]. However, despite their versatility and their high transfection efficiencies, the use of viral vectors presents major drawbacks related to high levels of immunogenicity, the cost and difficulty of large-scale production and inherent safety risks[28].

1.1.2.2. Non-viral vectors

Non-viral vectors are generally synthetic materials, making it easier to control their physicochemical properties to condense and protect nucleic cargo, increase cellular uptake, endosomal escape and nuclear delivery (if needed), while maintaining low cytotoxicity and immunogenicity. While synthetic vehicles overcome the difficulty of large-scale production presented by viral vectors, they fail to achieve the same high transfection efficiency levels[27,30]. The reason lies fundamentally on the numerous extra- and intracellular obstacles that viruses have had to overcome through years of evolution. Different non-viral vector candidates have been developed for specific applications where gene delivery is needed, leading to a vast array of options based on the chemistry, size or type of interaction with the cargo, among others. Metallic nanoparticles, mesoporous silica nanoparticles, and polypeptide vectors are a few examples. This section will only briefly review the two families of materials that have been more widely studied and bind nucleic acids through electrostatic interactions, forming nano-scaled discrete particles through self-assembly with the cargo. These systems are lipoplexes and polyplexes[31].

1.1.2.2.1. Lipoplexes

Lipoplexes are formed by cationic lipids or mixes of cationic lipids with neutral lipids. Cationic lipids present two well-differentiated moieties, a positively charged polar head and a hydrophobic tail (generally unsaturated) of variable length. Both parts are chemically connected (usually by ether, ester or amide bonds) and are of critical importance in the spontaneous formation of the discrete nanoparticles named lipoplexes. The formation occurs when the positively charged lipids complex the negatively charged DNA or RNA, encapsulating and protecting this material[32,33]. Moreover, the predominant positive charge on the surface of lipoplexes facilitates their internalization in cells by interacting electrostatically with the negatively charged plasmatic membrane. Both moieties also play a role in the cytotoxicity and efficiency of transfection[32,34]. In fact, chemical modifications on the positive hydrophobic head can be done to improve both parameters. The cationic lipids that are most common are DOTAP (1,2-Dioleoyl-3-trimethylammonium propane) and DOTMA (1,2-di-O-octadecenyl-3-trimethylammonium propane). They can be used together with the co-lipids DOPE (1,2-dioleoyl-sn-glycerophosphatidylethanolamine), DOPC (1,2-dioleoyl-sn-glycerophosphatidylcholine) or cholesterol. Generally, these co-lipids are used as a strategy to increase the lipoplexes' stability and transfection efficiency[35]. However, their major disadvantage is the difficulty to reach a compromise between these two parameters.

1.1.2.2.2. Polyplexes

Polyplexes are formed following the same mechanism than cationic lipids, but the interaction with the negatively charged polynucleotides occurs through a positively charged polymer instead. In these cationic polymers, the positive charge is normally produced by protonated amine groups in the structure, at neutral or acidic pH[7,36,37]. Moreover, polymers are generally easy to modify to tune properties such as stability or transfection efficiency. Interestingly, cationic polymers are able to condense the DNA or RNA much further than cationic lipids do[37]. This enables the delivery of higher doses of nucleic acids without increasing the amount of material used, thus decreasing overall cytotoxicity. Polymers can also be engineered to be soluble in aqueous solution, bioreducible and hydrolytically degradable. The polyplex gold standard is poly(ethylenimine) (PEI), widely used to achieve relatively high transfection efficiency in different cells, and is typically used as a commercial positive control in transfection experiments[7]. However, its cytotoxicity prevents the delivery of high doses of polynucleotides. This limitation can be overcome by using other polymers such as poly(lactic-co-glycolic acid) (PLGA), but similar to cationic lipids, it is challenging to find a compromise between transfection efficiency, stability and cytotoxicity. Hence, there is a need to engineer new polymer formulations. In our research group, we have studied and optimised a class of cationic polymers, poly(β-amino ester)s, which present high versatility, tunability and high transfection rates with cytotoxicities similar to those of available lipidic and polymeric commercial controls.

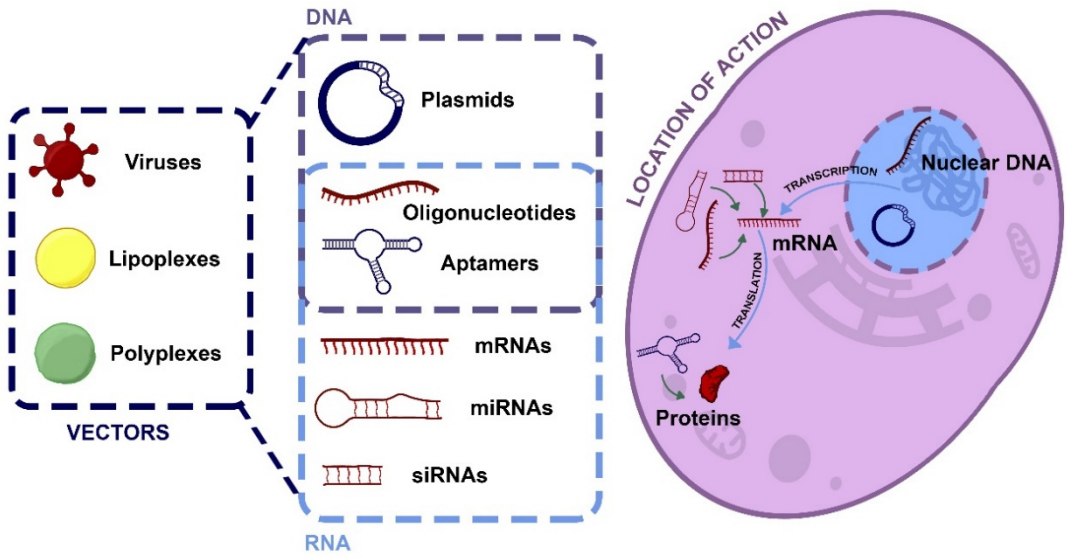

Figure 1.1. Representation of the different vectors and polynucleotides reviewed and brief schematization of their functions.

1.1.2.3. Poly(β-amino ester)s

PBAEs are found within the cationic polymers family and are considered one of the most powerful alternatives, not only when compared to liposomes and viruses, but also to other similar polymers[38,39]. PBAEs are generally synthesized by addition polymerization, a reaction in which acrylate-ended molecules react with amines following a Michael type addition mechanism[40,41]. A wide range of amines can be used, providing this kind of polymers with great versatility. For example, certain chemical groups can be added to perform desired functions or to tune the polarity. Additionally, the acrylate endings unlock more possibilities of chemical modification to gain additional features. Furthermore, metabolites formed have low toxicity, being therefore biocompatible polymers. Positive charges in these polymers interact with negatively charged nucleic acids to form polyplexes[42]. Polyplexes' positive overall net charge also allows them to interact to cell membranes and enter the cytoplasm via endosomal transport. This positive net charge can be enhanced by adding oligopeptides moieties to the ends of PBAE chains. In recent years, a large number of oligopeptide-modified PBAEs (OM-PBAEs) has been described showing high transfection efficiency and excellent biocompatibility in different cancer cell lines, both *in vitro*[43–45] and *in vivo*[46,47]. In addition to this, the tuneability of PBAEs enable the design of cell-specific and cell-targeted nanoparticles for polynucleotides delivery in other cells, showing high promise towards clinical success.

However, efficient transfection of human primary cells remains a challenge, hampering the progress of new gene therapies for numerous non-cancerous pathologies such as the one studied in the present thesis, diabetic foot ulcers[48,49]. To improve the transfection efficiency to non-cancerous cells and, consequently, the efficacy of potential treatments, it is critical to fully understand the internalization and delivery of the cargo into the cells.

1.1.2.4. Uptake and cell trafficking

The mechanisms followed by nanosized vehicles to enter the cells have been widely studied. Nowadays, there is unanimity among the scientific community in recognizing endocytosis as the internalization process (schematization in **Figure 1.2.**). This pathway is triggered after the interaction of these positively charged vectors with the negatively charged cellular membrane[50]. There is still discussion on what transport proteins mediate the endocytosis process. Endocytosis includes phagocytosis, pinocytosis and receptor-mediated endocytosis. However, it seems that the internalization generally occurs through a receptor-mediated endocytosis process known as clathrin-dependent endocytosis, especially for particles with a size ranging 100-200 nm[51,52]. Other internalization pathways are possible, but they are not as frequent. These pathways are known as clathrin-independent endocytoses (e.g., caveolae-mediated internalization) followed by particles presenting sizes other than the range mentioned above.

The particles containing polynucleotides are internalized inside an endosome. To achieve successful delivery, they must escape the endosome before it progresses towards a lysosome, the cell's digestive organelle. The most common mechanism to escape the endosome is known as the proton sponge effect, favoured by polymers that present high buffering capacity at the late endosomal pH range between 5.0 and 7.5[53–55]. The interaction of these polyplexes with endosomal membranes produces a locally weakened area that can then undergo rupture by the increase of osmotic forces. After the endosome's rupture, nanoparticles are released in the cytoplasm. RNAs and some DNAs (e.g., aptamers or antisense oligonucleotides), will act here, following different processes depending on the type of RNA/DNA and mechanism of action (e.g., mRNA will be translated to proteins in the ribosomes). In contrast, most DNA (e.g., plasmid DNA or antigene oligonucleotides) must cross the nuclear membrane. In non-dividing cells, the internalization of the nucleic acids up to 40,000 g/mol will occur passively through the nuclear pores[50]. Otherwise, specific signals are needed for an active transport. Finally, DNA (plasmid DNA, for example) will benefit from the transcription and translation machinery to finally express proteins of interest.

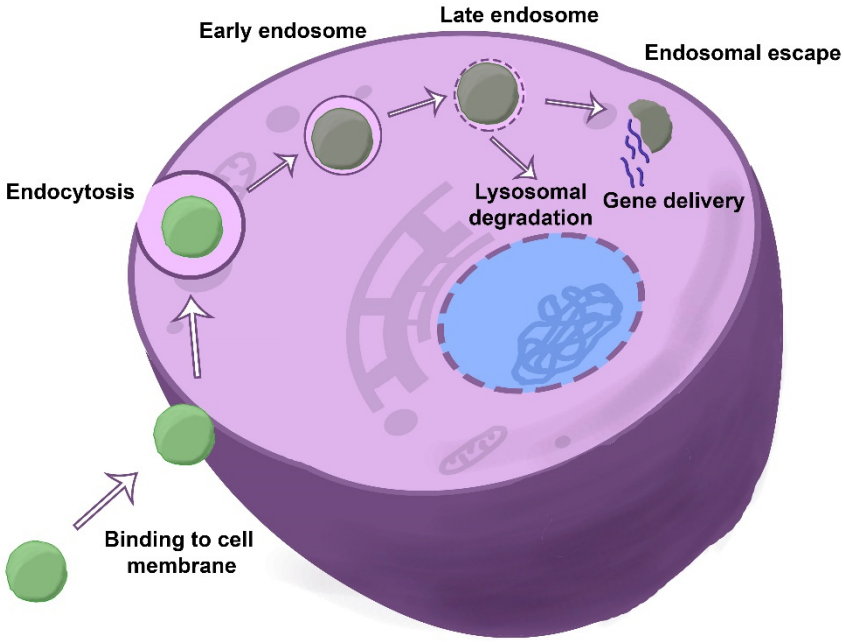

Figure 1.2. Schematic representation of polyplexes internalization.

Based on previous studies involving cell-trafficking and endosomal escape, a promising PBAE formulation is optimized in this chapter. mRNA and other different protein-coding nucleic acids are used to enable efficient transfection of human dermal fibroblasts. This cell type is categorized as hard-to-transfect primary mammalian cells[49]. In fact, Lipofectamine™ and Jet Prime™ reagents and different electroporation methods are commonly used, but giving low transfection efficiencies. Moreover, none of these are translatable. Fibroblasts are involved in many different stages of wound healing, and they have been reported to have altered gene expression profile in chronic wounds. Hence, the development of efficient delivery vectors for fibroblasts is key for the creation of new gene therapies for wound healing. In the future, the versatility and tunability of these newly PBAEs combinations will allow for further modifications with tissue- and cell-specific transfection.

1.2. Materials and methods

Reagents and solvents were obtained from Sigma–Aldrich and Panreac and used as received unless otherwise stated. Oligopeptides were purchased from Ontores Biotechnologies Inc. and used as hydrochloride salts. Plasmid reporter green fluorescent protein (pmaxGFP) (3486 bp), GFP-encoding mRNA CleanCap EGFP (5moU), Firefly Luciferase reporter (FLuc) and CleanCap FLuc mRNA 5-methoxyuridine were acquired from Amaxa, Tebu-Bio, Promega Corporation and TriLink respectively. HDFs from adult skin were purchased from ATCC (ATCC PCS-201-030). Media and supplements for cell culture (DMEM, phosphate-buffered saline (PBS), glutamine and penicillin−streptomycin solution, trypsin-EDTA 0.25 %) were obtained from Gibco, Hyclone, and Invitrogen. ^{1}H-NMR spectra were recorded in a 400 MHz Varian (Varian Inc. NMR Instruments, Claredon Hills, IL, USA) and methanol-d^{4} was used as solvent unless otherwise stated.

1.2.1. Synthesis and characterization of OM-PBAE polymers

The first step in the preparation of functional PBAEs is the formation of the acrylate-terminated backbones. This polymer formation occurs via Michael addition polymerization, reacting primary amines with diacrylates. PBAEs used in the present thesis were the ones named as C32 and C6 (see **Figure 1.3.**) and were synthesized following a procedure previously described in the literature by Dosta *et al*[43–45]. Specifically, C32 polymer was obtained stirring 5-amino-1-pentanol (7.7 g, 75 mmol) and 1,4-butanediol diacrylate (18 g, 82 mmol) together at 90 ºC for 20 h. For C6 polymer, 5-amino-1-pentanol (3.9 g, 38 mmol) was firstly mixed with 1-hexylamine (3.8 g, 38 mmol). Then, 1,4-butanediol diacrylate (18 g, 82 mmol) was added to the mixture and heated at 90 ºC for 20 h. The resulting products were characterized by ^{1}H-NMR and compared to PBAE backbones characterization in our previous works to confirm that the number of repeated units of the polymer was n = 7. PBAE backbones were stored at -20 ºC.

Once the acrylate-terminated PBAE backbones are formed, different oligopeptides are used to modify both endings of the chains. PBAEs C6 were modified with the oligopeptides Cys-Arg-Arg-Arg or CRRR (CR3) and Cys-His-His-His or CHHH (CH3) to form the C6CR3 and C6CH3 formulations, respectively, whereas the C32 backbone was only modified using the CR3 oligopeptide to form the PBAE formulation C32CR3. In this reaction, the oligopeptides must be in the hydrochloride form but since peptides were purchased as trifluoro acetic acid (TFA) salts, the first step was the substitution of trifluoro acetic acid for hydrochloride as

counterions. Generally, oligopeptides (100 mg) were dissolved in HCl 0.1 M (10 mL) and frozen at -80 ºC for an hour. The solution was then freeze-dried and dissolved in the necessary volume of DMSO to reach a concentration of 100 mg/mL. A polymer solution of the desired PBAE backbone was used at the same concentration and same solvent and added dropwise to the peptide hydrochloride solution at a PBAE/peptide molar ratio of 1:2.5. At this point, triethylamine was added to the solution in a peptide/triethylamine molar ratio of 1:8. The mixture was allowed to react at room temperature for 48 h. Precipitation of the OM-PBAEs occurred after adding the mixture dropwise to a solution of diethyl ether/acetone (4:1) and centrifuging at 4,000 rpm for 10 min. This process was repeated three times and the polymers were dried under vacuum overnight and dissolved to be kept in aliquots of 100 mg/mL using DMSO as solvent. All OM-PBAEs were characterized by ^{1}H-NMR as described in our previous works[43–45].

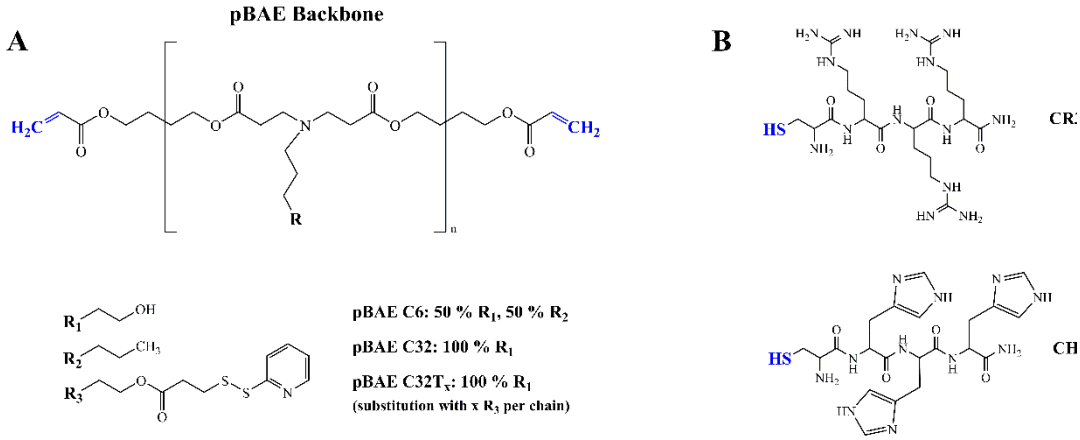

Figure 1.3. Schematic representation of the PBAEs used in the present thesis. A) PBAE backbones of the formulations. B) Oligopeptides used to modify the terminations of the polymer backbones.

1.2.2. Polyplexes formation and characterization

The PBAE nanoparticles were prepared using the oligopeptide-modified C6 and C32 PBAEs. The formulations used for the polyplexes were C6CR3, C32CR3 and C6RH (C6CR3/C6CH3 in a 6:4 ratio). Plasmid reporter green fluorescent protein (pGFP), EGFP mRNA (mRNA-GFP), firefly luciferase reporter plasmid (pFLUC) or mRNA-FLuc were encapsulated in the particles and used in transfections. PBAEs and polynucleotides were kept in stocks at 100 mg/mL in DMSO and 1 mg/mL in nuclease-free water, respectively. For polyplexes formation, the protocols based on our previous works were followed without changes[43–45]. The starting

solutions were diluted separately in sodium acetate (AcONa) buffer at pH 5.2. The concentration of AcONa salts used was 12.5 mM for C6 or 25 mM for C32. The final volume of the PBAE and the polynucleotide solutions was the same and it was calculated to reach a polynucleotide final concentration of 0.03 mg/mL. The PBAE/polynucleotide weight ratio when mixed depended on the formulation: the ratio in the final mix was 25:1 for C6 and 50:1 for C32. The mixing process is a critical step and influences both the size and polydispersity. Hence, the polynucleotide solution was added over the PBAE solution by pipetting and incubated at 25 ºC for 30 min. Analysis of the particle size, polydispersity and zeta potential was performed in a Nanosizer ZS instrument (Malvern Instruments, UK), after diluting the polyplexes' solution 10-fold with phosphate-buffered saline (PBS) 1x.

1.2.3. HDFs culture

Primary HDFs were cultured at 37°C and 5% CO_2 with supplemented DMEM (4.5 g glucose/mL, without glutamine, pH = 7.2) with glutamine (2 mM), 1% penicillin−streptomycin mixture and 10% fetal bovine serum (FBS). HDFs used in every experiment at passage below 4.

1.2.4. HDFs transfection and cell viability

HDFs were seeded at 10,000 cells per well in 96-well plates and incubated 24 h at 37ºC in 5% CO_2 atmosphere. The transfection was performed when cells reached 80% confluence. The different formulations studied consisted of polyplexes formed by OM-PBAE-encapsulated pGFP, pFLuc, mRNA-GFP and mRNA-FLuc polynucleotides. Polyplexes solutions were prepared at a concentration of 0.03 µg/µL as described above and were diluted 10-fold in non-supplemented DMEM. Cells were transfected with 100 µL of the previous solution to a final dose of 0.3 µg polynucleotide per well. HDFs were incubated for 3 h and the transfection media was removed and replaced by fresh supplemented media. Polyplus-transfection Jet Prime and JetMESSENGER were used as positive control in DNA and RNA experiments, respectively. The manufacturer's recommended concentration was used, which corresponds to a lower concentration than that used for PBAE nanoparticles, due to the toxicity of JetPrime and JetMESSENGER. Untreated cells were used as negative controls. Cells were imaged with a fluorescence microscope (Nikon Eclipse T32000-U) after 24 h incubation in the case of mRNA and 48 h for plasmid DNA. For quantification of the transfection, cells were detached by incubating for 5 min with trypsin-ethylenediaminetetraacetic acid (EDTA) at 37°C in 5% CO_2 atmosphere. Transfection efficiency was then measured by flow cytometry (FACS;

NovoCyte Flow Cytometer, ACEA Biosciences Inc.). In case of using FLuc reporters, luciferase activity was quantified using the Luciferase Assay System Kit (Promega), and photon emission was measured in a Synergy HT luminometer (BioTek). Cell viability of the formulations studied was performed using Presto Blue viability assay, following the manufacturer's instructions. Negative control consisted of untreated cells and positive control consisted of cells transfected using the Polyplus reagent.

1.2.5. Statistical Analysis

GraphPad Prism 8.0.1 software was used for the statistical analysis. Statistical differences between groups were studied by ordinary one-way ANOVA with post-hoc Tukey HSD test. The significance of the difference in the data is *$p < 0.05$, **$p < 0.01$, ***$p < 0.001$, and ****$p < 0.0001$.

1.3. Results and discussion

1.3.1. Synthesis and characterization of oligopeptide end-modified PBAEs

The chemical structure of PBAEs backbone plays a crucial role in the formation of polyplexes and their behaviour as transfection agents. In the present thesis, we synthesized and studied two families of PBAE polymers with varying polarity by controlling the molar stoichiometry of specific amine groups following an aza-Michael reaction mechanism[56] (**Scheme 1.1.**). PBAE C32 was obtained combining monomers 1,4-butanediol diacrylate and 5-amino-1-pentanol. C6 PBAE was synthesized by conjugate addition of 5-amino-1-pentanol and hexylamine to a slight excess of 1,4-butanediol diacrylate. Thus, hydrophobicity was controlled by the molar stoichiometry of hydrophilic and hydrophobic amines, with the C32 polymer being more hydrophilic than the C6 polymer (**Figure 1.3.**). The structure of the resulting polymers was characterized by ^{1}H-NMR. Integrals of signals inside and outside the repeating units were compared to confirm that the PBAE polymers were formed by 7 repeating units.

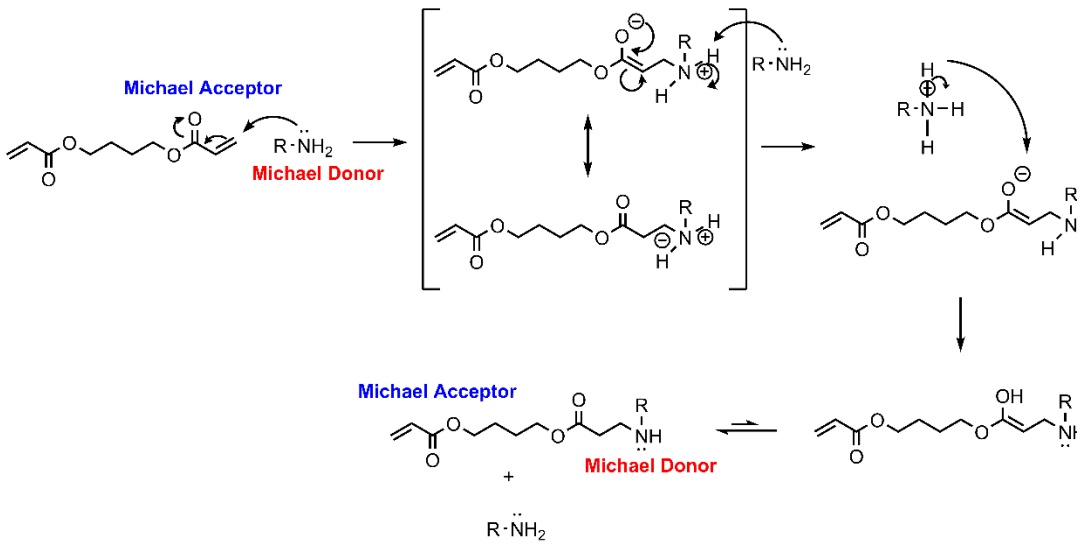

Scheme 1.1. Mechanism of the aza-Michael addition reaction

Finally, the different PBAE acrylate-ended backbones (C6 and C32) were modified with cysteine-terminated CR3 or CH3 oligopeptides through Michael-type addition[57] (**Scheme 1.2.**). Characterization of the oligopeptide-end polymers by ^{1}H-NMR showed a complete modification by disappearance of the acrylate signals.

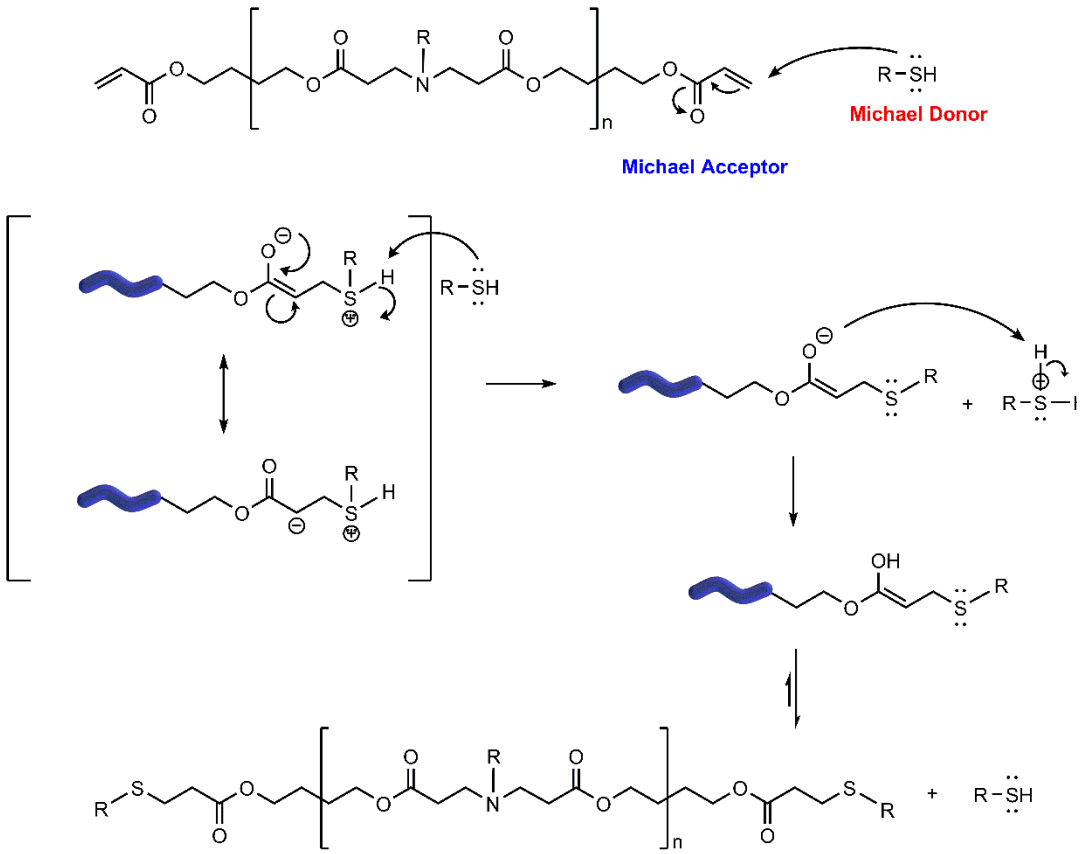

Scheme 1.2. Mechanism of the Michael addition reaction between thiols and acrylates.

1.3.2. PBAE polyplexes formation and characterization

Different cancer cell lines have been successfully transfected using a wide variety of PBAE formulations. However, transfection of primary human cells, such as fibroblasts, is challenging and typically yields very low transfection efficiency[49]. To maximize fibroblast transfection, we have based our current study on previously observed patterns that yielded optimal transfection efficiency in cancer cell lines[43–45,47]. Hence, the hydrophobicity/hydrophilicity ratio

and the ability to escape the endosome were tuned following the following rationale. The initial stage in the cell transfection process involves the interaction of the vehicle with cell membranes. It is known that amphiphilic or hydrophobic compounds present higher affinities for biological lipid membranes. As an example, hexyl groups in polyplexes tend to enhance endocytosis and hence, transfection efficiency[51,58]. However, Dosta *et al.* found that polyplexes formed entirely by hexyl groups were less stable and gave worse results in terms of cell transfection[43]. C6 polyplexes, composed of hexyl and 1-pentanol moieties in a 1:1 ratio, emerged as promising transfection agents, showing improved stability with high transfection efficiency. Another factor to consider in the transfection process is the internalization and the endosomal escape. The latter is facilitated by the proton sponge effect[53,59], which is mediated by polymers that present high buffering capacity. The interaction of these polyplexes with endosomal membranes produces a locally weakened area that will undergo rupture upon an increase in osmotic forces. This increase is likely to happen when polymers buffering effect is found at the endosomal pH range between 5.0 and 7.5[55]. Taking this into consideration, Segovia *et al.* tested different formulations of OM-PBAEs and showed that buffering capacity is controlled by incorporating certain amino acids in the oligopeptide modifiers[45]. In particular, histidine moieties showed the highest buffering capacity, leading to the most effective endosomal escape. However, polyplexes made of histidine-ended OM-PBAEs presented lower nucleic acid encapsulation efficiencies and lower cell transfection than those containing arginine-ended OM-PBAEs. On the other hand, arginine-ended OM-PBAEs presented lower buffering capacity, unlikely to facilitate endosomal escape. Polyplexes formed by mixture of both arginine- and histidine-ended polymers (C32CR3 and C32CH3) in a 1:1 ratio gave unprecedented transfection efficiency by combining the high encapsulation and cell entry, facilitated by arginine, and high endosomal escape, enabled by histidine.

Based on previous data, we hypothesized that the use of alcohol pendant groups combined with hydrocarbon chains (C6 formulation) would maximize oligonucleotide encapsulation, enable cellular membrane crossing and facilitate endosomal escape in primary HDFs. In addition, published data supports the hypothesis that a mixture of arginine-ended (CR3) and histidine-ended (CH3) PBAEs will lead to an improvement in transfection efficiency in HDF. Hybrid polyplexes formed by C6CR3/C6CH3 polymers with a 6:4 molar ratio (named C6RH from now on) showed efficient encapsulation of GFP-mRNA into nanoparticles of similar size, polydispersity index and Z-potential to its predecessors C32CR3 and C6CR3 (**Table 1.1.**), that proved to be optimal for cellular uptake and *in vivo* use in the past.

Table 1.1. Hydrodynamic diameter, polydispersity index and Z-potential of the formulations encapsulating mRNA-GFP studied in the present work (n=3).

NANOPARTICLE FORMULATION	Hydrodynamic diameter (nm; by DLS)	PDI (by DLS)	Z-Potential (mV; by DLS)
C32CR3	187 ± 14	0.12 ± 0.03	35 ± 2
C6CR3	132 ± 4	0.20 ± 0.02	30 ± 1
C6RH	127 ± 1	0.15 ± 0.01	30 ± 1

C6RH can also encapsulate other genetic material, such as plasmid DNA, and genetic material encoding other proteins, such as luciferase (**Table 1.2.**). C6CH3- and C32CH3-only polyplexes were not investigated in the present thesis owing to their null transfection efficiency observed in the past.

Table 1.2. Hydrodynamic diameter and polydispersity index of the formulations studied in the present work encapsulating different polynucleotides (n=3).

	pGFP		pLUC		mRNA-LUC	
NANOPARTICLE FORMULATION	**Hydrodynamic diameter** (nm; by DLS)	**PdI** (by DLS)	**Hydrodynamic diameter** (nm; by DLS)	**PdI** (by DLS)	**Hydrodynamic diameter** (nm; by DLS)	**PdI** (by DLS)
C32CR3	173 ± 3	0.18 ± 0.05	206 ± 2	0.17 ± 0.01	161 ± 5	0.19 ± 0.01
C6CR3	99 ± 3	0.13 ± 0.03	134 ± 1	0.11 ± 0.04	132 ± 3	0.23 ± 0.02
C6RH	150 ± 2	0.11 ± 0.01	140 ± 3	0.18 ± 0.02	110 ± 1	0.13 ± 0.01

1.3.3. Transfection efficiency and cytotoxicity of OM-PBAE polyplexes

Transfection efficiency was evaluated 24 h post-transfection with GFP-mRNA polyplexes, compared to controls. In **Figure 1.4.**, fluorescence microscopy images show GFP expression in dermal fibroblasts before their quantification by flow cytometry. Overall, C6RH polyplexes demonstrated superior transfection efficiency of HDFs with GFP-mRNA (74.0±3.9% transfected cells), compared to the previously developed formulations (20.5±6.6% and 53.4±10.0% with C32CR3 and C6CR3, respectively) and the commercially available transfection reagent PolyPlus JetMESSENGER (49.3±5.3% transfected cells, **Figure 1.5.**).

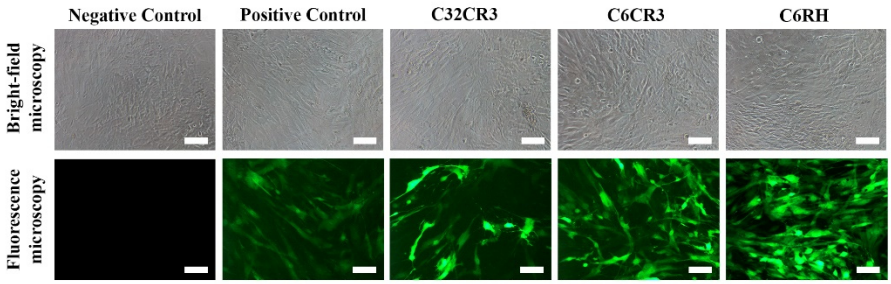

Figure 1.4. Bright-field and fluorescence microscopy images of HDFs transfected with the formulation C6RH loaded with GFP-mRNA. Negative control: untreated cells; Positive control: Polyplus JetMESSENGER transfection reagent.

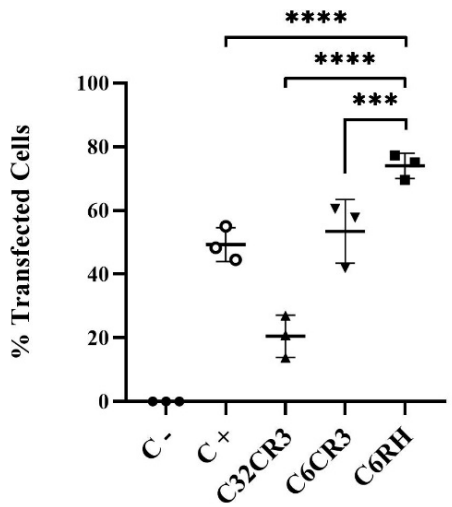

Figure 1.5. Transfection efficiency in % of transfected cells using different PBAE nanoparticles loaded with GFP-mRNA obtained by FACS (n=3). Negative control: untreated cells; Positive control: Polyplus JetMESSENGER transfection reagent.

These results demonstrate that by tuning the hydrophilicity of the PBAE backbone and the oligopeptide modification ratios, polyplexes can be more readily internalized in HDFs and successfully escape the endosome, leading to an overall enhanced transfection efficiency and concomitant increase in reporter protein expression, while eliciting minimal toxicity

(**Figure 1.6.**). Moreover, FACS data show that not only are there more GFP-expressing fibroblasts when transfecting with C6RH, but they have higher fluorescence emission intensity with lower dispersion, compared to commercial control and previous formulations (**Figure 1.7.**). The intensity values obtained from the fluorescence images are collected in **Figure 1.8**. Coinciding with the results observed from the FACS data, C6RH formulation presented the highest intensity in comparison to the positive control (72.8±29.9 AU and 27.1±5.5 AU for C6RH and the Polyplus control, respectively). In addition, the other PBAE formulations studied could not reach the C6RH intensity levels (48.2±27.5 AU and 50.3±21.5 AU for C32CR3 and C6CR3, respectively).

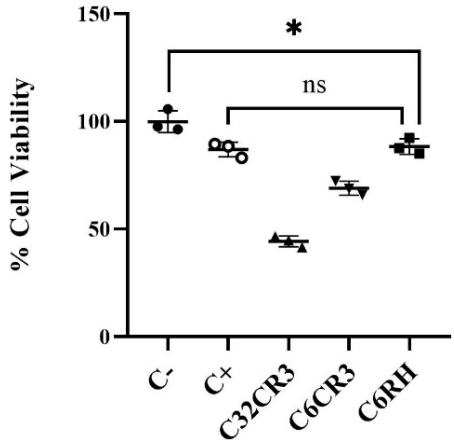

Figure 1.6. Cell viability after transfection in Figure 1.5 (n=3). Negative control: untreated cells; Positive control: Polyplus JetMESSENGER transfection reagent.

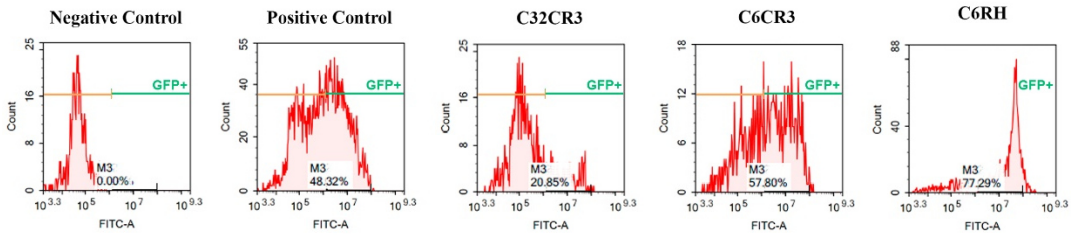

Figure 1.7. FACS graphs obtained in the transfection experiments using GFP-mRNA-loaded C6RH polyplexes. Negative control: untreated cells; Positive control: Polyplus JetMESSENGER transfection reagent.

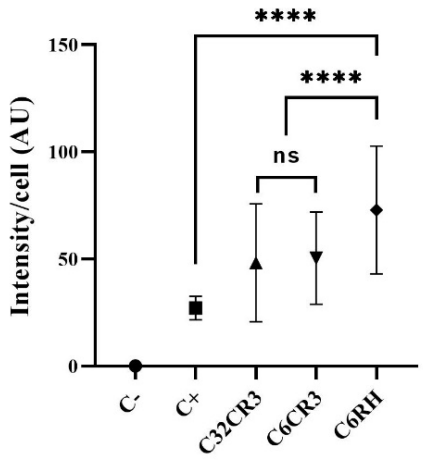

Figure 1.8. Transfection intensity per cell in AU of fibroblasts using the formulations studied. Negative control: untreated cells; Positive control: Polyplus JetMESSENGER transfection reagent.

Overall, C6RH polyplexes have a more homogeneous, robust and efficient transfection in HDF, and hence are ideal candidates for RNA therapies to skin fibroblasts. Interestingly, the levels of GFP expression after transfection with C6RH polyplexes loaded with plasmid DNA were also higher (22.7±1.9% cells transfected) than those shown by the previous formulations (0.2±0.1% and 6.0±0.5% with C32CR3 and C6CR3, respectively) and the commercially available positive control (12.2±0.5% cells transfected), thus indicating that C6RH polyplexes have an enhanced ability to also cross the nuclear membrane and deliver genetic material to the nucleus, a unique feature of these polyplexes. Transfection efficiency with pDNA is lower than that observed with mRNA, which is due to the inherent nature of transcription and translation mechanisms. RNA only needs to enter the cell via endosomal internalization and reach the ribosomes in the cytoplasm where it is translated into the reporter protein. However, DNA must also cross the nuclear membrane and reach the cell nucleus, where it is transcribed into mRNA and then the latter is translated into the reporter protein in the cytoplasmic ribosomes. For this reason, higher levels of mRNA expression than pDNA expression are expected. To confirm the broad applicability of this approach, we verified that these polyplexes successfully deliver mRNA and plasmid DNA encoding other proteins (such as luciferase, **Figure 1.9. A and B**) obtaining similar trends. Additionally, the stability of the promising formulation C6RH was studied when mixed with the hydrogel-forming polymers C32TCR3 and C32T*CR3 that will appear in the next chapter (**Figure 1.10.**). As it can be seen in **Figure 1.3.**, C32TCR3 is a C32CR3 polymer in which one out of seven hydroxyl groups have been modified to incorporate the thiopyridyl group that reacts with thiols, and will be used later to

crosslink the hydrogel. C32T*CR3 polymer is the result of the reaction of the thiopyridyl group in C32TCR3 polymers with 2-mercaptoethanol, and mimics the exact chemistry of the polymers formed after degradation of the hydrogel. This experiment aims to understand the stability of the C6RH polyplexes in contact with degradation by-products of the hydrogel, and whether these by-products might affect overall transfection efficiency. The data show that the transfection efficiency of C6RH in HDF is not affected by C32TCR3 or C32T*CR3, (75.0±4.8% and 75.6±3.3%, respectively) demonstrating that these particles are stable in contact with both the hydrogel and its degradation products.

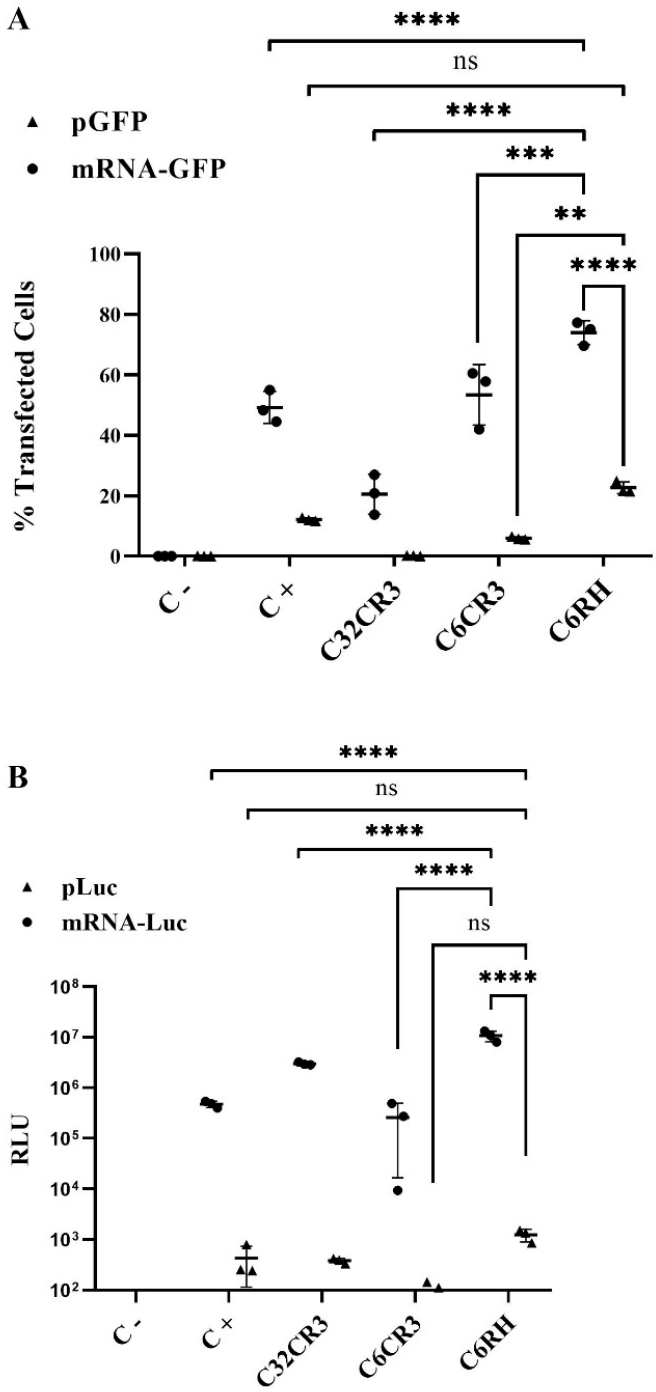

Figure 1.9. A) Transfection efficiency in % of transfected HDFs using mRNA and pDNA coding for the GFP. B) Transfection efficiency in % of transfected HDFs using luciferase-mRNA and pDNA (n=3). Negative control: untreated cells; Positive control: Polyplus JetMESSENGER transfection reagent.

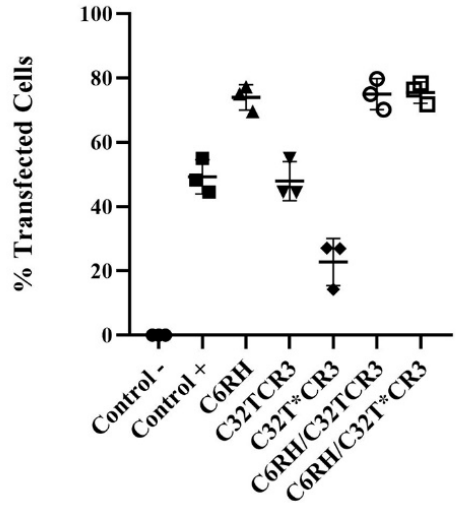

Figure 1. 10. Transfection efficiency of HDFs in % transfected cells using C6RH formulation mixed with the polymer C32TCR3 and C32T*CR3 (n=3). Negative control: untreated cells; Positive control: Polyplus JetMESSENGER transfection reagent.

1.4. Concluding remarks

The delivery of specific nucleic acids arises as an interesting approach to treat diseases or medical conditions characterized by a dysregulation of gene expression. The vast variety of polynucleotides of different nature opens the possibility to both silence overexpressed proteins or to promote expression of proteins of interest. However, the efficacy of these treatments is limited by the optimal internalization of the therapeutic nucleic acids into cells. Hence, carriers that protect and deliver this cargo in an efficient way are required. In this chapter, polyplexes formed with the C6RH formulation were proposed as a new delivery vehicle. This formulation showed similar hydrodynamic diameters, polydispersity indexes and Z-potentials than its predecessor C6CR3. Moreover, different types of nucleic acids encoding for different proteins can be loaded into these polyplexes without compromising the polyplex stability and physical properties.

The transfection experiments carried out unveiled unprecedented transfection efficiencies in human dermal fibroblasts when using mRNA-loaded C6RH polyplexes encoding for different reporter proteins. Furthermore, the new formulation was able to reach the nucleus when plasmid DNA was delivered. C6RH polyplexes demonstrated high stability when mixed with other PBAE polymers that can potentially add new interesting features (such as local and sustained delivery from a hydrogel) without compromising the transfection efficiencies.

C6RH polyplexes emerge as new candidates for RNA delivery to human dermal fibroblasts, and will be used in subsequent experiments for local delivery from the hydrogel wound dressing. It is noteworthy that the transfection efficiencies obtained when encapsulating pDNA are quite promising, especially taking into consideration that human skin-derived fibroblasts are inherently difficult to transfect. All in all, C6RH is a promising formulation for a potential therapeutic use for gene delivery applications in primary cells due to its versatility, high transfection efficiency and low toxicity, and is suitability for the delivery of both DNA and RNA.

1.5. References

(1) Balmayor, E. R. Synthetic MRNA – Emerging New Class of Drug for Tissue Regeneration. *Curr. Opin. Biotechnol.* **2022**, *74*, 8–14. https://doi.org/10.1016/j.copbio.2021.10.015.

(2) Damase, T. R.; Sukhovershin, R.; Boada, C.; Taraballi, F.; Pettigrew, R. I.; Cooke, J. P. The Limitless Future of RNA Therapeutics. *Front. Bioeng. Biotechnol.* **2021**, *9* (March), 1–24. https://doi.org/10.3389/fbioe.2021.628137.

(3) Patil, S. D.; Rhodes, D. G.; Burgess, D. J. DNA-Based Therapeutics and DNA Delivery Systems: A Comprehensive Review. *AAPS J.* **2005**, *7* (1), E61–E77. https://doi.org/10.1208/aapsj070109.

(4) Kole, R.; Krainer, A. R.; Altman, S. RNA Therapeutics: Beyond RNA Interference and Antisense Oligonucleotides. *Nat. Rev. Drug Discov.* **2012**, *11* (2), 125–140. https://doi.org/10.1038/nrd3625.

(5) Kaczmarek, J. C.; Kowalski, P. S.; Anderson, D. G. Advances in the Delivery of RNA Therapeutics: From Concept to Clinical Reality. *Genome Med.* **2017**, *9* (1), 60–75. https://doi.org/10.1186/s13073-017-0450-0.

(6) Ramasamy, T.; Munusamy, S.; Ruttala, H. B.; Kim, J. O. Smart Nanocarriers for the Delivery of Nucleic Acid-Based Therapeutics: A Comprehensive Review. *Biotechnol. J.* **2021**, *16* (2), 1900408. https://doi.org/10.1002/biot.201900408.

(7) Zhang, P.; Wagner, E. History of Polymeric Gene Delivery Systems. *Top. Curr. Chem.* **2017**, *375* (2), 26–64. https://doi.org/10.1007/s41061-017-0112-0.

(8) Thomas, T. J.; Tajmir-Riahi, H.-A.; Pillai, C. K. S. Biodegradable Polymers for Gene Delivery. *Molecules* **2019**, *24* (20), 3744. https://doi.org/10.3390/molecules24203744.

(9) Ullah, I.; Muhammad, K.; Akpanyung, M.; Nejjari, A.; Neve, A. L.; Guo, J.; Feng, Y.; Shi, C. Bioreducible, Hydrolytically Degradable and Targeting Polymers for Gene Delivery. *J. Mater. Chem. B* **2017**, *5* (18), 3253–3276. https://doi.org/10.1039/C7TB00275K.

(10) Caplen, N. J. Gene Therapy Progress and Prospects. Downregulating Gene Expression: The Impact of RNA Interference. *Gene Ther.* **2004**, *11* (16), 1241–1248. https://doi.org/10.1038/sj.gt.3302324.

(11) Gonçalves, G. A. R.; Paiva, R. de M. A. Gene Therapy: Advances, Challenges and Perspectives. *Einstein (São Paulo)* **2017**, *15* (3), 369–375. https://doi.org/10.1590/s1679-45082017rb4024.

(12) Wang, W.; Zhu, H. Z.; Xue, J. L. RNAi as a Gene Therapy Approach. *Prog. Biochem.*

Biophys. **2004**, *31* (7), 590–595. https://doi.org/10.1517/eobt.3.4.575.21204.

(13) Ibraheem, D.; Elaissari, A.; Fessi, H. Gene Therapy and DNA Delivery Systems. *Int. J. Pharm.* **2014**, *459* (1–2), 70–83. https://doi.org/10.1016/j.ijpharm.2013.11.041.

(14) Herweijer, H.; Wolff, J. A. Progress and Prospects: Naked DNA Gene Transfer and Therapy. *Gene Ther.* **2003**, *10* (6), 453–458. https://doi.org/10.1038/sj.gt.3301983.

(15) Bai, H.; Lester, G. M. S.; Petishnok, L. C.; Dean, D. A. Cytoplasmic Transport and Nuclear Import of Plasmid DNA. *Biosci. Rep.* **2017**, *37* (6), 1–17. https://doi.org/10.1042/BSR20160616.

(16) Bobbin, M. L.; Rossi, J. J. RNA Interference (RNAi)-Based Therapeutics: Delivering on the Promise? *Annu. Rev. Pharmacol. Toxicol.* **2016**, *56* (1), 103–122. https://doi.org/10.1146/annurev-pharmtox-010715-103633.

(17) Portnoy, V.; Huang, V.; Place, R. F.; Li, L. C. Small RNA and Transcriptional Upregulation. *Wiley Interdiscip. Rev. RNA* **2011**, *2* (5), 748–760. https://doi.org/10.1002/wrna.90.

(18) Tokatlian, T.; Segura, T. SiRNA Applications in Nanomedicine. *Wiley Interdiscip. Rev. Nanomedicine Nanobiotechnology* **2010**, *2* (3), 305–315. https://doi.org/10.1002/wnan.81.

(19) Whitehead, K. A.; Langer, R.; Anderson, D. G. Knocking down Barriers: Advances in SiRNA Delivery. *Nat. Rev. Drug Discov.* **2009**, *8* (2), 129–138. https://doi.org/10.1038/nrd2742.

(20) Setten, R. L.; Rossi, J. J.; Han, S. ping. The Current State and Future Directions of RNAi-Based Therapeutics. *Nat. Rev. Drug Discov.* **2019**, *18* (6), 421–446. https://doi.org/10.1038/s41573-019-0017-4.

(21) Hannon, G. J. RNA Interference. *Nature* **2002**, *418* (6894), 244–251. https://doi.org/10.1038/418244a.

(22) Lam, J. K. W.; Chow, M. Y. T.; Zhang, Y.; Leung, S. W. S. SiRNA Versus MiRNA as Therapeutics for Gene Silencing. *Mol. Ther. - Nucleic Acids* **2015**, *4* (September), e252. https://doi.org/10.1038/mtna.2015.23.

(23) Kwok, A.; Raulf, N.; Habib, N. Developing Small Activating RNA as a Therapeutic: Current Challenges and Promises. *Ther. Deliv.* **2019**, *10* (3), 151–164. https://doi.org/10.4155/tde-2018-0061.

(24) Chu, Y.; Yue, X.; Younger, S. T.; Janowski, B. A.; Corey, D. R. Involvement of Argonaute Proteins in Gene Silencing and Activation by RNAs Complementary to a Non-Coding Transcript at the Progesterone Receptor Promoter. *Nucleic Acids Res.* **2010**, *38* (21), 7736–7748. https://doi.org/10.1093/nar/gkq648.

(25) Anguela, X. M.; High, K. A. Entering the Modern Era of Gene Therapy. *Annu. Rev. Med.* **2019**, *70* (1), 273–288. https://doi.org/10.1146/annurev-med-012017-043332.

(26) Robbins, P. D.; Ghivizzani, S. C. Viral Vectors for Gene Therapy. *Pharmacol. Ther.* **1998**, *80* (1), 35–47. https://doi.org/10.1016/S0163-7258(98)00020-5.

(27) Nayerossadat, N.; Ali, P.; Maedeh, T. Viral and Nonviral Delivery Systems for Gene Delivery. *Adv. Biomed. Res.* **2012**, *1* (2), 27–37. https://doi.org/10.4103/2277-9175.98152.

(28) Thomas, C. E.; Ehrhardt, A.; Kay, M. A. Progress and Problems with the Use of Viral Vectors for Gene Therapy. *Nat. Rev. Genet.* **2003**, *4* (5), 346–358. https://doi.org/10.1038/nrg1066.

(29) Kootstra, N. A.; Verma, I. M. Gene Therapy with Viral Vectors. *Annu. Rev. Pharmacol. Toxicol.* **2003**, *43*, 413–439. https://doi.org/10.1146/annurev.pharmtox.43.100901.140257.

(30) Mintzer, M. A.; Simanek, E. E. Nonviral Vectors for Gene Delivery. *Chem. Rev.* **2009**, *109* (2), 259–302. https://doi.org/10.1021/cr800409e.

(31) Rafael, D.; Andrade, F.; Arranja, A.; Luís, S.; Videira, M. Lipoplexes and Polyplexes: Gene Therapy. *Encycl. Biomed. Polym. Polym. Biomater.* **2015**, 4335–4347. https://doi.org/10.1081/e-ebpp-120050058.

(32) Wasungu, L.; Hoekstra, D. Cationic Lipids, Lipoplexes and Intracellular Delivery of Genes. *J. Control. Release* **2006**, *116* (2 SPEC. ISS.), 255–264. https://doi.org/10.1016/j.jconrel.2006.06.024.

(33) Zhi, D.; Bai, Y.; Yang, J.; Cui, S.; Zhao, Y.; Chen, H.; Zhang, S. A Review on Cationic Lipids with Different Linkers for Gene Delivery. *Adv. Colloid Interface Sci.* **2018**, *253*, 117–140. https://doi.org/10.1016/j.cis.2017.12.006.

(34) Lv, H.; Zhang, S.; Wang, B.; Cui, S.; Yan, J. Toxicity of Cationic Lipids and Cationic Polymers in Gene Delivery. *J. Control. Release* **2006**, *114* (1), 100–109. https://doi.org/10.1016/j.jconrel.2006.04.014.

(35) Fasbender, A.; Marshall, J.; Moninger, T. O.; Grunst, T.; Cheng, S.; Welsh, M. J. Effect of Co-Lipids in Enhancing Cationic Lipid-Mediated Gene Transfer in Vitro and in Vivo. *Gene Ther.* **1997**, *4* (7), 716–725. https://doi.org/10.1038/sj.gt.3300459.

(36) Aggarwal, R.; Targhotra, M.; Kumar, B.; Sahoo, P. .; Chauhan, M. K. Polyplex: A Promising Gene Delivery System. *Int. J. Pharm. Sci. Nanotechnol.* **2019**, *12* (6), 4681–4686. https://doi.org/10.37285//ijpsn.2019.12.6.1.

(37) Hayat, S. M. G.; Farahani, N.; Safdarian, E.; Roointan, A.; Sahebkar, A. Gene Delivery Using Lipoplexes and Polyplexes: Principles, Limitations and Solutions. *Crit. Rev.*

Eukaryot. Gene Expr. **2019**, *29* (1), 29–36. https://doi.org/10.1615/CritRevEukaryotGeneExpr.2018025132.

(38) Lynn, D. M.; Langer, R. Degradable Poly(β-Amino Esters): Synthesis, Characterization, and Self-Assembly with Plasmid DNA. *J. Am. Chem. Soc.* **2000**, *122* (44), 10761–10768. https://doi.org/10.1021/ja0015388.

(39) Karlsson, J.; Rhodes, K. R.; Green, J. J.; Tzeng, S. Y. Poly(Beta-Amino Ester)s as Gene Delivery Vehicles: Challenges and Opportunities. *Expert Opin. Drug Deliv.* **2020**, *17* (10), 1395–1410. https://doi.org/10.1080/17425247.2020.1796628.

(40) Cheng, W.; Wu, D.; Liu, Y. Michael Addition Polymerization of Trifunctional Amine and Acrylic Monomer: A Versatile Platform for Development of Biomaterials. *Biomacromolecules* **2016**, *17* (10), 3115–3126. https://doi.org/10.1021/acs.biomac.6b01043.

(41) Chen, J.; Huang, S.-W.; Liu, M.; Zhuo, R.-X. Synthesis and Degradation of Poly(Beta-Aminoester) with Pendant Primary Amine. *Polymer (Guildf).* **2007**, *48* (3), 675–681. https://doi.org/10.1016/j.polymer.2006.12.008.

(42) Wilson, D. R.; Suprenant, M. P.; Michel, J. H.; Wang, E. B.; Tzeng, S. Y.; Green, J. J. The Role of Assembly Parameters on Polyplex Poly(Beta-amino Ester) Nanoparticle Transfections. *Biotechnol. Bioeng.* **2019**, *116* (5), 1220–1230. https://doi.org/10.1002/bit.26921.

(43) Dosta, P.; Ramos, V.; Borrós, S. Stable and Efficient Generation of Poly(β-Amino Ester)s for RNAi Delivery. *Mol. Syst. Des. Eng.* **2018**, *3* (4), 677–689. https://doi.org/10.1039/c8me00006a.

(44) Dosta, P.; Segovia, N.; Cascante, A.; Ramos, V.; Borrós, S. Surface Charge Tunability as a Powerful Strategy to Control Electrostatic Interaction for High Efficiency Silencing, Using Tailored Oligopeptide-Modified Poly(Beta-Amino Ester)s (PBAEs). *Acta Biomater.* **2015**, *20*, 82–93. https://doi.org/10.1016/j.actbio.2015.03.029.

(45) Segovia, N.; Dosta, P.; Cascante, A.; Ramos, V.; Borrós, S. Oligopeptide-Terminated Poly(ß-Amino Ester)s for Highly Efficient Gene Delivery and Intracellular Localization. *Acta Biomater.* **2014**, *10* (5), 2147–2158. https://doi.org/10.1016/j.actbio.2013.12.054.

(46) Segovia, N.; Pont, M.; Oliva, N.; Ramos, V.; Borrós, S.; Artzi, N. Hydrogel Doped with Nanoparticles for Local Sustained Release of SiRNA in Breast Cancer. *Adv. Healthc. Mater.* **2015**, *4* (2), 271–280. https://doi.org/10.1002/adhm.201400235.

(47) Fornaguera, C.; Guerra-Rebollo, M.; Ángel Lázaro, M.; Castells-Sala, C.; Meca-Cortés, O.; Ramos-Pérez, V.; Cascante, A.; Rubio, N.; Blanco, J.; Borrós, S. MRNA Delivery System for Targeting Antigen-Presenting Cells In Vivo. *Adv. Healthc. Mater.*

2018, *7* (17), 1–11. https://doi.org/10.1002/adhm.201800335.

(48) Koster, J.; Waterham, H. R. *Peroxisomes*; Schrader, M., Ed.; Methods in Molecular Biology; Springer New York: New York, NY, **2017**; Vol. 1595. https://doi.org/10.1007/978-1-4939-6937-1.

(49) Gresch, O.; Altrogge, L. Transfection of Difficult-to-Transfect Primary Mammalian Cells. In *Methods in Molecular Biology*; **2012**; Vol. 801, pp 65–74. https://doi.org/10.1007/978-1-61779-352-3_5.

(50) Pichon, C.; Billiet, L.; Midoux, P. Chemical Vectors for Gene Delivery: Uptake and Intracellular Trafficking. *Curr. Opin. Biotechnol.* **2010**, *21* (5), 640–645. https://doi.org/10.1016/j.copbio.2010.07.003.

(51) Khalil, I. A.; Futaki, S.; Niwa, M.; Baba, Y.; Kaji, N.; Kamiya, H.; Harashima, H. Mechanism of Improved Gene Transfer by the N-Terminal Stearylation of Octaarginine: Enhanced Cellular Association by Hydrophobic Core Formation. *Gene Ther.* **2004**, *11* (7), 636–644. https://doi.org/10.1038/sj.gt.3302128.

(52) Kaksonen, M.; Roux, A. Mechanisms of Clathrin-Mediated Endocytosis. *Nat. Rev. Mol. Cell Biol.* **2018**, *19* (5), 313–326. https://doi.org/10.1038/nrm.2017.132.

(53) Bus, T.; Traeger, A.; Schubert, U. S. The Great Escape: How Cationic Polyplexes Overcome the Endosomal Barrier. *J. Mater. Chem. B* **2018**, *6* (43), 6904–6918. https://doi.org/10.1039/C8TB00967H.

(54) Smith, S. A.; Selby, L. I.; Johnston, A. P. R.; Such, G. K. The Endosomal Escape of Nanoparticles: Toward More Efficient Cellular Delivery. *Bioconjug. Chem.* **2019**, *30* (2), 263–272. https://doi.org/10.1021/acs.bioconjchem.8b00732.

(55) Behr, J. P. The Proton Sponge: A Trick to Enter Cells the Viruses Did Not Exploit. *Chimia (Aarau).* **1997**, *51* (1–2), 34. https://doi.org/10.2533/chimia.1997.34.

(56) Nigam, M.; Rush, B.; Patel, J.; Castillo, R.; Dhar, P. Aza-Michael Reaction for an Undergraduate Organic Chemistry Laboratory. *J. Chem. Educ.* **2016**, *93* (4), 753–756. https://doi.org/10.1021/acs.jchemed.5b00615.

(57) Nair, D. P.; Podgórski, M.; Chatani, S.; Gong, T.; Xi, W.; Fenoli, C. R.; Bowman, C. N. The Thiol-Michael Addition Click Reaction: A Powerful and Widely Used Tool in Materials Chemistry. *Chem. Mater.* **2014**, *26* (1), 724–744. https://doi.org/10.1021/cm402180t.

(58) Takigawa, D. Y.; Tirrell, D. A. Disruption of Phospholipid Packing by Branched Poly(Ethylenimine) Derivatives. *Macromolecules* **1985**, *18* (3), 338–342. https://doi.org/10.1021/ma00145a006.

(59) Varkouhi, A. K.; Scholte, M.; Storm, G.; Haisma, H. J. Endosomal Escape Pathways

for Delivery of Biologicals. *J. Control. Release* **2011**, *151* (3), 220–228. https://doi.org/10.1016/j.jconrel.2010.11.004.

Chapter 2: 4-arm PEG-SH/C32T$_x$CR3 PBAE Hydrogels: preparation and characterization

This page is intentionally left blank

4-arm PEG-SH/C32T$_x$CR3 PBAE Hydrogels: preparation and characterization

Matching the characteristics of the wound microenvironment is critically important for successful wound healing. Wound dressings that can maintain a moist environment and form non-toxic by-products upon degradation have demonstrated to favour wound closure. Hence, it is not surprising that hydrogels have gained momentum in recent years as a viable approach to treat wounds.

In this chapter, the preparation of a family of hydrogels based on thiolated branched PEG molecules crosslinked using hydrophilic thiol-reactive PBAE polymers is described. Different formulations of hydrogels are explored by tuning the crosslinking nature and the polymer ratios. Finally, the characterization of the physicochemical properties of these formulations will inform of their suitability as a delivery platform for wound healing.

2.1. Introduction

The previous chapter described the optimisation of a new formulation of PBAE polyplexes to transfect human dermal fibroblasts. Due to the localised nature of wounds, it becomes clear that the optimal approach to deliver these nanoparticles is by using a local delivery depot, such as a wound dressing. This strategy not only maximises the efficient dose that reaches the wound, but also protects nanoparticles from degradation and enables sustained release over time. The latter is of key importance to match the temporal biology of wound healing. Finally, injectability of the wound dressing is a desired characteristic, especially when dealing with chronic wounds and ulcers. Injectable materials can adapt to irregular topologies, typical in these wounds, and maximise the contact with delivered therapeutics. Amongst the biomaterials family, hydrogels- stand out as one of the best candidates[1–4]. Their mechanical properties are similar to those of tissues, and their physicochemical nature allows them to absorb large amounts of water or biological fluids, easily mimicking human tissues with high compatibility[5–7]. Additionally, this kind of material can easily be chemically and physically modified to tune its characteristics, thus allowing the recent emergence of new smart hydrogels with a wide range of applications. Biomedical hydrogels are used as contact lenses, in cosmetics, drug delivery and other applications involving tissue engineering such as the one discussed in the present thesis[8–12].

2.1.1. Hydrogels for tissue engineering

Hydrogels are a class of materials formed by insoluble three-dimensional polymeric networks with the ability to swell by absorbing water and biological fluids, due to the predominant hydrophilic nature of the forming chains[13]. Hydrogels are easily customisable through polymer chemistry, making it possible to engineer these materials to meet specific physicochemical features. Porosity, swelling, viscosity and other mechanical properties can be finely controlled, having important implications in their behaviour and performance[14]. In this sense, hydrogels can be presented in a wide range of states from liquid-like to solid-like, and show features such as biocompatibility, low immunogenicity, controlled biodegradability and adhesion to specific substrates, among other relevant properties[5–7]. In addition to resembling tissues, hydrogels can act as scaffolds to enable cell growth, to encapsulate cells and to deliver molecules of interest, such as growth factors, genes or drugs[15–18]. More importantly, hydrogels can be engineered to be implantable or injectable in a minimally invasive manner.

Hydrogels can be classified following different criteria, but the most common way is based on the source of the hydrogel-forming polymers. The source of the polymers can be natural or synthetic depending on whether the hydrogels are derived from biologic materials or from exploiting chemical synthetic pathways using one or more kinds of monomers[19]. Natural hydrogels are commonly made of collagen, gelatin, silk fibroin or polysaccharides, among others. They present high biocompatibility and biodegradability making them suitable for cell adhesion, proliferation and regeneration. However, some polymers can trigger immune responses upon contact to the human body. They are generally poorly soluble, making difficult to add chemical modifications, and manufacturing processes tend to be costly[20–22]. In contrast, synthetic polymers such as those made of acrylic acids, acrylamides, acrylates, glycols or vinyls are easily modifiable, cost-effective, scalable and easy to manufacture. However, unreactive monomers and degradation by-products might increase the cytotoxicity[23–25]. Often, hybrid hydrogels composed of both synthetic and natural materials present as an alternative to balance these properties[6].

Another classification widely used is related to the nature of the bonds in the hydrogel structure. In this sense, hydrogels can be physical or chemical. Physical hydrogels are formed mainly by weak bonding, for example electrostatic forces between cationic and anionic polymers, hydrogen bonds, affinity or recognition of biomolecules, hydrophobic interactions, physical entanglements of polymer chains or combination of two or more of the above-mentioned. They are also called reversible hydrogels as they are formed only by non-covalent

interactions. In contrast, chemical hydrogels are formed by the crosslinking of molecules by covalent bonding, thus forming a continuous network[26]. Widely used crosslinking methods include radical polymerisation using vinyl monomers or vinyl-functionalized polymers together with a crosslinker and a radical initiator, click reactions, enzyme-mediated reactions, Michael additions or the use of Schiff-base chemistry. Moreover, some of these methods enable copolymerization of different monomers, which leads to tuneable polymers with special features like control of backbone polarity or inclusion of specific targeting moieties[23]. A summary of different crosslinking methods is shown in **Figure 2.1**.

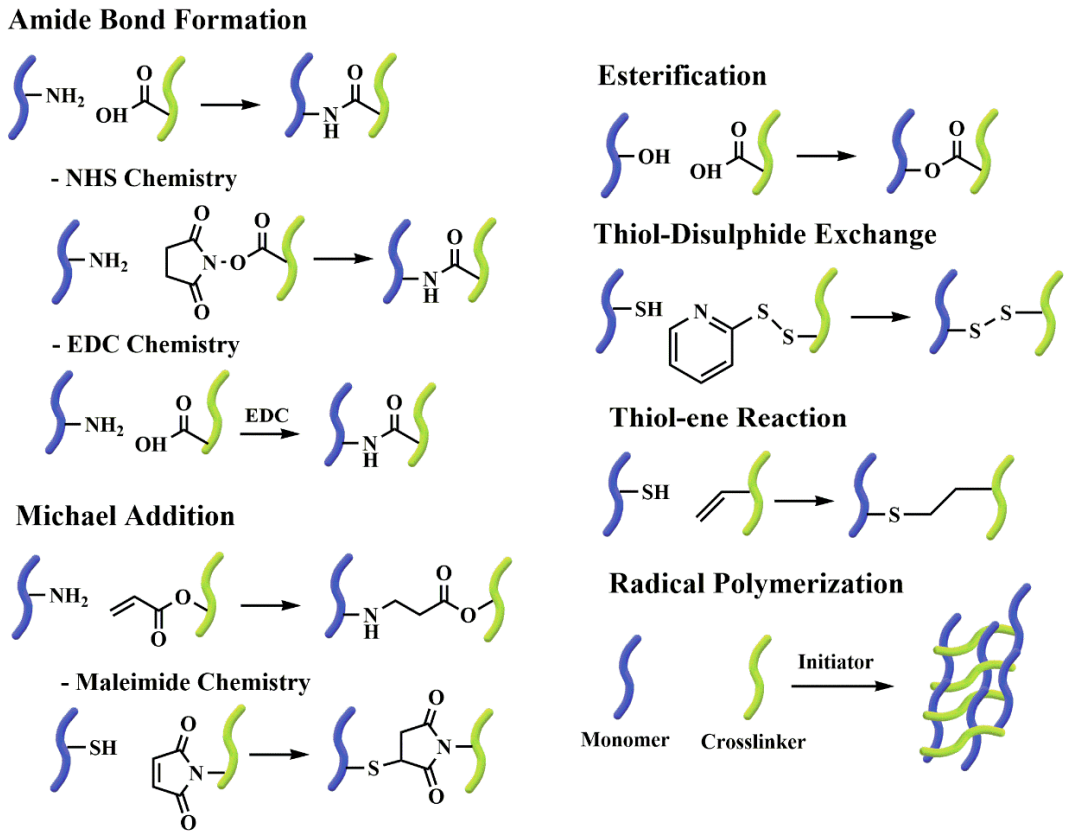

Figure 2.1. Summary of different crosslinking methods used in the formation of chemical hydrogels. Reproduced from[27] with permission from the Royal Society of Chemistry.

Overall, the nature of the polymers, the crosslinking strategies and/or the possible physical interactions between chains, along with the modifications that these can include, will dictate the micro- and macrostructure of the final hydrogel. The importance and further implications

of these properties on the hydrogel structure and behaviour are discussed in the next sections.

2.1.1.1. Porosity and swelling

The porosity of a hydrogel is the volumetric fraction of pores. Pores can be located on the surface of the material or the internal structure and they are influenced by the composition and crosslinking density of the hydrogel-forming polymeric networks. Porosity is defined with the average pore size, the pore size distribution and the pore interconnection. These parameters can be easily measured by different types of microscopies such as confocal microscopy or cryo-SEM and they play a decisive role in the mechanical properties of the hydrogel, and the absorption and effective diffusion of water or media of interest inside them[28]. Swelling is the ability to retain these liquids inside their structure. Its extent generally depends on the hydrophilicity of the hydrogel-forming polymers, the crosslinking density and the porosity. Interestingly, these parameters are directly implicated in the biodegradability. From the moment of swelling, the network can start to disintegrate and dissolve at a specific rate if it is formed by degradable bonds[29]. One of the methods that is widely used to measure the swelling ratio consists of measuring the ratio of weights before and after swelling[30,31].

Therefore, the characterization of swelling is highly important, since this parameter will also affect the permeation of water, nutrients and drugs, but also the rate of degradation of the material, the mechanical behaviour, and hence the release of the therapeutic agents entrapped.

2.1.1.2. Mechanical properties

Mechanical properties of biomaterials define their suitability for a particular application. For example, depending on the timescale of the intended biological process, hydrogels might require rapid or slow degradation, and depending on the tissues and organs in contact, they may need to withstand compressive or tensile forces without failing[32–34]. Matching mechanical properties is especially important when in contact with tissues, since cells surrounding the material can undergo specific differentiation into other lineages through a process called mechanotransduction[35]. Rheological properties, measured by rheometry, are the most informative and relevant to understand biomedical hydrogels[36]. The main rheological technique to characterize hydrogels is small-amplitude oscillatory shear (SAOS). The hydrogel is located between two disks (or between a disk and a cone) and a small-amplitude torsional oscillation is applied generating a shear flow in the sample[36]. This technique provides

the values of storage modulus (G') and loss modulus (G''). Storage modulus is a parameter that measures how much energy can be elastically stored by the hydrogel, giving a measure of the solid-state behaviour of the sample. On the other hand, the loss modulus is the quantification of the energy lost or dissipated by the material, representing the liquid-state behaviour. These two moduli can be inferred from the plateau zone in the G' or G'' versus strain graph, the linear viscoelastic region (LVR), where the hydrogel structure is stretched but not damaged. Hydrogels showing higher values of G' than G'' present a behaviour that is more similar to a solid than a liquid, also known as viscoelastic behaviour. In contrast, a G'' higher than G' indicates a more liquid-like behaviour. Hence, hydrogel formulations with higher G' values will be stiffer. Once the stress is withdrawn, the energy stored elastically is used by the material to return to its initial form. Moreover, formulations generally increase the storage modulus when increasing the degree of crosslinking. Once the internal structure of the hydrogel is starting to break, G' falls abruptly and G'' increases, meaning the energy applied cannot be stored anymore and it is dissipated. This technique also allows to study the gelation time of a formulation, the entanglement, glass transition and some other details of the chain architecture[36,37].

Other techniques used to characterize mechanical properties of hydrogels are tensile testing, compression testing or indentation. In tensile tests, two grips hold a strip of the hydrogel and a tensile force is applied. Stress-strain data is provided by the equipment and it can be used to calculate the Young's modulus, yield strength or the ultimate tensile strength[24]. A hydrogel that is going to be implanted or injected in a zone that experiments compressive forces must be characterized using compression tests. The sample is located between two plates and compressive forces are applied[24]. The measurement of the compression distance is then used in theoretical models to obtain values for stiffness and the Young's modulus. Finally, the hardness of a hydrogel to deformation can be measured by indentation[33].

There is a considerable number of properties and mechanical parameters that can be characterized in hydrogels. These are mainly affected by the swelling, the porosity, and the crosslinking rate, which, in turn, can be controlled by tuning the physicochemical properties of the polymers forming the hydrogel. In the next section, the requirements that hydrogels must meet for an appropriate performance in wound healing are reviewed.

2.1.1.3. Hydrogels in wound healing

Wound dressings (alone or in combinations with drugs like antibiotics) are the preferred approach for treating chronic wounds. When engineering new dressings to promote healing, mimicking some of the wound site characteristics presents some key advantages. It is widely known that the moisture in the wound is one of the most important[38–40]. A moist environment facilitates the migration of epithelial cells, protecting them from dehydration and scab formation and enhancing their viability, thus providing the most favourable environment for the growth of new tissue. Additionally, a good influx of oxygen increases fibroblast migration, replication and the collagenous dermal matrix synthesis and posterior remodelling. The ability of hydrogels to absorb and retain biological fluids makes them optimal candidates to promote and maintain moisture in the wound site.

In view of the above, an ideal wound dressing should cover the wound site and protect it while maintaining a moist environment, allow the exchange in and out of gases such as oxygen, water vapour and carbon dioxide[41,42]. Additionally, it should serve as a barrier to bacteria and absorb the excess of exudate to avoid contamination and prevent maceration of the adjacent skin[40,43]. In terms of manipulation, it should be free of toxic or particulated components and its removal must be non-traumatic[44]. In the recent years, and thanks to advances in tissue engineering, a vast number of new materials have been proposed to treat different kinds of both acute and chronic wounds. Strategies ranging from the application of ointments to the implantation of skin grafts have been described[45,46]. However, the complexity of the tissue repair process requires the use of materials that can perform a wide range of functions to meet the requirements previously mentioned. Hydrogels possess high versatility to meet such conditions. Their capability to absorb liquids allows them to hydrate the wound and help in autolytic debridement, facilitating the wound cleaning[47–49]. Additionally, this also aids to a correct granulation and epithelization, allowing the activation and optimal functioning of growth factors, cells and enzymes. In fact, hydrogels have been shown to absorb exudates and promote cell migration[50]. They are easy manipulated and handled by nurses and they have a cooling and soothing effect in painful ulcers[46]. Moreover, hydrogels are easy to modify to acquire tuneable features, enabling their use as delivery platforms of drugs, growth factors or genes, among others. Furthermore, polymers such as PEG present antibacterial activity[51]. In fact, the latter polymer has been widely used in wound healing applications. For example, Xu *et al*[52] presented an injectable hydrogel formed by crosslinking hyperbranched multi-acrylated PEG macromers using thiolated hyaluronic acid. In their work, this hydrogel was used to deliver stem cells in order to treat diabetic foot ulcers showing an enhanced wound

healing in diabetic murine animal model. A branched PEG was also used by Hao *et al*[53] for the preparation of hydrogel/adhesives as liquid first-aid for trauma emergency. In this case, the PEG containing aldehyde groups was crosslinked using polyethyleneimine *via* Schiff base reaction. The material showed a high adhesive strength and excellent antibacterial ability and fast haemostatic capacity both *in vitro* and *in vivo*. Other examples of hydrogels commonly used in wound healing are those based on methacrylated gelatin[54,55], chitosan[56,57], alginate[58,59] or polyvinyl alcohol[60,61]. Given the ideal combination of properties that hydrogel offer, it is not surprising that several hydrogels have been commercially approved in the last few years (e.g., AquaDerm™, ActivHeal®, Suprasorb® or Purilon®), further reinforcing the fact that they are one of the best options to treat wounds[62,63].

In this chapter, we designed a family of injectable hydrogels, that meets the general requirements for optimal wound healing reviewed previously, based on thiolated 4-armed PEG molecules crosslinked with thiol-reactive hydrophilic PBAE C32CR3. These starting materials show interesting characteristics such as biocompatibility, biodegradability and, in the case of PEG, antibacterial properties. The main objective in this chapter is to produce hydrogels that can incorporate PBAE polyplexes optimized in the previous chapter, protecting them from degradation and enabling their sustained release over time. We hypothesize that having the same polymer in the hydrogel's network as in the polyplexes (i.e., PBAE) will stabilize the nanoparticles and keep them therapeutically active for longer. The release kinetics of polyplexes entrapped in the hydrogel structure is highly dependent on the degradation profile. Hence, several formulations of these hydrogels are explored by changing the polymers ratio or nature of crosslinking (physical entanglement or chemical crosslinking). The preparation of the hydrogel-forming PBAEs will be discussed first in this chapter, followed by the development and characterisation of the different PBAE-PEG hydrogel formulations. The encapsulation of the PBAE polyplexes in the hydrogel and the release kinetics studies will be discussed in the next chapter.

2.2. Materials and methods

The reagents and solvents used in the synthesis were obtained from Sigma–Aldrich and Panreac and used as received unless otherwise stated. Oligopeptides were purchased from Ontores Biotechnologies Inc. including TFA as a counterion, but they were used as hydrochloride salts (detailed conversion in the section *Materials and methods* in Chapter 1). HDFs from adult skin was purchased from ATCC (ATCC PCS-201-030). Cell culture medium, supplements and other compounds used in tissue culture (DMEM, PBS, glutamine, penicillin−streptomycin solution and trypsin-EDTA 0.25 %) were obtained from Gibco, Hyclone, and Invitrogen. ^{1}H-NMR spectra were recorded in a 400 MHz Varian (Varian NMR Instruments, Claredon Hills, IL, USA) and methanol-d_4 was used as solvent unless otherwise stated.

2.2.1. Synthesis and characterization of C32 PBAE backbones

The initial step to prepare the hydrogel is to synthesize the hydrogel-forming polymers. For that purpose, two PBAE formulations based on the hydrophilic C32CR3 polymer are used in the present work. Hence, only the acrylate-ended C32 backbone is needed (**Scheme 2.1. A**). Details on its synthesis are found in the previous chapter. Briefly, the C32 backbone is obtained after mixing 5-amino-1-penthanol (7.7 g, 75 mmol) and 1,4-butanediol diacrylate (18 g, 82 mmol) at 90 ºC for 20 h. A characterization by ^{1}H-NMR confirmed the success of the reaction and the number of repeated units of the polymer, being n = 7.

2.2.2. Synthesis and characterization of C32T and C32T$_2$ PBAE backbones

As it was mentioned previously, the hydrogels studied in this work consist of the crosslinking of 4-arm PEG-SH molecules using C32CR3 PBAEs. Hence, PBAE chains must react with the thiol groups of the PEG molecules. For that reason, the C32 backbone synthesized must be modified adding a thiol-reactive moiety (C32T$_x$, where x is the number of the thiol-reactive groups per polymer chain). The thiol-reactive group used in the present work is the 3-(2-pyridyldithio)propanoic (SPDP) acid (see **Scheme 2.1. A**). To prepare this organic acid, the solution must be systematically purged using argon and protected from light. Aldrithiol-2 (1 g, 4.46 mmol) is dissolved in a flask with ethanol and, then, glacial acetic acid (0.134 mL) is added dropwise to the solution while stirring. Finally, the 3-mercaptopropionic acid (0.237 g, 2.23 mmol) is added and the mixing is allowed to react for 2 h at room temperature. The resulting product must be purified by column chromatography. Specifically, the column is

packed using basic activated alumina as the stationary phase and a solution formed by dichloromethane/ethanol/acetic acid in a 60:40:1 proportion as the mobile phase.

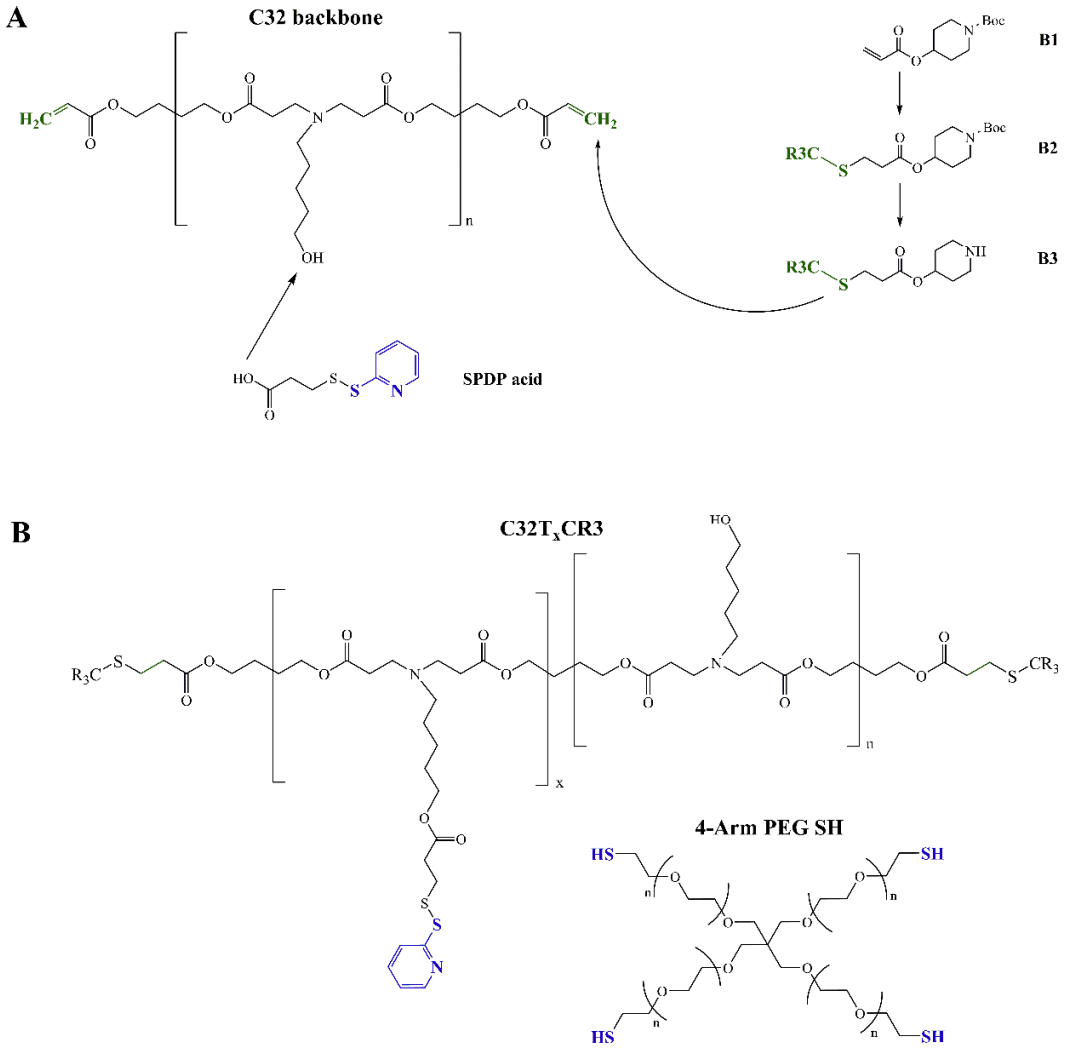

Scheme 2.1. Schematic representation of the synthesis (A) of the different hydrogel-forming polymers used in the present thesis (B).

Typically, impurities present a yellowish colour and leave the column first. The rest of the fractions are collected and the solvent is eliminated using a rotary evaporator to unveil a white product (SPDP acid). The incorporation of the SPDP moieties to the C32 polymer occurs by esterification reaction between the SPDP carboxylic acids and the hydroxyls of the PBAE, process known as Steglich esterification. The quantity of SPDP groups per chain is controlled

by the molar quantities used in the reaction thus obtaining the formulations explored in the present thesis, the C32T and the C32T$_2$ depending on whether the C32 backbone presents one or two SPDP groups, respectively. For the C32T backbone, the C32 polymer (1 g, 0.4 mmol), SPDP (0.130 g, 0.6 mmol) and a spatula tip of 4-dimethylaminopyridine (DMAP) are dissolved in anhydrous dichloromethane. The solution is cooled for 30 min at 4 ºC. At that very moment, N,N'-dicyclohexylcarbodiimide (DCC) (0.155 g, 0.75 mmol) is added and the solution is allowed to react at room temperature overnight, always keeping the mixture in an inert atmosphere and protected from light. Finally, to precipitate and separate the DCC salts after the reaction and obtain the pure product, the mixing is dissolved in a solution of acetonitrile/ethyl acetate in a 1:1 ratio and kept at 4 ºC for 3 h. In the case of the C32T$_2$, the same synthetic pathway is followed, but altering the C32 to SPDP ratio (1 g, 0.4 mmol and 0.215 g, 1.0 mmol, respectively) and DCC (0.250 g, 1.2 mmol). The C32T$_x$ backbones are characterized by ^{1}H-NMR and the ratio of the integrals of signals of the terminal acrylates at δ = 5.8 – 6.4 ppm and the thiopyridyl group at δ = 7.0 – 8.5 ppm is used to quantify the number of SPDP groups per chain.

2.2.3. Synthesis and characterization of CR3 oligopeptide-modified C32T and C32T$_2$ PBAE polymers

The PBAEs used to form the different hydrogel formulations are C32TCR3 and C32T$_2$CR3.The acrylates of the PBAE backbones C32T and C32T$_2$ synthesized above are therefore modified using the oligopeptide CR3. However, this oligopeptide is conjugated to the acrylate groups in the polymer through a terminal thiol and therefore can also react with the thiol-reactive SPDP, decreasing the number of these moieties available to form the hydrogel with the 4-arm PEG-SH. Hence, the oligopeptide CR3 is modified to prevent this reaction and favour Michael addition to the terminal acrylates. First, 1-boc-4-hydroxypiperidine (100 mg, 0.50 mmol) and triethylamine (0.115 mL, 0.80 mmol) are dissolved in dichloromethane and cooled to 0 ºC. Then, acryloyl chloride (0.044 mL, 0.52 mmol) is added. The mixture is stirred overnight at room temperature to obtain the product B1 (**Scheme 2.1. A**). This product is washed with water and a saturated solution of sodium bicarbonate in a separatory funnel and finally dried under vacuum. The product B1 (90 mg, 0.24 mmol) and the CR3 peptide (200 mg, 0.33 mmol) are dissolved separately in 0.5 mL of DMSO and mixed dropwise. The solution is stirred overnight at room temperature to protect the thiol of the cysteine. The residue obtained is precipitated by adding this mixture dropwise to a solution of diethyl ether/acetone at a ratio 4:1 and centrifuging at 4,000 rpm for 10 min to isolate the compound B2 (**Scheme 2.1. A**). Finally, the boc group of the B2 compound must

be removed to form the compound B3. This occurs dissolving the B2 (100 mg, 0.110 mmol) in a TFA (0.483 mL) and dichloromethane (0.887 mL) solution. The mixing is stirred for 4 h at room temperature and dried using the rotary evaporator. The resulting oil is dissolved in a solution of dichloromethane/methanol at a 5:1 ratio and passed through an Amberlyst A21 column. The oil obtained is again concentrated under vacuum to obtain the compound B3 (**Scheme 2.1. A**) and reacted immediately with the desired C32T$_x$ polymer, in a polymer to B3 molar ratio of 1:2.5. The structure of the CR3-modified PBAEs C32TCR3 and C32T$_2$CR3 were confirmed by ^{1}H-NMR.

2.2.4. 4-arm PEG-SH/C32TCR3 hydrogel formation

Hydrogel matrix formation occurs by the crosslinking of 4-arm PEG-SH molecules (Mn = 5,000) with C32T$_x$CR3 PBAE in different PEG/PBAE ratios (**Scheme 2.1. B**). For the formation of this hydrogel, the 4-arm PEG-SH and C32TCR3 were separately dissolved in DMSO at a concentration of 250 mg/mL. An aliquot of the PBAE solution was added over an aliquot of the PEG solution to achieve the desired PEG/PBAE molar ratio after mixing. The solution was mildly vortexed and incubated at room temperature for a minute. Then, the mixture was frozen at -80 ºC for an hour and immediately lyophilized overnight. The residue obtained was reconstituted with water to form the hydrogel. PEG/PBAE molecular ratios prepared were 1:1, 1:2 and 1:4.

2.2.5. 4-arm PEG-SH/C32T$_2$CR3 hydrogel formation

The C32T$_2$CR3 polymer, with two thiol-reactive thiopyridyl groups per chain, allows the chemical crosslinking forming a continuous polymeric network in situ. For its preparation, a similar procedure is followed. The 4-arm PEG-SH and C32T$_2$CR3 were separately dissolved in DMSO at a concentration of 500 and 250 mg/mL, respectively. The PBAE solution is added over the PEG solution achieving a specific PEG/PBAE ratio after mixing. The mixture is mildly shaken and incubated at room temperature for 30 min. As an exception, the freeze-drying step is not necessary since the hydrogel is formed in situ when mixing the starting solutions and reconstituting with water after the incubation time. Additionally, each sample must be washed with deionized water five times to fully eliminate DMSO traces. The hydrogels prepared present a PEG/PBAE molecule ratios of 1:1 (HG11, one PEG is cross-linked with one linear C32T$_2$CR3) and 1:4 (HG14, a PEG molecule is cross-linked using four C32T$_2$CR3 PBAE).

2.2.6. Hydrogel degradation

The hydrogel formulations to test are HG11 and HG14. They are prepared following the previous protocols, but the polymer C32T$_2$CR3 is tagged with fluorescein in a percentage of 2.5 % or 5.0 % (w/w) for the formulation HG11 and HG14, respectively. Each sample is immersed in 200 µL of PBS (1x) and incubated at 37 ºC. The supernatant is collected and the fluorescence intensity is measured using a Tecan Infinite 200 PRO plate and cuvette reader at each timepoint. The 200 µL of solution collected are replaced by the same volume of fresh PBS solution. The degradation is followed by tracking the loss of fluorescence of each replicate at each timepoint and the hydrogel integrity is calculated using these values relative to the total fluorescence.

2.2.7. Swelling ratio

Hydrogel formulations HG11 and HG14 are prepared in duplicates for each swelling experiment. Specifically, the swelling is studied following two drying procedures. The first one consists in drying the samples at 37 ºC for 24 h in a lab oven whereas in the other alternative method the samples are frozen at -80 ºC and lyophilized overnight. After each drying method, the samples are weighed. Then, the hydrogel formulations are immersed in 1 mL of Milli-Q water for 30 min. The samples are squeezed occasionally using tweezers to facilitate a complete water absorption. Swollen hydrogels are weighed and the swelling ratio is calculated using the **Equation 2.1.**:

$$Swelling\ (\%) = \frac{Ws\text{-}Wd}{Wd} \cdot 100$$

Equation 2.1. Swelling ratio

W_s and W_d represent the weight of the swollen and the dried hydrogel, respectively.

2.2.8. Confocal microscopy characterization

Confocal microscopy is used to study the porosity of the formulations HG11 and HG14. Hydrogels are prepared using a C32T$_2$CR3 polymer tagged with fluorescein isothiocyanate (FITC) in a 0.5 % proportion (w/w). Samples are prepared as detailed in the previous sections, immersed in optimal cutting temperature compound (OCT) and frozen at -80 ºC overnight. The hydrogels are sliced with a cryotome obtaining slices of 25 and 50 µm thickness. The

slices are imaged using a Leica SP8 confocal microscope (Leica Microsystems). Image processing and pore size distribution are done with ImageJ-Fiji software.

2.2.9. Scanning Electron Microscopy characterization

The hydrogels studied are prepared as described above. The different samples are frozen at -80 ºC and freeze-dried overnight. No sputtering is used to coat the samples prior to visualization and imaging.

2.2.10. Hydrogels rheological characterization

Formulations HG11 and HG14 are prepared and used immediately in the mechanical testing. The storage (G') and loss (G'') moduli are measured as a function of the strain at 25 ºC with the rheometer Ar2000ex (TA Instruments) using 8 mm cross-hatched plate. Depending on the sample a different gap value was set maintaining an initial normal force used was 0.1 N.

2.2.11. Cytotoxicity of the degradation products

Hydrogels HG11 and HG14 triplicates are prepared as described above. The samples are immersed in 1 mL of supplemented culture medium without FBS and incubated at 37 ºC. At 24, 72 and 168 h timepoints, three aliquots of 200 µL per sample were collected and replaced with fresh medium. The reagents used to form these formulations are also dissolved separately in culture medium using the same quantity as used in the hydrogels. Before using the aliquots, 10 % FBS is added to each sample. In this experiment, fibroblasts are seeded at a 10,000 cells per well density in a 96-well plate. Cells are grown using the collected 200 µL aliquots containing the degradation products of the hydrogels or the starting reagents. Cell viability assays are performed using Presto Blue reagent (Invitrogen) at 24 h following the manufacturer's instructions.

2.2.12. Statistical Analysis

GraphPad Prism 8.0.1 software was used for the statistical analysis. Statistical differences between groups were studied by ordinary one-way ANOVA with post-hoc Tukey HSD test. The significance of the difference in the data is *$p < 0.05$, **$p < 0.01$, ***$p < 0.001$, and ****$p < 0.0001$.

2.3. Results and discussion

The formation of the different hydrogel formulations studied occurs by crosslinking commercially available PEG molecules that present four thiolated arms using the PBAE C32CR3. For that, the C32 backbone is modified to incorporate the thiol reactive group SPDP. This chapter will start with the preparation of hydrogel-forming PBAEs, followed by the design and characterisation of PBAE-PEG hydrogels.

2.3.1. Synthesis and characterization of CR3 oligopeptide-modified C32TCR3 and C32T$_2$CR3

Two different thiol-reactive C32CR3 are used in the present work, the C32TCR3 with only one SPDP group per chain, and the C32T$_2$CR3 with two SPDP groups. The structure of the synthesized polymers, the incorporation of the oligopeptides and the number of SPDP per chain were confirmed by ^{1}H-NMR. As an example, the C32T$_2$CR3 spectra are collected in **Figure 2.2.** The first step is the addition of the SPDP groups to the C32 backbones. The signals produced by this moiety are highlighted in blue in **Figure 2.2. A.** The terminal acrylates of the PBAE backbone can also be seen highlighted in green. The ratio between the integral value of a proton in the SPDP group and a proton in the acrylate was calculated to obtain the number of SPDP groups added per chain. Finally, the obtainment of the C32T$_2$CR3 polymer was confirmed in **Figure 2.2. B.** In this case, it can be seen how the acrylates' signals disappears, meaning that the addition of the CR3 oligopeptide occur in both ends of the polymer. Moreover, the SPDP signals are still present. The number of SPDPs per chain was calculated again after the addition of the oligopeptides. However, since the acrylates' signals have been substituted, the ratio is now obtained dividing the integral value of a proton in the SPDP group by the integral value of a proton outside the repeated unit of the polymer. The PBAEs synthesized were used after the successful modifications of the acrylates and the correct number of SPDPs were confirmed by this technique.

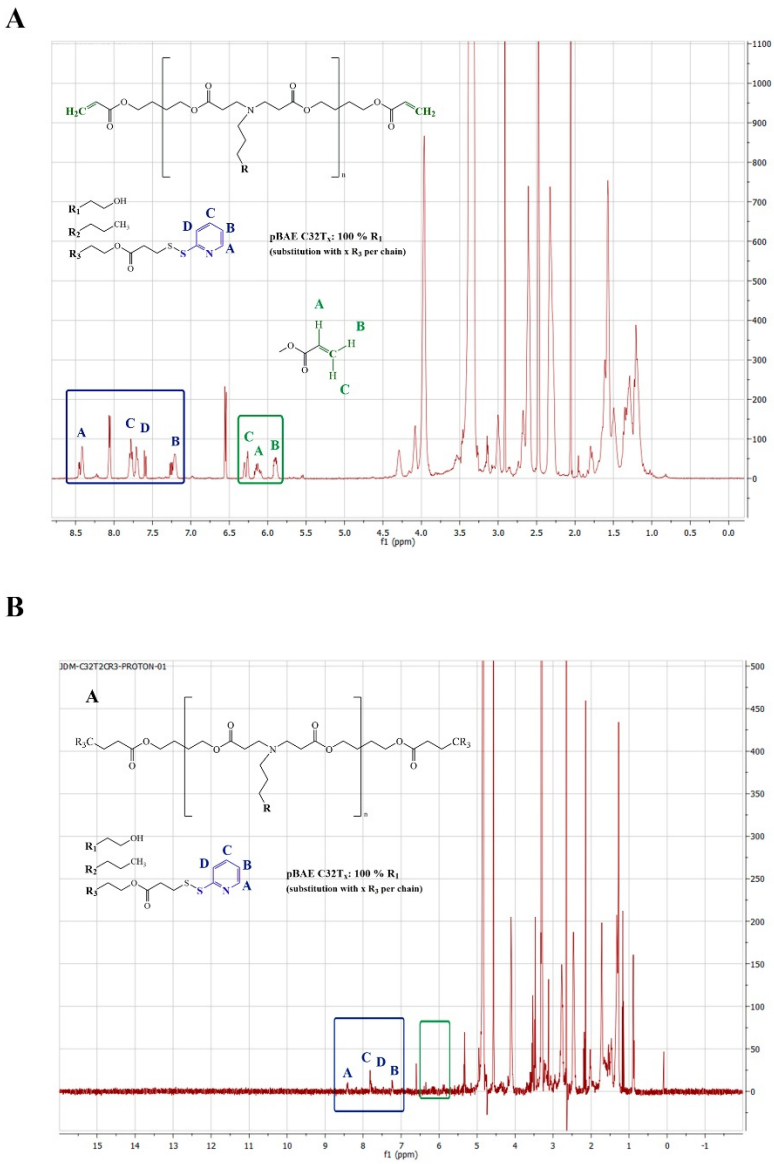

Figure 2.2. ^{1}H-NMR spectra of the A) C32T$_2$ backbone and B) C32T$_2$CR3 polymer. Blue square: thiopyridyl signals; Green square: acrylates signals.

2.3.2. Formation of hydrogels 4-arm PEG-SH/C32TCR3 and 4-arm PEG-SH/C32T$_2$CR3

Different hydrogel formulations are prepared with the goal of studying their formation, characteristics and mechanical properties, to guarantee the optimal performance for the intended application (**Table 2.1.**). Two general families are prepared depending on whether a physical or a chemical hydrogel is formed. The physical hydrogels were formed by reacting 4-arm PEG SH molecules with the C32TCR3 polymer. Since the PBAE has only one thiol-

reactive SPDP group, the network formed is not continuous (there is no covalent crosslinking leading to three-dimensional structures). This means that the hydrogel is formed mostly by physical interactions (e.g., hydrogen or Van der Waals bonding) or entanglement of the polymeric chains. Hence, we hypothesise that this group of formulations should present a more rapid degradation, suitable for a complete nanoparticle release in a few hours to days. The physical hydrogel formulations studied had PEG/PBAE molecular ratios of 1:1, 1:2 and 1:4, meaning that one 4-arm PEG-SH molecule reacts with one, two or four C32TCR3 molecules. It must be highlighted that physical hydrogels were formed after lyophilising the mixing and reconstituting the resulting solid with water. The ideal hydrogel-based wound dressing should effectively deliver the cargo in a sustained manner over time, and in a time frame that matches the healing process (2-10 days depending on the phase of wound healing). These hydrogel formulations degraded completely in a few hours at 37ºC, and hence are not good candidates for this application. Other drawbacks of fast degradation and nanoparticle release is the lack of control over the dosage delivered to the wound and the increase in cytotoxicity to cells in the wound. Moreover, fast release led to high experimental variability, with replicates of the same sample showing different behaviours. Lyophilised products, like the physical hydrogel described herein, present clear advantages in terms of manufacture and distribution. However, and given the irregular topology of chronic wounds, injectability (not provided by the physical hydrogel developed) is a more desired property to maximise the contact area with the wound surface. For these reasons involving the fabrication process, the performance and the translational aspect, these formulations must be discarded. Alternatively, chemical hydrogels were formed by crosslinking the PEG molecules with the PBAE C32T$_2$CR3. This PBAE presents two thiol-reactive groups thus forming a continuous, three-dimensional, covalent network. The PEG/PBAE ratios studied for this family of hydrogels are 1:1 and 1:4, where thiol groups are in 2-fold excess of thiol-reactive groups or thiol-reactive groups are in a 2-fold excess of thiol groups, respectively. From now on, these two formulations will be referred as HG11 and HG14. The formation was confirmed visually (**figure 2.3. A and B**) and by ^{1}H-NMR, after the leaving group of the SPDP moiety (pyridine-2-thione) signal disappears (**figure 2.3 C.**).

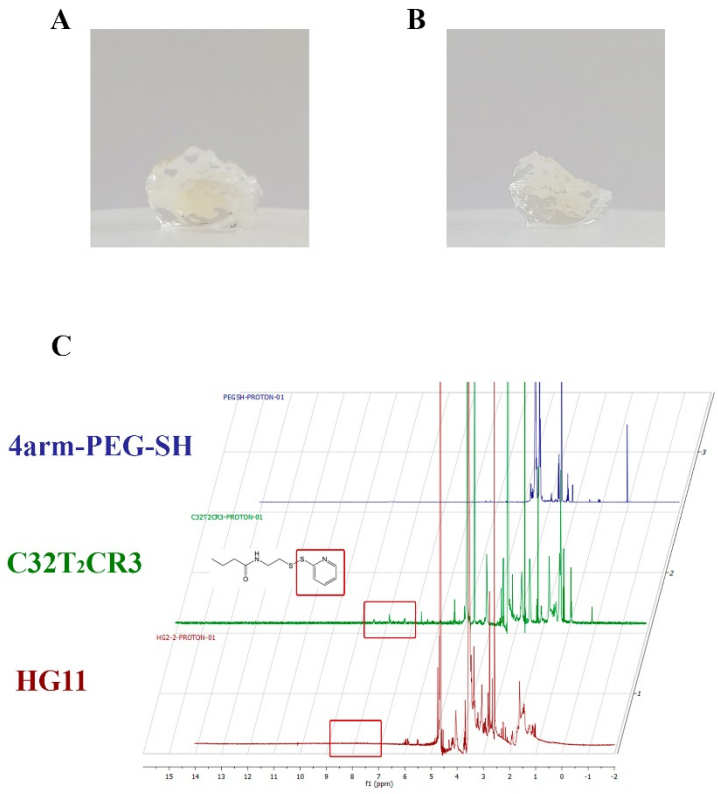

Figure 2.3. Images of the formulation A) HG11 and B) HG14 and C) ^{1}H-NMR spectrum confirming the HG11 formation.

Table 2.1. Details on the hydrogel formulations studied in the present work.

Name	PBAE	PEG/PBAE molecular ratio	Formation	Comments
HG$_{phys}$11	C32TCR3	1:1	Physical	Redissolved in a few hours
HG$_{phys}$12	C32TCR3	1:2	Physical	Redissolved in a few hours
HG$_{phys}$14	C32TCR3	1:4	Physical	Redissolved in a few hours
HG11	C32T$_2$CR3	1:1	Chemical	Formation in situ, adapts the shape of the container
HG14	C32T$_2$CR3	1:4	Chemical	Formation in situ, adapts the shape of the container

2.3.3. Structure, degradation and mechanical characterization

The behaviour and performance of a material in an *in vitro* or *in vivo* setting are determined by its physicochemical and mechanical properties. As discussed earlier, physical hydrogels present suboptimal properties, making them unsuitable for wound healing applications. Hence, only chemical hydrogels' formulations HG11 and HG14 will be studied in detail in this section.

The first characteristic tested was the swelling ratio of both formulations, following the protocol described in the *Materials and Methods* section, after drying the samples in a lab oven or through lyophilization. Interestingly, HG11 and HG14 swelling ratios were similar when hydrogels were subjected to the same drying method (**Figure 2.4.**), indicating the PEG/PBAE ratio does not have an impact in the swelling ratio. However, the drying method considerably influenced this parameter, with swelling ratios of around 2.5% and 15% for both formulations after oven-drying or lyophilization, respectively. This can be explained by the efficiency in the extraction of water, which is superior in the case of the lyophilization. In contrast, the oven-drying method is more likely to leave water molecules trapped inside the hydrogel networks, which result in a decrease of the swelling ratio after application of **Equation 2.1**.

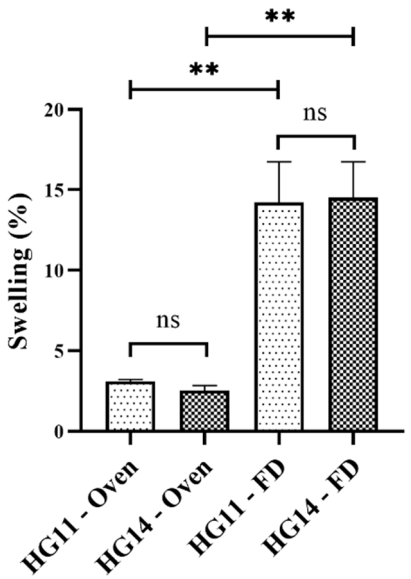

Figure 2.4. Swelling ratio of formulations HG11 and HG14 after an oven-drying (Oven) or freeze-drying process (FD) (n=2).

To better understand the behaviour of the hydrogel formulations, the microstructure and porosity were studied next. HG11 and HG14 samples were prepared with a fluorescent tag following the protocols described, frozen at -80ºC and cryosectioned. The slices were imaged by confocal microscopy. The formulation HG11 presented pores that were uniformly distributed throughout the slice, with sizes that varied from 5 to 100 µm (**Figure 2.5. and Figure 2.6 A**), while HG14 hydrogel showed pores ranging from 1 to 1,000 µm (**Figure 2.5. and Figure 2.6 B**). It can be observed that this latter formulation presents a higher portion of smaller pores, due to the increase in crosslinking caused by a 4-fold more PBAE than PEG. As a result, the median pore sizes are 16.9 µm and 7.6 µm for the formulations HG11 and HG14, respectively. However, despite presenting a distinct pore size distribution, the average pore sizes are not statistically significantly different (17.9±8.0 and 17.6±35.9 µm for the HG11 and HG14 formulations, respectively). This correlates with the similarity obtained in the swelling ratio values. The increase in crosslinking density in the HG14 formulation produces a tighter microstructure with smaller pores, and hence lower swelling ratios would be expected. However, the presence of much larger pores in HG14 formulation, not observed in HG11 formulation, increases the water contact surface, increasing in turn the swelling ratio to similar values than those obtained for formulation HG11[64,65].

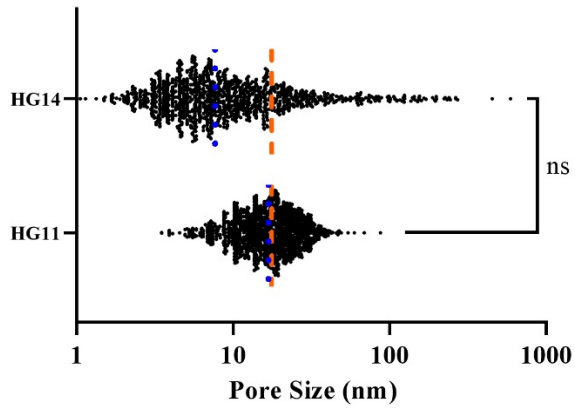

Figure 2.5. Pore size distribution of hydrogels HG11 and HG14. Orange bar: mean; blue bar: median.

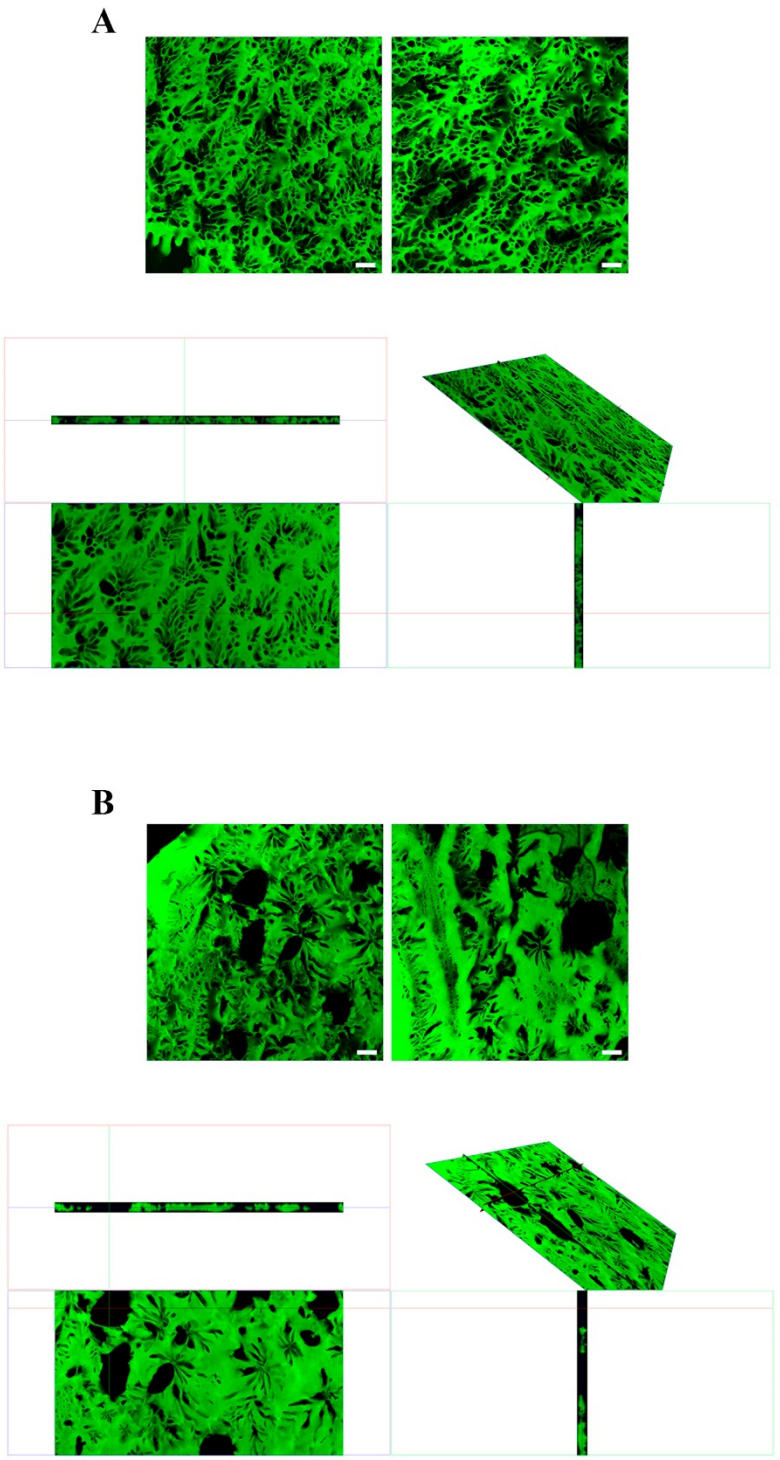

Figure 2.6. A) and B) Confocal microscopy images and 3D reconstruction of 50 µm thickness slices of HG11 and HG14 formulations, respectively. Scale bar: 100 µm.

Due to the important implication of the porosity in the degradation of hydrogels, this parameter was studied next. Hydrogels were tagged with fluorescein and the degradation was tracked by fluorescence loss (as a surrogate measurement for weight loss). Once all the fluorescence values were obtained, the integrity of the formulations was calculated as described in the *Materials and Methods* section. As it can be seen in **Figure 2.7.**, HG11 formulation was completely degraded after 8 days whereas HG14 hydrogels lasted 15 days. Interestingly, the initial burst of degradation was more pronounced in the formulation HG11 than in the HG14, representing a loss of integrity of 37% and 15%, respectively. This correlates with the smaller median pore size and higher crosslinking density for HG14 formulation compared to HG11 (**Figure 2.5.**). After a few days, the bigger pores of the HG14 formulation (presenting larger sizes than those of HG11 formulation) caused a more pronounced loss of integrity, leading to HG14 hydrogels to break into large pieces.

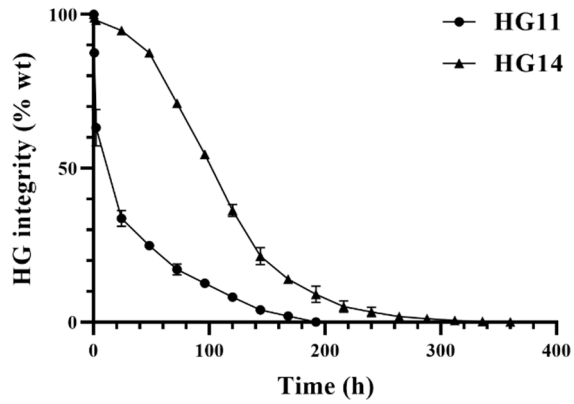

Figure 2.7. Degradation of hydrogels HG11 and HG14 in % of the hydrogel integrity (n=3).

Rheological characterization was performed to obtain the storage and loss moduli (**Figure 2.8. A and B**). Though the morphology of the samples gave generally unstable G'' values, G' was higher for both formulations, hence confirming a viscoelastic behaviour of the hydrogels. Formulation HG14 showed higher G' values than HG11, meaning that HG14 samples can store more energy elastically. After the linear viscoelastic region, G' decreases slowly due to the inability to store this energy elastically, suggesting the development of microfractures that can grow to produce cracks. In fact, the samples of the HG14 formulation appeared broken after rheometry testing. This is likely due to their large pores, as observed by confocal microscopy, facilitating points of increased stress levels that may lead to the creation and

propagation of fractures. This also means that despite HG14 presenting higher initial values of G', this formulation is more brittle. SEM imaging (**Figure 2.9.**) confirmed this hypothesis, as several cracks were observed in HG14 structure after the lyophilization process required to prepare the samples for imaging. It must be remarked that the SEM images were only used for this purpose and not to study their structure or pore sizes, since the samples collapse after the freeze-drying, losing the original morphology.

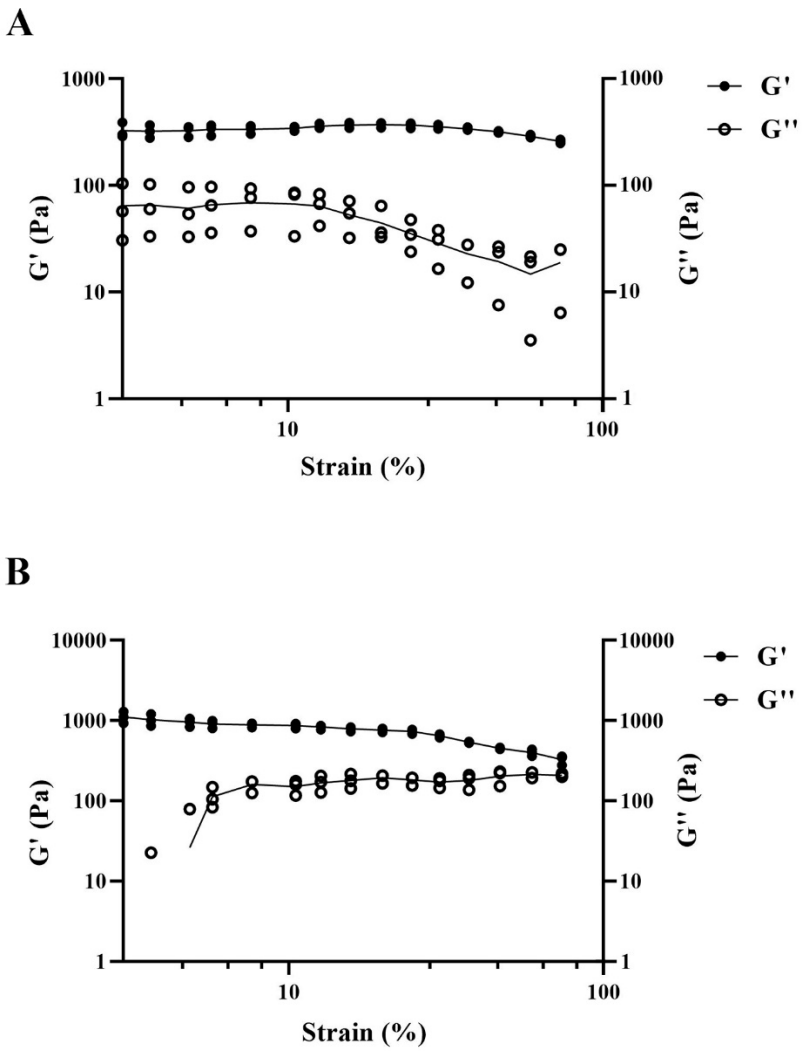

Figure 2.8. A) and B) G' and G'' versus strain (%) of formulations HG11 and HG14, respectively (n=3).

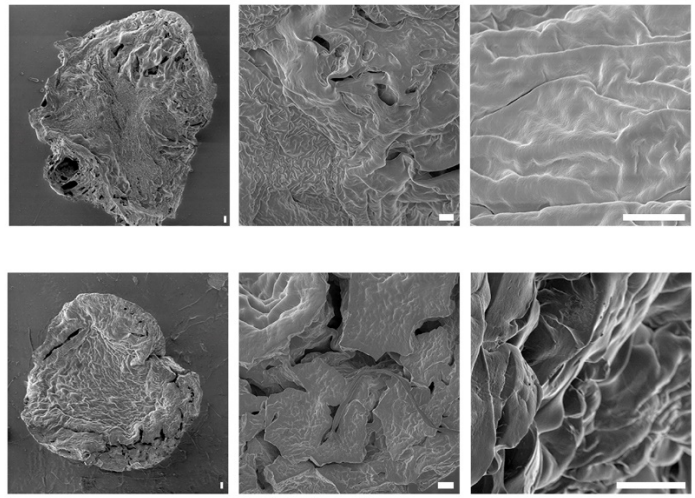

Figure 2.9. SEM images of up: HG11 formulation and; down: HG14 formulation. SEM scale bar: 50 µm.

Formulations HG11 and HG14 have presented substantial differences in terms of morphology and internal microstructure leading to distinct mechanical behaviour and degradation kinetics. However, their performance as wound dressings is not limited to these properties. For example, a high toxicity might compromise the efficacy of the treatment. In this sense, the next section will explore how hydrogel degradation by-products affect fibroblasts viability.

2.3.4. Cytotoxicity of the degradation products

The cytotoxicity of the materials was studied measuring the viability of human dermal fibroblasts after 24 hours in media containing the degradation by-products of the hydrogels released at the time intervals 0−24 h, 24−72 h, and 72−168 h, as described in the *Materials and Methods* section. The starting reagents of the hydrogel (PEG and PBAE) were also dissolved in medium at the same concentration used to prepare the materials. The results are shown in **Figure 2.10**. The degradation by-products of HG11 formulation collected after 24, 72 and 168 h showed no significant cytotoxicity. In contrast, the degradation products of HG14 hydrogels collected after 24 h degradation caused a toxicity of approximately 75%. No cytotoxicity was observed when cells were exposed to by-products released after the first 24 h. Hence, this toxicity is most likely produced by the burst release during the early stages of degradation. This seems to be in disagreement with the data shown in the previous section, where the burst release of degradation products was more pronounced in the HG11 formulation. However, these were relative numbers (% of PBAE released over total PBAE). It

is important to note that formulation HG14 contains 4-fold higher PBAE content than HG11, leading to a higher total concentration of degradation products in contact with the cells in this initial burst, causing the decrease in the cell viability observed. Indeed, the study of the cytotoxicity of the individual starting reagents revealed that, while the 4-arm PEG-SH caused no significant cell death, PBAEs were toxic at high concentrations compared to the negative control. This confirmed that the hydrogel's initial PBAE burst can be toxic if too high PBAE solid contents are used, and suggested that HG11 formulation may be more suitable for wound healing.

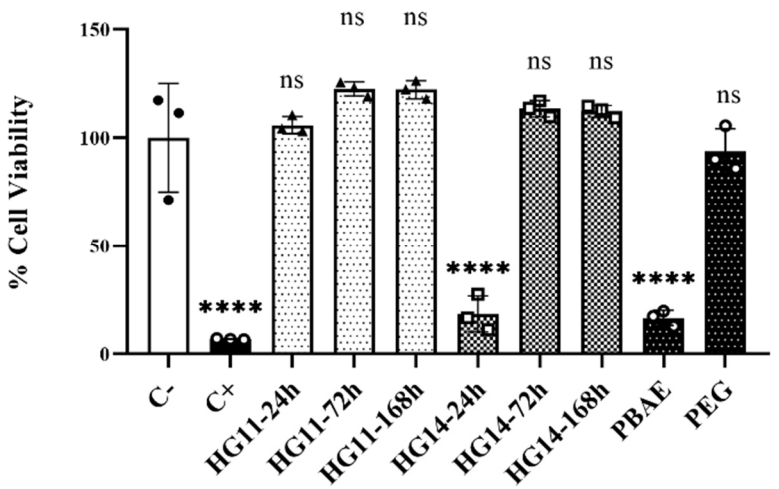

Figure 2.10. Human dermal fibroblasts viability after 24 h growing in culture medium containing the degradation products of hydrogels HG11 and HG14 after degradation intervals 0-24 h (HG11-24h and HG14-24h), 24-72 h (HG11-72h and HG14-72h) and 72-168 h (HG11-168h and HG14-168h) or containing the starting hydrogel-forming polymers (n=3).

2.4. Concluding remarks

Wound healing is a complex process involving many biomolecules, which act in an orchestrated fashion to completely close the injury. Any error or slowdown in any of the wound healing stages might change the status of the wound from acute to chronic, leading to additional complications for the patient. We now understand that the characteristics of the wound microenvironment play an important role in the successful resolution of injury. Parameters such as the interchange of gas molecules (e.g., oxygen or carbon dioxide) or the moisture of the wound site are found to play a decisive role in the progress of healing. On this basis, different biomaterials have been engineered in the last decade to meet these requirements and improve the outcomes from current treatments, such as ointments or gauzes. Hydrogels have stood out as one of the best strategies to accelerate the wound closure. Their high water content, tissue-like mechanical properties and easy tuneability have enabled the design of smart materials for the treatment of wounds.

Herein, different hydrogel formulations based on crosslinked thiolated 4-arm PEG molecules and thiol-reactive C32CR3 PBAE polymers were prepared. Specifically, two PBAE polymers were used, with varying numbers of thiol-reactive groups (SPDP) per chain. The PBAE C32TCR3, with one SPDP group, formed hydrogels by non-covalent interactions and entanglements, leading to their instant redissolution with aqueous media at 37 ºC. In contrast, C32T$_2$CR3 polymers, containing two SPDP groups per chain, were able to covalently crosslink the PEG molecules into a continuous, covalent network. The hydrogels formed by physical interactions were discarded, owing to their suboptimal properties (too fast degradation), unsuitable for lengthy wound healing applications. The chemical hydrogel formulations HG11 and HG14 were further characterized to fully understand the effects of increasing the polymer ratios.

The microstructure of formulations HG11 and HG14 was studied by confocal microscopy. HG11 presented a more regular pore size throughout the material than HG14. The latter formulation, in contrast, presented a greater majority of smaller pores than that observed in HG11 correlating with the increased solid content of PBAE. However, formulation HG14 also showed pores that were much bigger, leading to overall similar swelling ratios than HG11 hydrogel. This also influenced the degradation kinetics. HG11 was completely degraded in 8 days whereas HG14 degraded in almost double the time (15 days), due to the increased crosslinking caused by the formation of four times more chemical bonds. The smaller pores

of HG14 decreased the initial burst release during degradation (relative to the total amount of PBAE). However, the bigger pores in this formulation's structure caused an acceleration of the degradation kinetics after a few days and the fracture of the samples. This behaviour was confirmed by rheometry, where formulation HG14 showed higher values of storage modulus, yet the samples were broken after the test. In terms of cytotoxicity, the initial burst release of PBAE in formulation HG14 produced high levels of cytotoxicity. No cytotoxicity was observed for formulation HG11 at any release time point (24, 48 or 72 hours).

Additionally, the hydrogel formulations herein prepared are injectable, having the ability to adapt to the irregular topology of chronic wounds and ulcers. Maximising the contact area between the hydrogel and the wound will improve the delivery of active substances and the efficacy of the treatment. In the next chapter, the two hydrogel formulations studied will be doped using the polyplexes that were optimized in Chapter 1 to enable the sustained and local delivery of gene therapy to the wound.

2.5. References

(1) Ovington, L. G. Advances in Wound Dressings. *Clin. Dermatol.* **2007**, *25* (1), 33–38. https://doi.org/10.1016/j.clindermatol.2006.09.003.

(2) Agarwal, A.; McAnulty, J. F.; Schurr, M. J.; Murphy, C. J.; Abbott, N. L. Polymeric Materials for Chronic Wound and Burn Dressings. *Adv. Wound Repair Ther.* **2011**, 186–208. https://doi.org/10.1533/9780857093301.2.186.

(3) Falanga, V. The Chronic Wound: Impaired Healing and Solutions in the Context of Wound Bed Preparation. *Blood Cells, Mol. Dis.* **2004**, *32* (1), 88. https://doi.org/10.1016/j.bcmd.2003.09.020.

(4) Selvakumar, G. Biomaterials and Wound Healing : A Mini Review. **2020**, *1*, 13.

(5) Hoffman, A. S. Hydrogels for Biomedical Applications. *Adv. Drug Deliv. Rev.* **2012**, *64* (SUPPL.), 18. https://doi.org/10.1016/j.addr.2012.09.010.

(6) Palmese, L. L.; Thapa, R. K.; Sullivan, M. O.; Kiick, K. L. Hybrid Hydrogels for Biomedical Applications. *Curr. Opin. Chem. Eng.* **2019**, *24*, 143–157. https://doi.org/10.1016/j.coche.2019.02.010.

(7) Li, Y.; Yang, H. Y.; Lee, D. S. Advances in Biodegradable and Injectable Hydrogels for Biomedical Applications. *J. Control. Release* **2021**, *330* (August 2020), 151–160. https://doi.org/10.1016/j.jconrel.2020.12.008.

(8) Jeong, K.-H.; Park, D.; Lee, Y.-C. Polymer-Based Hydrogel Scaffolds for Skin Tissue Engineering Applications: A Mini-Review. *J. Polym. Res.* **2017**, *24* (7), 112. https://doi.org/10.1007/s10965-017-1278-4.

(9) Gaharwar, A. K.; Peppas, N. A.; Khademhosseini, A. Nanocomposite Hydrogels for Biomedical Applications. *Biotechnol. Bioeng.* **2014**, *111* (3), 441–453. https://doi.org/10.1002/bit.25160.

(10) Guan, X.; Avci-Adali, M.; Alarçin, E.; Cheng, H.; Kashaf, S. S.; Li, Y.; Chawla, A.; Jang, H. L.; Khademhosseini, A. Development of Hydrogels for Regenerative Engineering. *Biotechnol. J.* **2017**, *12* (5), 1600394. https://doi.org/10.1002/biot.201600394.

(11) Mandal, A.; Clegg, J. R.; Anselmo, A. C.; Mitragotri, S. Hydrogels in the Clinic. *Bioeng. Transl. Med.* **2020**, *5* (2), 1–12. https://doi.org/10.1002/btm2.10158.

(12) Cascone, S.; Lamberti, G. Hydrogel-Based Commercial Products for Biomedical Applications: A Review. *Int. J. Pharm.* **2020**, *573*, 118803–118821. https://doi.org/10.1016/j.ijpharm.2019.118803.

(13) Bartkowiak, G.; Frydrych, I. Superabsorbents and Their Medical Applications. *Handb. Med. Text.* **2011**, 505–546. https://doi.org/10.1533/9780857093691.4.505.

(14) Li, X.; Sun, Q.; Li, Q.; Kawazoe, N.; Chen, G. Functional Hydrogels with Tunable Structures and Properties for Tissue Engineering Applications. *Front. Chem.* **2018**, *6* (OCT), 1–20. https://doi.org/10.3389/fchem.2018.00499.

(15) Ren, B.; Chen, X.; Ma, Y.; Du, S.; Qian, S.; Xu, Y.; Yan, Z.; Li, J.; Jia, Y.; Tan, H.; Ling, Z.; Chen, Y.; Hu, X. Dynamical Release Nanospheres Containing Cell Growth Factor from Biopolymer Hydrogel via Reversible Covalent Conjugation. *J. Biomater. Sci. Polym. Ed.* **2018**, *29* (11), 1344–1359. https://doi.org/10.1080/09205063.2018.1460140.

(16) Spicer, C. D. Hydrogel Scaffolds for Tissue Engineering: The Importance of Polymer Choice. *Polym. Chem.* **2020**, *11* (2), 184–219. https://doi.org/10.1039/c9py01021a.

(17) Nicodemus, G. D.; Bryant, S. J. Cell Encapsulation in Biodegradable Hydrogels for Tissue Engineering Applications. *Tissue Eng. - Part B Rev.* **2008**, *14* (2), 149–165. https://doi.org/10.1089/ten.teb.2007.0332.

(18) Mathew, A. P.; Uthaman, S.; Cho, K. H.; Cho, C. S.; Park, I. K. Injectable Hydrogels for Delivering Biotherapeutic Molecules. *Int. J. Biol. Macromol.* **2018**, *110*, 17–29. https://doi.org/10.1016/j.ijbiomac.2017.11.113.

(19) Gyles, D. A.; Castro, L. D.; Silva, J. O. C.; Ribeiro-Costa, R. M. A Review of the Designs and Prominent Biomedical Advances of Natural and Synthetic Hydrogel Formulations. *Eur. Polym. J.* **2017**, *88* (01), 373–392. https://doi.org/10.1016/j.eurpolymj.2017.01.027.

(20) Kabir, S. M. F.; Sikdar, P. P.; Haque, B.; Bhuiyan, M. A. R.; Ali, A.; Islam, M. N. Cellulose-Based Hydrogel Materials: Chemistry, Properties and Their Prospective Applications. *Prog. Biomater.* **2018**, *7* (3), 153–174. https://doi.org/10.1007/s40204-018-0095-0.

(21) Gomez-Florit, M.; Pardo, A.; Domingues, R. M. A.; Graça, A. L.; Babo, P. S.; Reis, R. L.; Gomes, M. E. Natural-Based Hydrogels for Tissue Engineering Applications. *Molecules* **2020**, *25* (24), 1–29. https://doi.org/10.3390/molecules25245858.

(22) Catoira, M. C.; Fusaro, L.; Di Francesco, D.; Ramella, M.; Boccafoschi, F. Overview of Natural Hydrogels for Regenerative Medicine Applications. *J. Mater. Sci. Mater. Med.* **2019**, *30* (10), 115. https://doi.org/10.1007/s10856-019-6318-7.

(23) Hao, Y.; Fowler, E. W.; Jia, X. Chemical Synthesis of Biomimetic Hydrogels for Tissue Engineering. *Polym. Int.* **2017**, *66* (12), 1787–1799. https://doi.org/10.1002/pi.5407.

(24) Madduma-Bandarage, U. S. K.; Madihally, S. V. Synthetic Hydrogels: Synthesis, Novel Trends, and Applications. *J. Appl. Polym. Sci.* **2021**, *138* (19), 50376. https://doi.org/10.1002/app.50376.

(25) Li, J.; Wu, C.; Chu, P. K.; Gelinsky, M. 3D Printing of Hydrogels: Rational Design Strategies and Emerging Biomedical Applications. *Mater. Sci. Eng. R Reports* **2020**, *140* (December 2019), 100543. https://doi.org/10.1016/j.mser.2020.100543.

(26) Bustamante-Torres, M.; Romero-Fierro, D.; Arcentales-Vera, B.; Palomino, K.; Magaña, H.; Bucio, E. Hydrogels Classification According to the Physical or Chemical Interactions and as Stimuli-Sensitive Materials. *Gels* **2021**, *7* (4), 1–25. https://doi.org/10.3390/gels7040182.

(27) Duran-Mota, J. A.; Oliva, N.; Almquist, B. D. Chapter 19. Nanobiomaterials for Smart Delivery. In *Soft Matter for Biomedical Applications*; 2021; pp 475–498. https://doi.org/10.1039/9781839161124-00475.

(28) Annabi, N.; Nichol, J. W.; Zhong, X.; Ji, C.; Koshy, S.; Khademhosseini, A.; Dehghani, F. Controlling the Porosity and Microarchitecture of Hydrogels for Tissue Engineering. *Tissue Eng. - Part B Rev.* **2010**, *16* (4), 371–383. https://doi.org/10.1089/ten.teb.2009.0639.

(29) Holback, H.; Yeo, Y.; Park, K. Hydrogel Swelling Behavior and Its Biomedical Applications. In *Biomedical Hydrogels*; Elsevier, 2011; pp 3–24. https://doi.org/10.1533/9780857091383.1.3.

(30) Zhang, K.; Feng, W.; Jin, C. Protocol Efficiently Measuring the Swelling Rate of Hydrogels. *MethodsX* **2020**, *7* (December 2019), 100779. https://doi.org/10.1016/j.mex.2019.100779.

(31) Park, H.; Guo, X.; Temenoff, J. S.; Tabata, Y.; Caplan, A. I.; Kasper, F. K.; Mikos, A. G. Effect of Swelling Ratio of Injectable Hydrogel Composites on Chondrogenic Differentiation of Encapsulated Rabbit Marrow Mesenchymal Stem Cells In Vitro. *Biomacromolecules* **2009**, *10* (3), 541–546. https://doi.org/10.1021/bm801197m.

(32) Kickhöfen, B.; Wokalek, H.; Scheel, D.; Ruh, H. Chemical and Physical Properties of a Hydrogel Wound Dressing. *Biomaterials* **1986**, *7* (1), 67–72. https://doi.org/10.1016/0142-9612(86)90092-X.

(33) Oyen, M. L. Mechanical Characterisation of Hydrogel Materials. *Int. Mater. Rev.* **2014**, *59* (1), 44–59. https://doi.org/10.1179/1743280413Y.0000000022.

(34) Tse, J. R.; Engler, A. J. Preparation of Hydrogel Substrates with Tunable Mechanical Properties. *Curr. Protoc. Cell Biol.* **2010**, No. SUPPL. 47, 1–16. https://doi.org/10.1002/0471143030.cb1016s47.

(35) Narasimhan, B. N.; Horrocks, M. S.; Malmström, J. Hydrogels with Tunable Physical Cues and Their Emerging Roles in Studies of Cellular Mechanotransduction. *Adv. NanoBiomed Res.* **2021**, *1* (10), 2100059. https://doi.org/10.1002/anbr.202100059.

(36) Zuidema, J. M.; Rivet, C. J.; Gilbert, R. J.; Morrison, F. A. A Protocol for Rheological Characterization of Hydrogels for Tissue Engineering Strategies. *J. Biomed. Mater. Res. - Part B Appl. Biomater.* **2014**, *102* (5), 1063–1073. https://doi.org/10.1002/jbm.b.33088.

(37) Ramazani-Harandi, M. J.; Zohuriaan-Mehr, M. J.; Yousefi, A. A.; Ershad-Langroudi, A.; Kabiri, K. Rheological Determination of the Swollen Gel Strength of Superabsorbent Polymer Hydrogels. *Polym. Test.* **2006**, *25* (4), 470–474. https://doi.org/10.1016/j.polymertesting.2006.01.011.

(38) Verdier-Sévrain, S.; Bonté, F. Skin Hydration: A Review on Its Molecular Mechanisms. *J. Cosmet. Dermatol.* **2007**, *6* (2), 75–82. https://doi.org/10.1111/j.1473-2165.2007.00300.x.

(39) Sharman, D. Moist Wound Healing: A Review of Evidence, Application and Outcome. *Diabet. Foot J.* **2003**, *6* (3), 112–120.

(40) Weller, C. Interactive Dressings and Their Role in Moist Wound Management. In *Advanced Textiles for Wound Care*; Elsevier, 2009; pp 97–113. https://doi.org/10.1533/9781845696306.1.97.

(41) Guo, S.; DiPietro, L. A. Critical Review in Oral Biology & Medicine: Factors Affecting Wound Healing. *J. Dent. Res.* **2010**, *89* (3), 219–229. https://doi.org/10.1177/0022034509359125.

(42) Sen, C. K. Wound Healing Essentials: Let There Be Oxygen. *Wound Repair Regen.* **2009**, *17* (1), 1–18. https://doi.org/10.1111/j.1524-475X.2008.00436.x.

(43) Mayet, N.; Choonara, Y. E.; Kumar, P.; Tomar, L. K.; Tyagi, C.; Du Toit, L. C.; Pillay, V. A Comprehensive Review of Advanced Biopolymeric Wound Healing Systems. *J. Pharm. Sci.* **2014**, *103* (8), 2211–2230. https://doi.org/10.1002/jps.24068.

(44) Jones, V.; Grey, J. E.; Harding, K. G. Wound Dressings. *BMJ* **2006**, *332* (7544), 777–780. https://doi.org/10.1136/bmj.332.7544.777.

(45) Kathawala, M. H.; Ng, W. L.; Liu, D.; Naing, M. W.; Yeong, W. Y.; Spiller, K. L.; Van Dyke, M.; Ng, K. W. Healing of Chronic Wounds: An Update of Recent Developments and Future Possibilities. *Tissue Eng. Part B Rev.* **2019**, *25* (5), 429–444. https://doi.org/10.1089/ten.teb.2019.0019.

(46) Powers, J. G.; Higham, C.; Broussard, K.; Phillips, T. J. Wound Healing and Treating Wounds Chronic Wound Care and Management. *J. Am. Acad. Dermatol.* **2016**, *74* (4), 607–625. https://doi.org/10.1016/j.jaad.2015.08.070.

(47) da Silva, L. P.; Reis, R. L.; Correlo, V. M.; Marques, A. P. Hydrogel-Based Strategies to Advance Therapies for Chronic Skin Wounds. *Annu. Rev. Biomed. Eng.* **2019**, *21*

(1), 145–169. https://doi.org/10.1146/annurev-bioeng-060418-052422.

(48) Dumville, J. C.; O'Meara, S.; Deshpande, S.; Speak, K. Hydrogel Dressings for Healing Diabetic Foot Ulcers. *Cochrane Database Syst. Rev.* **2013**, *2017* (12). https://doi.org/10.1002/14651858.CD009101.pub3.

(49) Koehler, J.; Brandl, F. P.; Goepferich, A. M. Hydrogel Wound Dressings for Bioactive Treatment of Acute and Chronic Wounds. *Eur. Polym. J.* **2018**, *100*, 1–11. https://doi.org/10.1016/j.eurpolymj.2017.12.046.

(50) Brett, D. A Review of Collagen and Collagen-Based Wound Dressings. *Wounds* **2008**, *20* (12), 347–356.

(51) Nalawade, T.; Sogi, S. P.; Bhat, K. Bactericidal Activity of Propylene Glycol, Glycerine, Polyethylene Glycol 400, and Polyethylene Glycol 1000 against Selected Microorganisms. *J. Int. Soc. Prev. Community Dent.* **2015**, *5* (2), 114–119. https://doi.org/10.4103/2231-0762.155736.

(52) Xu, Q.; A, S.; Gao, Y.; Guo, L.; Creagh-Flynn, J.; Zhou, D.; Greiser, U.; Dong, Y.; Wang, F.; Tai, H.; Liu, W.; Wang, W.; Wang, W. A Hybrid Injectable Hydrogel from Hyperbranched PEG Macromer as a Stem Cell Delivery and Retention Platform for Diabetic Wound Healing. *Acta Biomater.* **2018**, *75*, 63–74. https://doi.org/10.1016/j.actbio.2018.05.039.

(53) Hao, Y.; Yuan, C.; Deng, J.; Zheng, W.; Ji, Y.; Zhou, Q. Injectable Self-Healing First-Aid Tissue Adhesives with Outstanding Hemostatic and Antibacterial Performances for Trauma Emergency Care. *ACS Appl. Mater. Interfaces* **2022**, *14* (14), 16006–16017. https://doi.org/10.1021/acsami.2c00877.

(54) Rehman, S. R. ur; Augustine, R.; Zahid, A. A.; Ahmed, R.; Tariq, M.; Hasan, A. Reduced Graphene Oxide Incorporated GelMA Hydrogel Promotes Angiogenesis For Wound Healing Applications. *Int. J. Nanomedicine* **2019**, *Volume 14*, 9603–9617. https://doi.org/10.2147/IJN.S218120.

(55) Yan, L.; Han, K.; Pang, B.; Jin, H.; Zhao, X.; Xu, X.; Jiang, C.; Cui, N.; Lu, T.; Shi, J. Surfactin-Reinforced Gelatin Methacrylate Hydrogel Accelerates Diabetic Wound Healing by Regulating the Macrophage Polarization and Promoting Angiogenesis. *Chem. Eng. J.* **2021**, *414* (August 2020), 128836. https://doi.org/10.1016/j.cej.2021.128836.

(56) Liu, H.; Wang, C.; Li, C.; Qin, Y.; Wang, Z.; Yang, F.; Li, Z.; Wang, J. A Functional Chitosan-Based Hydrogel as a Wound Dressing and Drug Delivery System in the Treatment of Wound Healing. *RSC Adv.* **2018**, *8* (14), 7533–7549. https://doi.org/10.1039/C7RA13510F.

(57) Patrulea, V.; Ostafe, V.; Borchard, G.; Jordan, O. Chitosan as a Starting Material for Wound Healing Applications. *Eur. J. Pharm. Biopharm.* **2015**, *97*, 417–426. https://doi.org/10.1016/j.ejpb.2015.08.004.

(58) Zhao, X.; Liu, L.; An, T.; Xian, M.; Luckanagul, J. A.; Su, Z.; Lin, Y.; Wang, Q. A Hydrogen Sulfide-Releasing Alginate Dressing for Effective Wound Healing. *Acta Biomater.* **2020**, *104*, 85–94. https://doi.org/10.1016/j.actbio.2019.12.032.

(59) Summa, M.; Russo, D.; Penna, I.; Margaroli, N.; Bayer, I. S.; Bandiera, T.; Athanassiou, A.; Bertorelli, R. A Biocompatible Sodium Alginate/Povidone Iodine Film Enhances Wound Healing. *Eur. J. Pharm. Biopharm.* **2018**, *122*, 17–24. https://doi.org/10.1016/j.ejpb.2017.10.004.

(60) Hussein, Y.; El-Fakharany, E. M.; Kamoun, E. A.; Loutfy, S. A.; Amin, R.; Taha, T. H.; Salim, S. A.; Amer, M. Electrospun PVA/Hyaluronic Acid/L-Arginine Nanofibers for Wound Healing Applications: Nanofibers Optimization and in Vitro Bioevaluation. *Int. J. Biol. Macromol.* **2020**, *164*, 667–676. https://doi.org/10.1016/j.ijbiomac.2020.07.126.

(61) Venkataprasanna, K. S.; Prakash, J.; Vignesh, S.; Bharath, G.; Venkatesan, M.; Banat, F.; Sahabudeen, S.; Ramachandran, S.; Devanand Venkatasubbu, G. Fabrication of Chitosan/PVA/GO/CuO Patch for Potential Wound Healing Application. *Int. J. Biol. Macromol.* **2020**, *143*, 744–762. https://doi.org/10.1016/j.ijbiomac.2019.10.029.

(62) Jones, A.; Vaughan, D. Hydrogel Dressings in the Management of a Variety of Wound Types: A Review. *J. Orthop. Nurs.* **2005**, *9* (SUPPL. 1), S1–S11. https://doi.org/10.1016/S1361-3111(05)80001-9.

(63) Aswathy, S. H.; Narendrakumar, U.; Manjubala, I. Commercial Hydrogels for Biomedical Applications. *Heliyon* **2020**, *6* (4), e03719. https://doi.org/10.1016/j.heliyon.2020.e03719.

(64) Khan, S.; Ranjha, N. M. Effect of Degree of Cross-Linking on Swelling and on Drug Release of Low Viscous Chitosan/Poly(Vinyl Alcohol) Hydrogels. *Polym. Bull.* **2014**, *71* (8), 2133–2158. https://doi.org/10.1007/s00289-014-1178-2.

(65) Mahkam, M.; Doostie, L. The Relation between Swelling Properties and Cross-Linking of Hydrogels Designed for Colon-Specific Drug Delivery. *Drug Deliv. J. Deliv. Target. Ther. Agents* **2005**, *12* (6), 343–347. https://doi.org/10.1080/10717540590952627.

Chapter 3: 4-arm PEG SH/C32T$_2$CR3 hydrogels doped with C6RH polyplexes

This page is intentionally left blank

4-arm PEG SH/C32T2CR3 hydrogels doped with C6RH polyplexes

A prolonged and sustained administration of drugs is often needed in different medical conditions to attain therapeutic effect. Specifically, in the case of ulcers, the length of administration must match the time needed to heal the ulcer. Hence, controlled release of therapeutics from wound dressings over time is an ideal approach to treat chronic wounds.

In this chapter, the hydrogels prepared and characterized in the previous chapter are doped using the polyplexes optimized in Chapter 1 to complete the platform for the delivery of genes to HDFs. First, the effects of incorporating the nanoparticles on the degradation kinetics of the hydrogels were studied. In turn, this has an impact on the release kinetics of the polyplexes from each formulation, leading to different transfection efficiencies when directly in contact with fibroblasts *in vitro*. Hence, this chapter describes the development and optimization of a hydrogel-based wound dressing doped with polyplexes to deliver genes to fibroblasts.

3.1. Introduction

Localised ailments, such as chronic dermal wounds, can greatly benefit from local delivery of therapeutics, as opposed to systemic administration. Local treatments present numerous advantages, such as higher specificity to the end organ without adding targeting moieties, facilitating their manufacturing and reducing the costs. They also enable the possibility to safely administer higher doses of the therapeutics with minimal systemic toxicity. Moreover, the use of biomaterials, such as hydrogels, as drug-loaded matrices protect the cargo and elicit spatiotemporally control over the release[1]. Hydrogels, particularly, can also be designed with certain desirable properties like injectability, which maximises the contact surface with the injured tissue, as described earlier in this thesis. In light of the above, therapeutic-loaded biomaterials are an especially interesting approach to treating wounds[2–5] in which long-term delivery of drugs[6,7], growth factors[8,9] or genes[10,11] is needed, as is the case with chronic wounds. Because this approach ultimately delivers the drug of interest in a more efficient manner, lower doses and frequency of administration are needed, which translates into a decrease in the cost of treatment and an increase in patient safety and compliance.

Any biomaterial can be easily modified to meet the desired release kinetics. However, controlling the initial burst release, characteristic of most hydrogel-based delivery platforms, is typically challenging. Contrary to expectations, this burst release might be favourable in some applications, such as the one herein studied[12], by quickly reaching a therapeutic concentration, which is then maintained with a more sustained release over time. The control over the release stages is of paramount importance to tune the dosage administered. Upon release, the uptake of the therapeutic agents by the cells in the wound is controlled by their bioavailability at a physiologically relevant rate and extent to prevent rapid dilution in the wound fluids[13–18]. Understanding the factors controlling release kinetics is highly important in predicting how the delivery platform will eventually work for the application selected.

3.1.1. Release of therapeutics from delivery platforms

As it has been stated before, the rate of local delivery of drugs, genes or other molecules planned to be used in a treatment must be controlled to reach a prolonged and suitable therapeutic effect. The selection of the most appropriate release assay and the interpretation of the data obtained is not trivial. There are many conditions that can be controlled, while others are innate to the delivery platform or the drug itself. Depending on this, different mechanisms for the release of molecules can be found. In fact, the delivery of the therapeutic agents might be influenced by one or more than one mechanism, being the most common the release by diffusion, by the swelling of the networks, by erosion of the structure and by mechanical deformation[19,20]. The diffusion process occurs when the molecules of interest move from the material to the external medium. It is the typical mechanism for non-responsive hydrogels that release the therapeutics passively, and it is controlled by the quantity of drug in the delivery platform, its concentration and the diffusion coefficient. The latter is a parameter used to describe the ability of the released molecule to move in a certain solvent (strongly dependent on the size and form of the molecule released, but also the viscosity and temperature of the solvent). The diffusivity of the therapeutic from a hydrogel is also dictated by the ratio of mesh size to drug size, describing steric interactions[21]. This kind of release is described using the Higuchi equation or one of its different variants[22]:

$$\frac{M_t}{A} = \sqrt{(2 \cdot C_i - C_s) \cdot D \cdot C_s \cdot t}$$

Equation 3.1. Derived Higuchi equation

Where M_t is the cumulative amount of drug released at time t, A is the material's surface area, C_i is the initial concentration, C_s the solubility of the drug, D is the diffusion coefficient and t is the time of release. The **Equation 3.1.** shown above is an evolution of the classical Higuchi equation to correct some minor details that were not considered originally, involving the diffusion and the drug gradient. Specifically, the equation was updated to take into account the fact that the molecules released first are located in the external part. This increases the diffusion distance that has to be covered by the agents, thus decreasing the concentration gradient and eventually resulting in a deceleration of the release rate. For this reason, this equation derives from Fick's laws. Interestingly, it also shows that the release can be influenced by tuning the physicochemical properties of the hydrogel-forming polymers to control the crosslinking density and porosity, affecting the surface area of the material. Therefore, the appropriate selection of these polymers as starting reagents and the nature of the molecules released together with their concentration will have an impact on the kinetics[23].

Another mechanism among the ones previously listed that can influence the release kinetics involves the swelling of the material. It consists of the expansion of the hydrogel networks by the absorption of water and the solutes it may contain. The internalization of these dissolutions into the matrix is a complex process and it is associated to several parameters that act as the driving force. Some of the most relevant are the elastic force of the gel structure, the osmotic force of the dissolution absorbed within the networks and/or the capillary force[19,21,24]. Higher swellings normally result in a more rapid release, making it easier for loaded drugs to the escape. However, since this process is highly-dependent on the networks formed, the hydrogel-forming polymers can be modified to add a new level of control or responsiveness. As an example, it is common to use thermo- or pH-responsive polymers in certain settings or environments where the presence of specific cues such as local elevated temperatures or specific pH are used as triggers to increase the release rate[25].

The release can also be controlled by the network’s erosion or degradation. This mechanism is quite important in tissue regeneration, where not only a prolonged and sustained release is needed, but also a degradation of the material that matches the requirements of the healing tissues. In addition, the degradation products can be engineered to be safely eliminated from the body. Additional chemical bonds can be incorporated into polymers to form hydrogels with erodible points, leading to an increase of the mesh size as the networks degrade, and concomitant gradual increase of therapeutics release[26]. Ester bonds, for example, are widely used due to their biodegradability[27]. As in the previous mechanism, smart hydrogels can be

designed including bonds that can respond to certain stimuli such as redox cues[28,29] (e.g., reducible disulphide bonds) or the presence of enzymes (e.g., MMP-sensitive moieties[30]) to name a few examples.

The last release mechanism among the most common ones reviewed in the present thesis is the control through mechanical deformation. Briefly, it consists in the use of mechanical forces, ultrasounds or even magnetic fields to accelerate or delay the release of therapeutics. These driving forces can increase the mesh size, change the network structure or trigger a convective flow within the networks, having as a result direct implications in the delivery kinetics[31,32]. This release mechanism opens the possibility to a pulsatile release that can be beneficial for applications where the therapeutic effect must be stimulated using a repeated administration[33].

In the previous paragraphs, the most important release mechanisms have been reviewed. However, as it has been mentioned in some cases, there are different additional factors that can drive the release kinetics, such as temperature. Generally, temperature is set to 37ºC for applications in the biomedical field. Some materials are responsive to temperature, changing their swelling or even transitioning from a liquid-like state to a more solid-like state or viceversa. The medium used in the release experiment also plays an important role. For example, pH, salinity, redox state or presence of certain macromolecules can accelerate or decelerate the release of specific therapeutics. Hence, a release experiment must incorporate the parameters to mimic physiologically relevant conditions.

Release curves are obtained by tracking the drug or therapeutic delivered. Depending on the size and concentrations of the therapeutic, the suitable techniques for the detection and quantification differ[1], mostly based on the selectivity and sensitivity required for analysis. A wide variety of techniques can be used, but the most common ones are spectroscopy-based, such as UV-Vis and fluorescence spectroscopy of released analytes. While straightforward, these techniques can lack selectivity for the analyte. Alternatively, antibody-based techniques like enzyme-linked immunosorbent assays (ELISA) present high sensitivity and selectivity for the target, with low complexity and relatively low cost. In contrast, techniques like high-performance liquid chromatography-mass spectrometry (HPLC-MS) or reverse transcription quantitative real-time PCR (RT-qPCR) are used when a high sensitivity and selectivity is needed, with a concomitant increase in the complexity of the experiments and the cost. It must be highlighted again that the nature of the therapeutic is one of the most decisive factors,

since a RT-qPCR assay, for example, may not be appropriate to detect the release of an organic drug. Similarly, fluorescence spectroscopy may be a good option if the therapeutic released is fluorescent or if it can be tagged using a fluorescent moiety[1]. Other aspects, such as convenience, availability of equipment and cost can play a role in deciding which technique is the optimal one for each application.

Overall, the different mechanisms by which the release of a therapeutic occurs from a delivery platform have been described. However, therapeutics release rarely follow just one of these mechanisms, but rather a combination of two or more. The correct interpretation of the release profiles obtained provides valuable information about the mechanisms followed. More importantly, it will define whether the material suits the final application requirements or if further modifications and optimizations are needed.

3.1.2. Tunability of drug release

Different strategies have been engineered in the last few decades to increase the control over the release kinetics. Depending on the application, an acceleration or deceleration of the release might be needed. These control strategies can be classified into three different families depending on the working scale: atomic or molecular scale, mesh scale and macroscopic scale[34]. The first one is the smallest one, and is based on the affinity or binding between the drug and the network chains. In this sense, the interaction of the drug can be physically or chemically tuned to modify the release. This release control mechanism has an important impact in the initial burst[23,26]. The inclusion of hydrophobic domains or physical interactions like cation-anion (including groups such as phosphates, amines, aminoacids or carboxylates), hydrogen bonding, π-π stacking or antigen-antibody are few examples of strategies that can be used[23,35]. Additionally, stronger interactions can be achieved by covalently binding the drug to the network using bonds that may be responsive to stimulus, such as temperature or pH[25,36]. Another strategy is the formation of bonds that can be enzymatically cleaved to increase the release kinetics in the presence of a particular enzyme. The use of hydrolytically-degradable polymers in the matrix structure is also interesting to elicit matrix erosion-mediated release[25,36].

The next scale to control release is dictated by the mesh size, defined as the linear distance between two adjacent crosslinks. This size can be lengthened by using matrix-forming polymers with higher molecular mass, for example, which would typically lead to faster release kinetics due to the increased mobility of the drug[34]. However, this situation may change

depending on the type of drug and the network chains. The use of nano- or microparticles to encapsulate drugs is also a strategy that can be included in this scale, protecting the cargo and slowing down their release through steric hindrance[37,38]. Moreover, these particles can also be chemically conjugated to the networks, opening again the possibility to include stimuli-responsive moieties. Even though a vast number of modifications can be incorporated to the released therapeutic, the network itself can also include interesting properties. The use of certain polymers can render the matrix formed to show thermo-, pH- or electrical-responsiveness, increasing or decreasing the swelling in different circumstances after certain triggers are present, normally accelerating or decelerating the release, respectively[25].

The largest scale to control release of therapeutics is the macroscopic scale, including architectural factors. It is mainly based on the matrix porous structure and the swelling. These two factors have been reviewed in the beginning of this chapter and throughout the previous chapter, and they are tightly related to the control of crosslinking density, mesh size and the ability of certain hydrophilic polymer to absorb water absorption. Generally, a higher water content and larger pore sizes in a drug delivery system are linked to more rapid drug release. As described earlier, the type of drug also plays an important role, since hydrophobicity slows down the kinetics of the release[34,39].

It becomes clear that the engineering of new delivery platforms requires in depth understanding of the matrix, the therapeutic loaded and their interactions. Manipulation of their characteristics, such as the inclusion of breakable bonds, modification of the mesh size, porosity or swelling, are a few strategies to tune the release kinetics. As a result, the final mechanism of drug release is the product of many variables and tends to be complex. In the present case, the hydrogels optimized in Chapter 2 will be loaded with PBAE polyplexes developed in Chapter 1. Then, the degradation of various hydrogel formulations and the release of the particles will be studied to understand the impact of parameters such as the degree of crosslinking, the nature of the erodible chemical bonds, the concentration of the starting reagents and the polyplex-network interaction, among others. The data gathered will inform on the suitability of the prototype biodegradable drug delivery platforms as wound dressings to treat diabetic foot ulcers.

3.2. Materials and methods

Reagents and solvents were purchased from Sigma-Aldrich and Panreac and used as received unless otherwise stated. The specific reagents, materials and PBAE polymers synthesized used for the preparation of the polyplexes and the hydrogels in this chapter are the same than those used in the previous chapters, without further modifications. Cell culture procedures followed herein were the same than in the previous chapters and only few variations were done. These variations will be stated in the corresponding sections. The fluorophores cy3 and cy5 for the polymers and the nucleic acids tagging were purchased from Mirus and the manufacturer's protocol was followed.

3.2.1. Preparation of hydrogels HG11 and HG14 doped with PBAE polyplexes

The C6RH polyplexes were prepared following the same protocol described in Chapter 1. Briefly, the C6RH PBAE and the desired polynucleotide are dissolved in separate tubes using the AcONa buffer at pH 5.2. The solution containing the nucleic acids is added to the PBAE solution to get a final polynucleotide concentration of 0.3 mg/mL and in a PBAE/polynucleotide weight ratio of 25:1. This time, these nucleic acids final concentration is ten-fold higher compared to the one used in Chapter 1. This value was achieved after studying the incorporation of the polyplexes into the hydrogels, being the maximum concentration reachable without resulting in an aggregation of the particles. The volume of the nanoparticle solution in each hydrogel is 4 µL. Also, this volume was chosen after several trials to incorporate the maximum quantity of polyplexes without compromising the formation of the material. The hydrogels HG11 and HG14 are prepared following the protocols in Chapter 2. However, the polyplexes' solution is mixed with the PEG solution by pipetting up and down prior to forming the hydrogels. After the mixing is visually uniform, the C32T$_2$CR3 is added. The solution is mixed again by pipetting up and down. The hydrogels are formed, as in the previous chapter, after 30 min incubation and adding distilled water. To further understand these two polyplex-loaded formulations behaviour, different variations with or without the nanoparticles were additionally prepared. The characteristics of these variations are summarized in **Table 3.1.**

Table 3.1. Hydrogels' formulations studied in the present chapter with the detailed volumes and concentrations used. Concentration is given in mg/mL and volumes in µL.

Formulation	$[PEG]_i$	V_{PEG}	$[PBAE]_i$	V_{PBAE}	V_{NP}	V_{DMSO}	V_f
HG11	500	8	250	8	0	0	16
HG14	500	8	250	32	0	0	40
HG11-NP	500	8	250	8	4	0	20
HG14-NP	500	8	250	32	4	0	44
HG14-NP$_{1/2}$	500	8	250	32	2	2	44
HG11-500v	500	8	500	4	0	12	24
HG14-500v	500	8	500	16	0	0	24

3.2.2. Confocal microscopy

The microstructure of the C6RH-loaded hydrogels was studied by confocal microscopy following the same procedure described in the previous chapter without any variation. Polyplexes encapsulation inside the hydrogels and their distribution were also studied by confocal microscopy. The doped hydrogels were prepared as described above, but fluorophore tags were used to localize the nanoparticles. Specifically, the C6RH polymer solution contained a 2% (w/w) of polymers labelled using the fluorophore cy5. The pGFP plasmid used in this experiment was also tagged at a concentration of 10% (w/w) with cy3. Hence, the core and the shell of the polyplexes were labelled using different fluorophores to study their colocalization as a surrogate for nanoparticle stability inside the hydrogel structure. Hydrogels prepared and doped with tagged polyplexes were washed using distilled water a few times after their preparation and the 30 min of incubation to detach the polyplexes that may be weakly adsorbed on the surface. The images were taken using a Leica SP8 confocal microscope (Leica Microsystems) and the image processing, pore size distribution, analysis, and colocalization studies were done with ImageJ-Fiji software.

3.2.3. SEM microscopy

Hydrogels studied by SEM microscopy were prepared as described in the Section 3.2.1. No sputter coating was used for the image of the samples. This technique was not used to visualise the pores but to study how a lyophilization process affects the structure.

3.2.4. Degradation of hydrogel formulations

The degradation was studied in the same manner as described in the previous chapter, using 2.5% and 5% (w/w) of tagged polymer for HG11 and HG14 formulations, respectively. The collection of aliquots and the spectrophotometric measurements using a Tecan Infinite 200 PRO were done following the protocol described in the previous chapter.

3.2.5. Release of PBAE polyplexes

HG11 and HG14 doped with the C6RH polyplexes were prepared, but this time the pGFP used was labelled with cy3. The samples were immersed in PBS (1x) and a 200 µL aliquot was collected at each timepoint. The fluorescence intensity was measured and 200 µL of fresh PBS were added to the samples. The release of the nanoparticles was followed by tracking the fluorescence intensity of the release samples at each timepoint, relative to the total fluorescence after the hydrogels were completely degraded. This experiment was repeated again but tagging the C6RH polymer with cy3 instead of the nucleic acid, and samples were processed and measured as described above for the tagged pGFP.

3.2.6. Transfection of HDF using the C6RH-loaded hydrogels

Fibroblasts were seeded at a density of 40,000 cells per well in 48-well plates and incubated for 24 hours at 37ºC in a 5% CO_2 atmosphere. C6RH-loaded HG11 and HG14 samples were prepared in triplicates. In this study, the polyplexes encapsulated reporter mRNA-GFP. Hydrogels were washed using supplemented DMEM five times to eliminate DMSO traces, they were placed in the wells on top of the cells and covered with 250 µL of supplemented medium. The negative control consisted of the same hydrogels incorporating C6RH encapsulating non-coding DNA. Cells were imaged after 24 h of incubation using a fluorescence microscope and the transfection efficiency was quantified by flow cytometry under the same conditions as mentioned in Chapter 1. The positive control consisted of the formulation HG11 loaded with Polyplus JetMESSENGER polyplexes, adapting the protocol to incorporate the same quantity of mRNA per hydrogel than in the formulations HG11 and HG14. The cell viability was also assessed after the 24 h transfection using Presto Blue, following the manufacturer's instructions. In this case, the negative control consisted of untreated cells (0% toxicity) and the positive control was cells treated with a highly cytotoxic solution (representing 100% toxicity). The cell viability after transfection with the hydrogels containing Polyplus-loaded mRNA was also measured.

3.2.7. Statistical Analysis

GraphPad Prism 8.0.1 software was used for the statistical analysis. Statistical differences between groups were studied by ordinary one-way ANOVA with post-hoc Tukey HSD test. The significance of the difference in the data is *$p < 0.05$, **$p < 0.01$, ***$p < 0.001$, and ****$p < 0.0001$.

3.3. Results and discussion

The hydrogels HG11 and HG14 were optimized in the previous chapter to match the intended application. Moreover, the polyplexes' formulation C6RH prepared in Chapter 1 showed high transfection efficiency close to 80% in dermal fibroblasts. In the following paragraphs, the incorporation of these polyplexes into the hydrogel formulations and their interactions will be studied.

3.3.1. Preparation and microstructure characterization of C6RH-loaded hydrogels

The incorporation of nanoparticles inside hydrogels can be attained in different ways. As an example, a typical procedure consists in forming the hydrogels and immersing them in a solution containing the drug, which is introduced into the hydrogel by swelling. However, there is a risk that the nanoparticles distribution might not occur in a uniform manner. Another common approach consists in mixing the nanoparticles with one of the starting reagents, followed by the formation of the hydrogel. This procedure normally leads to more homogeneous distributions, as long as good miscibility of the components is achieved without disrupting the stability of any of them. The latter method was used in this study, aiming for a uniform distribution of the polyplexes inside the hydrogel formulations HG11 and HG14. The polyplexes were prepared, pre-mixed with the 4-arm PEG-SH solution, followed by hydrogel formation upon reaction with C32T$_2$CR3, as described in the *Materials and Methods* section. No visual differences were observed compared to the formation of hydrogels without polyplexes prepared in the previous chapter. Next, the distribution of the polyplexes inside the material was studied by confocal microscopy, using fluorescently labelled C6RH and nanoparticles. Confocal images in **Figure 3.1. A and B** showed that the polymer forming the nanoparticles (blue) and the plasmid (red) were co-localized, forming discrete dots. This fluorescence colocalization was further studied using ImageJ-Fiji software, giving a Pearson's R value of 0.97 and 0.90 for HG11 and HG14, respectively. The Manders' overlap coefficient was also obtained, since it is known to be more accurate for images with different intensities[40,41]. The coefficient also revealed high colocalization of the discrete fluorescent signals (HG11-NP: 0.91 and 1.00; HG14-NP: 0.98 and 0.84 for blue channel overlapping red channel and red channel overlapping blue channel, respectively). This means that the polyplexes stability was not disrupted upon hydrogel formation and they were successfully trapped within the hydrogels network. Additionally, the three-dimensional construct of the hydrogel showed that the polyplexes were uniformly distributed throughout the hydrogels' structures (**Figure 3.1. C and D**).

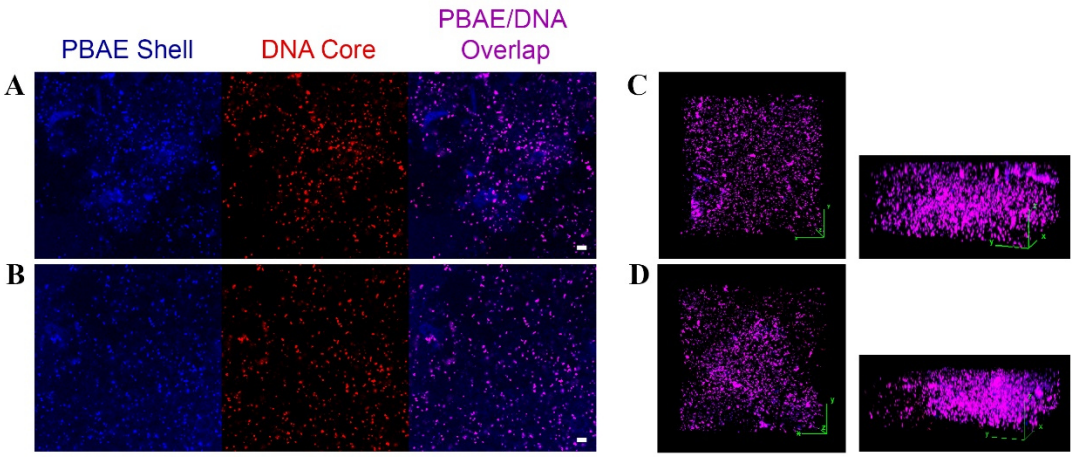

Figure 3.1. A) and B) Confocal microscopy images of hydrogels HG11 and HG14 doped with C6RH polyplexes, respectively (cy5-labelled PBAE shell: blue channel; cy3-labelled DNA core: red channel. Purple results from the PBAE and DNA signal overlap). C) Three-dimensional reconstruction of a section of 79 µm thickness of HG11 loaded with C6RH-cy5 encapsulating pGFP-cy3. D) Three-dimensional reconstruction of a section of 57 µm thickness of HG14 loaded with C6RH-cy5 encapsulating pGFP-cy3.

The successful doping of the hydrogels using the C6RH polyplexes is a meaningful step towards the use of the platforms as gene delivery systems. However, the incorporation of the polyplexes may interact with the networks and produce changes in the microstructure. To study this, the hydrogels doped with the PBAE nanoparticles were frozen at -80ºC, immersed in OCT and cryosectioned to observe the microstructure by confocal microscopy. The C32T$_2$CR3 was labelled with FITC, as described in the *Materials and Methods* section of the previous chapter. The images are shown in **Figure 3.2. A and B**.

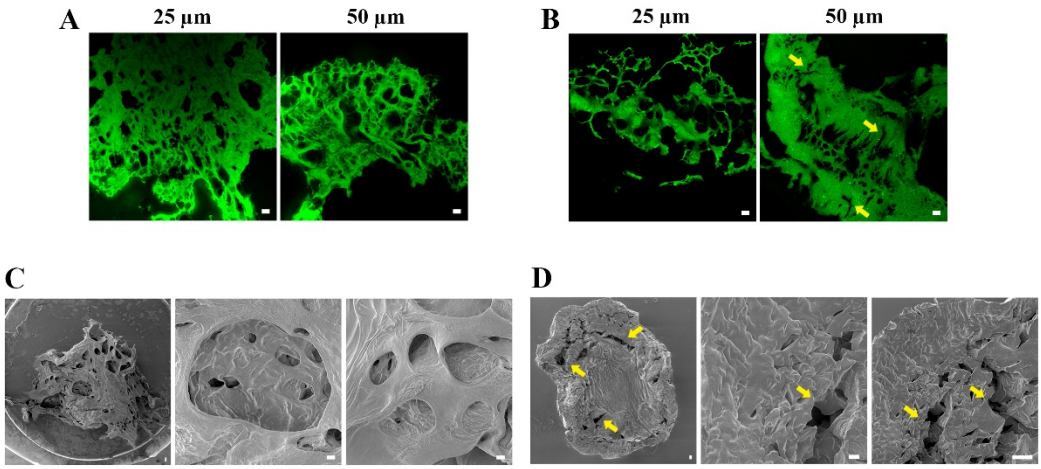

Figure 3.2. A) and B) Confocal microscopy images of 25 and 50 µm slices of FITC-labelled HG11 and HG14 doped with C6RH polyplexes, respectively. C) and D) SEM images of lyophilized hydrogels HG11 and HG14 doped with C6RH polyplexes, respectively. Scale bar: 50 µm.

The HG11 formulation containing the polyplexes showed a more uniform distribution of pores than HG14, which was challenging to section due to the high fragility of the material. In fact, some cracks and fissures can be observed in the fluorescence microscopy images in **Figure 3.1 B, yellow arrows**, as well as in the SEM images after the lyophilization of the materials (**Figure 3.2 C and D, yellow arrows**). Pore size distribution of the doped formulations was studied from the confocal microscopy images, and compared with the formulations without polyplexes (**Figure 3.3**). No significant difference was found between the mean pore size for formulations HG11 and HG14, whether empty (17.9±8.0 nm and 17.6±35.9 nm for HG11 and HG14, respectively) or doped with the nanoparticles (30.6±37.5 nm and 30.4±38.3 nm for HG11-NP and HG14-NP, respectively). However, there is a clear difference in the overall pore size distribution of the empty hydrogels, reflected in the median pore size for these formulations (16.9 nm and 7.6 nm for HG11 and HG14, respectively). This is consistent with an increase in crosslinking density in the HG14 formulation, leading to smaller pores. Nonetheless, HG14 also presents a small proportion of very large pores, as observed in confocal microscopy, which might be responsible for the increased fragility. Incorporating nanoparticles leads to an overall increase in both mean and median pore size, being more pronounced for the formulation HG14-NP compared to HG14. This indicates that, since PEG concentration is the same in both formulations, the quantity of PBAE in this material might

have reached a point of saturation, leading to destabilizing interactions in the structure. To confirm this phenomenon, the degradation and release kinetics of these formulations were studied.

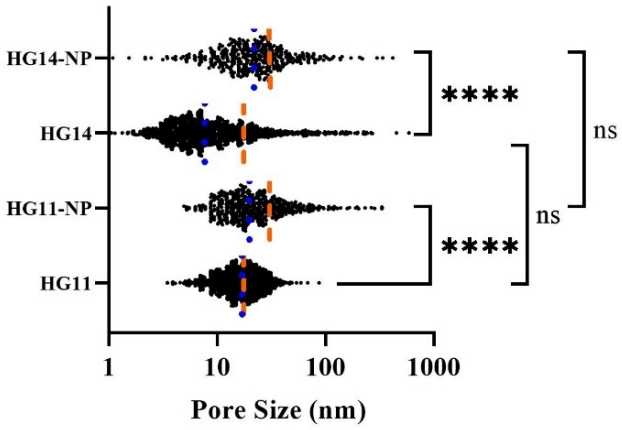

Figure 3.3. Pore size distribution comparison of the formulations HG11-NP and HG14-NP and formulations without polyplexes HG11 and HG14. Orange dotted lines: average pore sizes. Blue dotted lines: median pore sizes. The statistics shown are related to the mean values.

3.3.2. Degradation of C6RH-doped hydrogels

The detailed specifications for each formulation were shown in **Table 3.1.** The addition of the polyplexes impacted the release kinetics differently in each formulation (**Figure 3.4.**).

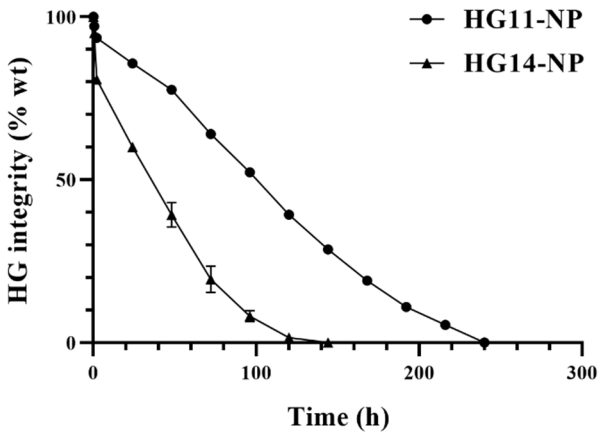

Figure 3.4. Degradation of hydrogels HG11-NP and HG14-NP, as percentage of hydrogel integrity (n=3).

For example, formulation HG11-NP required longer time for complete degradation, compared to formulation HG11 (without nanoparticles), being 240 h for HG11-NP versus 200 h for HG11. Contrarily, HG14-NP was completely degraded in roughly a third of the time compared to HG14 (144 h and 360 h, respectively) strengthening the theory of detrimental interactions due to a PBAE saturation of the system. Interestingly, the incorporation of the polyplexes in the HG11 formulation minimises the initial burst in the degradation, with a resulting almost zero-order degradation kinetics. As it is shown in **Table 3.1.**, the final volume for the HG14 formulations is larger than that of formulations HG11 (40 µl vs 16 µl, respectively). To eliminate this dilution factor as the reason of the acceleration of the degradation in HG14, the formulations HG11-500v and HG14-500v were prepared. These formulations did not contain polyplexes, and were prepared to maintain the original PEG/PBAE ratios in HG11 and HG14, with the same final volume for HG11 and HG14 (24 µl). The degradation profiles of these two new formulations are compared to the original HG11 and HG14 formulations (**Figure 3.5**). Interestingly, HG11-500v (having a higher final volume than HG11) decreased the initial burst and doubled the degradation time respect to the formulation HG11, whereas HG14-500v and HG14 presented almost identical degradation kinetics. Hence, it is suggested that the unexpected change in the degradation of HG14 formulation after adding polyplexes is not due to a dilution factor.

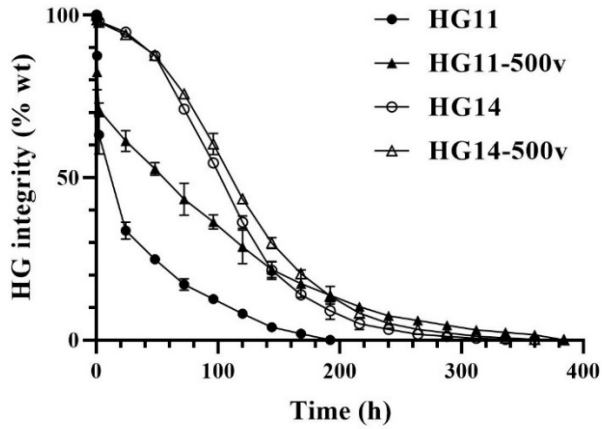

Figure 3.5. Comparison of the degradation profiles of hydrogels HG11-500v and HG14-500v to formulations HG11 and HG14 expressed in percentage of hydrogel integrity (n=3).

The effect of the addition of the nanoparticles was then studied. For that, the degradation of the formulation HG14-NP$_{1/2}$ was compared to formulations HG14 and HG14-NP. This new formulation presents the same volume of the polyplexes' solution, but half the concentration. We hypothesised that using less polyplexes should increase the degradation time if the interaction of C6RH particles with the networks is destabilizing the hydrogel structure. **Figure 3.6** corroborates our hypothesis, showing that the time for a complete degradation decreases gradually as the polyplex concentration increases. Hence, it is reasonable to hypothesize that there is an existing interaction between the C6RH PBAE of the nanoparticles with the C32T$_2$CR3 PBAE in the hydrogel networks, and that the 4-fold PBAE increase in formulation HG14 compared to HG11 exacerbates the overall destabilisation of the hydrogel network and acceleration of the degradation kinetics.

Overall, increasing the PBAE in the PEG/PBAE ratio increased the degradation time in the hydrogels studied. However, the incorporation of the polyplexes appears to destabilise the hydrogel structure as a function of PBAE concentration. This results in an acceleration of the release kinetics, studied next.

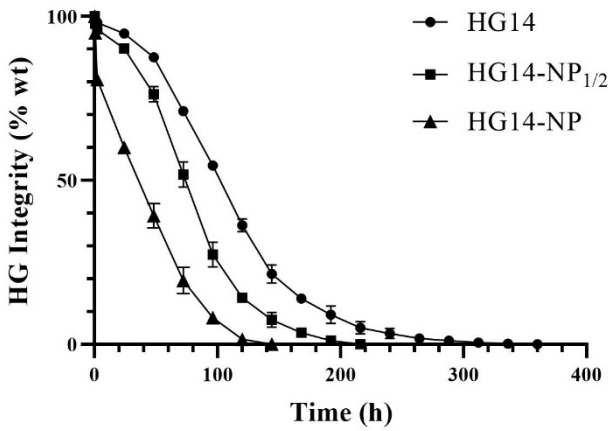

Figure 3.6. Comparison of the degradation profiles of formulations HG14, HG14-NP$_{1/2}$ and HG14-NP expressed in percentage of hydrogel integrity (n=3).

3.3.3. C6RH polyplexes release from hydrogels

The release of the polyplexes was studied by tracking the fluorescence intensity produced by the nanoparticles released. The release of PBAE (shell) and nucleic acid (core) in each formulation was followed separately, to avoid the Fluorescence Resonance Energy Transfer (FRET) between fluorophores. Measuring both shell and core separately provides evidence as to whether the particles are being released as unique entities (and hence are stable in the hydrogel) or separately, due to polyplexes' destabilization. The profiles obtained are shown in **Figure 3.7.** Similar kinetic profiles were obtained for the shell and core components of the polyplexes loaded in HG11-NP, meaning that the polymer and the nucleic acid of the nanoparticles were released at the same time. Hence, the stability of the polyplexes is maintained from the hydrogel doping procedure to their release. Contrarily, most of the C6RH PBAE of the polyplexes was released in the first hours for the formulation HG14-NP, whereas the nucleic acids were retained for approximately 48 h, after which there was a rapid increase in the release of polynucleotides. This coincided with the appearance of fractures in the material, consistent with our observations in the degradation experiments. The discrepancy in release kinetics of the core and shell of polyplexes loaded in HG14 indicates that they are not stable in the hydrogel structure. The initial burst release experimented only by the shell suggests that an electrostatic interaction may repel this polymer and the polymer in the hydrogel network, both positively charged PBAEs. Nucleic acids, being negatively charged, might remain in the positively charged hydrogel structure through attractive interactions and released once the hydrogel structure disintegrates. This supports our hypothesis that there is a destabilising interaction between PBAEs in the hydrogel network and in the polyplexes. However, the confirmation that the cause of this behaviour is due to a mechanism involving repulsive forces between the positively charged polymers need further research and it is beyond the scope of the present thesis.

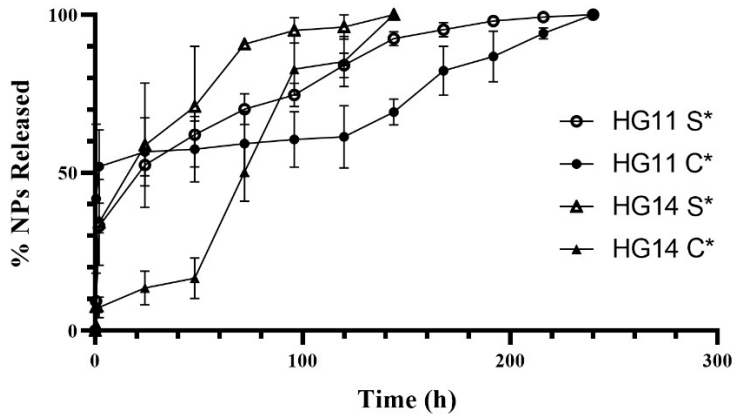

Figure 3.7. Release profiles of polyplexes released from the formulations HG11 and HG14. S*: The shell of the particles was labelled. C*: The core of the particles was labelled (n=3).

3.3.4. Transfection and fibroblasts viability using the C6RH-loaded hydrogels

The characteristic degradation of the hydrogels and the release of the polyplexes observed in the previous section will have an impact on the cell viability and transfection that will be studied hereunder. The polyplex-loaded HG11 and HG14 were prepared following the protocol described in the *Materials and Methods* section. Cells were transfected with mRNA GFP loaded in polyplexes delivered from HG11-NP and HG14-NP. Non-transfected cells and cells transfected using the HG11-NP and HG14-NP formulations encapsulating a scrambled RNA were used as negative controls. The transfection quantification in fibroblasts was performed after 24 h in contact with the formulations. As observed in **Figure 3.8**, HG11-NP was the only formulation showing significantly different transfection efficiency in comparison to the controls.

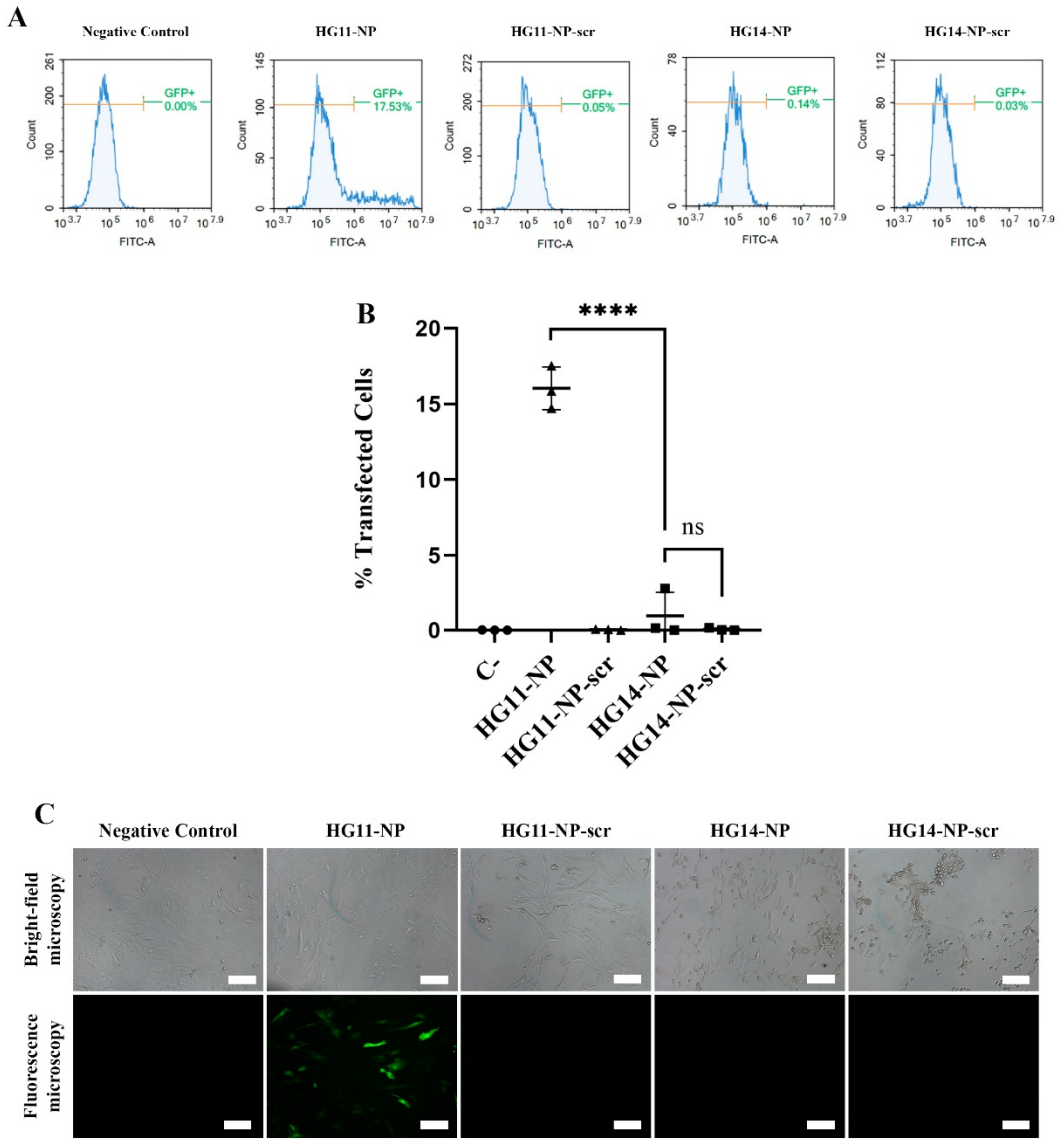

Figure 3.8. A) FACS graphs showing the percentage of the single dermal fibroblasts counted expressing GFP after transfection using the C6RH-loaded hydrogels HG11-NP and HG14-NP encapsulating mRNA-GFP or a scrambled RNA. B) Percentage of transfected cells and C) bright-field and fluorescence microscopy images 24 h after the transfection. (n=3). Scale bar: 100 µm.

The transfection efficiency of HG11-NP was lower than the one obtained with free nanoparticles (16.0±1.4 and 74.0±3.9 for HG11-NP and free nanoparticles, respectively). This can be explained by the experimental setup, as GFP expression was assessed 24 hours after

doped hydrogel administration to cells. At this time point, only up to 50% of nanoparticles had been released from the hydrogel, and not all released particles had the necessary time to be translated to GFP protein. Also, the expression of this protein increases in a gradual manner in the 24 h since the start of the mRNA transfection, and there might be an important cell-to-cell variability in the expression levels of GFP of transfected cells[42]. Thus, the fluorescence measured corresponds only to the cells transfected in the first few hours.

In addition to the previous experiment, the HG11 was loaded with the Polyplus JetMESSENGER positive control carrying the same quantity of mRNA, and no significant transfection was observed (**Figure 3.9**).

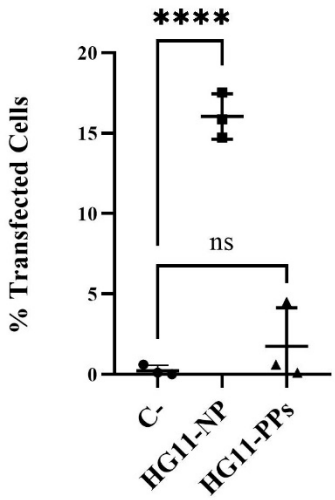

Figure 3.9. Transfection of HDFs using the formulation HG11-NP in comparison to the same formulation doped with mRNA-loaded JetMESSENGER positive control nanoparticles (PP) (n=3).

Interestingly, HG14-NP did not elicit any transfection compared to controls. This aligns with the slower delivery of nucleic acids at early time points observed in the release experiments, as well as with the instability of the polyplexes in this formulation. Altogether, the data supports the hypothesis that PBAEs in the hydrogel network and polyplexes experience destabilising interactions, rendering HG14 non-functional as a transfection platform. Additionally, the cell viability after the transfection was also measured, showing similar results to those obtained for the degradation products in the previous chapter (**Figure 3.10.**).

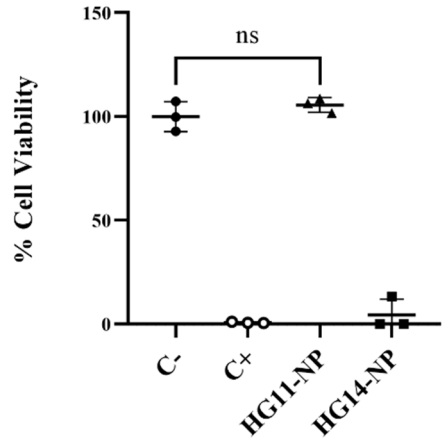

Figure 3.10. Fibroblasts viability after transfection using formulations HG11-NP and HG14-NP (n=3).

Hydrogel HG11-NP did not show statistically different cytotoxicity to the negative untreated control, while formulation HG14-NP elicited cytotoxicity comparable to that of the positive control consisting of a treatment with a toxic solution. This aligns with our hypothesis regarding the toxicity of PBAEs above a certain concentration, matching the cell viability obtained for the degradation products in the previous chapter.

Altogether, the formulation HG11-NP has shown the ability to transfect primary dermal cells with relatively high efficiency and without compromising the cell viability, and hence is a good wound dressing prototype to deliver RNA therapies to skin.

3.4. Concluding remarks

The suitability of a biomedical material for gene delivery depends on different factors that have been explored through the last and the present chapters. Properties such as biocompatibility, low cytotoxicity of the forming reagents, material performance and cell viability after using the platform have been characterized. Regarding treating wounds with dressings that deliver drugs, it is important that the release matches the time frame of wound healing, reaching a therapeutic concentration in the first hours and sustaining this effect over time. Ideally, the material should gradually be degraded to be eliminated from the body. For that, the study of the release and degradation kinetics is necessary and can give evidence for further improvements.

In this sense, hydrogel formulations HG11 and HG14 have been doped using the C6RH polyplexes. The study of this incorporation by confocal microscopy showed that the polyplexes can be successfully encapsulated inside both hydrogel structures after the formation. Moreover, the PBAE nanoparticles are homogeneously distributed through the whole hydrogel structure. However, observations of the microstructure of these formulations suggested that the addition of the polyplexes produced an increase in the mean and the median pore size, being more pronounced in the formulation HG14. This has a direct but different implication in the degradation of both formulations, increasing the complete degradation time in formulation HG11-NP and halving it in the case of the HG14-NP, compared to formulations without polyplexes. The release of nanoparticles is affected by the degradation of the hydrogels. For HG11-NP, the polyplexes were released in a sustained manner after the initial burst release, whereas the stability of the polyplexes released from HG14-NP seemed to be disrupted, delivering the polymer (shell) and the nucleic acids (core) with different kinetics (i.e., separately).

The kinetics and observations from the release experiments matched the results obtained in the transfection of HDFs using the complete platform, where only the formulation HG11-NP could efficiently transfect fibroblasts. Despite further modifications may be required, this formulation has high potential as an injectable dressing for gene therapy to the dermis to treat chronic wound. The polyplexes incorporated in the platform herein designed will be tuned in the next chapter to acquire the therapeutic effect aimed at accelerating the proliferation of diabetic fibroblasts for their further use in diabetic foot ulcers.

3.5. References

(1) Vigata, M.; Meinert, C.; Hutmacher, D. W.; Bock, N. Hydrogels as Drug Delivery Systems: A Review of Current Characterization and Evaluation Techniques. *Pharmaceutics* **2020**, *12* (12), 1–45. https://doi.org/10.3390/pharmaceutics12121188.

(2) Liang, Y.; Chen, B.; Li, M.; He, J.; Yin, Z.; Guo, B. Injectable Antimicrobial Conductive Hydrogels for Wound Disinfection and Infectious Wound Healing. *Biomacromolecules* **2020**, *21* (5), 1841–1852. https://doi.org/10.1021/acs.biomac.9b01732.

(3) Liang, Y.; He, J.; Guo, B. Functional Hydrogels as Wound Dressing to Enhance Wound Healing. *ACS Nano* **2021**, *15* (8), 12687–12722. https://doi.org/10.1021/acsnano.1c04206.

(4) Lokhande, G.; Carrow, J. K.; Thakur, T.; Xavier, J. R.; Parani, M.; Bayless, K. J.; Gaharwar, A. K. Nanoengineered Injectable Hydrogels for Wound Healing Application. *Acta Biomater.* **2018**, *70*, 35–47. https://doi.org/10.1016/j.actbio.2018.01.045.

(5) Zhao, X.; Wu, H.; Guo, B.; Dong, R.; Qiu, Y.; Ma, P. X. Antibacterial Anti-Oxidant Electroactive Injectable Hydrogel as Self-Healing Wound Dressing with Hemostasis and Adhesiveness for Cutaneous Wound Healing. *Biomaterials* **2017**, *122*, 34–47. https://doi.org/10.1016/j.biomaterials.2017.01.011.

(6) Sheng, Y.; Gao, J.; Yin, Z.-Z.; Kang, J.; Kong, Y. Dual-Drug Delivery System Based on the Hydrogels of Alginate and Sodium Carboxymethyl Cellulose for Colorectal Cancer Treatment. *Carbohydr. Polym.* **2021**, *269* (June), 118325. https://doi.org/10.1016/j.carbpol.2021.118325.

(7) Ha, W.; Yu, J.; Song, X. Y.; Zhang, Z. J.; Liu, Y. Q.; Shi, Y. P. Prodrugs Forming Multifunctional Supramolecular Hydrogels for Dual Cancer Drug Delivery. *J. Mater. Chem. B* **2013**, *1* (41), 5532–5538. https://doi.org/10.1039/c3tb20956c.

(8) Burdick, J. A.; Mason, M. N.; Hinman, A. D.; Thorne, K.; Anseth, K. S. Delivery of Osteoinductive Growth Factors from Degradable PEG Hydrogels Influences Osteoblast Differentiation and Mineralization. *J. Control. Release* **2002**, *83* (1), 53–63. https://doi.org/10.1016/S0168-3659(02)00181-5.

(9) Holland, T. A.; Bodde, E. W. H.; Cuijpers, V. M. J. I.; Baggett, L. S.; Tabata, Y.; Mikos, A. G.; Jansen, J. A. Degradable Hydrogel Scaffolds for in Vivo Delivery of Single and Dual Growth Factors in Cartilage Repair. *Osteoarthr. Cartil.* **2007**, *15* (2), 187–197. https://doi.org/10.1016/j.joca.2006.07.006.

(10) Seidlits, S. K.; Gower, R. M.; Shepard, J. A.; Shea, L. D. Hydrogels for Lentiviral Gene Delivery. *Expert Opin. Drug Deliv.* **2013**, *10* (4), 499–509.

https://doi.org/10.1517/17425247.2013.764864.

(11) Lei, P.; Padmashali, R. M.; Andreadis, S. T. Cell-Controlled and Spatially Arrayed Gene Delivery from Fibrin Hydrogels. *Biomaterials* **2009**, *30* (22), 3790–3799. https://doi.org/10.1016/j.biomaterials.2009.03.049.

(12) Cam, M. E.; Yildiz, S.; Alenezi, H.; Cesur, S.; Ozcan, G. S.; Erdemir, G.; Edirisinghe, U.; Akakin, D.; Kuruca, D. S.; Kabasakal, L.; Gunduz, O.; Edirisinghe, M. Evaluation of Burst Release and Sustained Release of Pioglitazone-Loaded Fibrous Mats on Diabetic Wound Healing: An in Vitro and in Vivo Comparison Study. *J. R. Soc. Interface* **2020**, *17* (162), 20190712. https://doi.org/10.1098/rsif.2019.0712.

(13) Son, Y. J.; Tse, J. W.; Zhou, Y.; Mao, W.; Yim, E. K. F.; Yoo, H. S. Biomaterials and Controlled Release Strategy for Epithelial Wound Healing. *Biomater. Sci.* **2019**, *7* (11), 4444–4471. https://doi.org/10.1039/c9bm00456d.

(14) Johnson, N.; Wang, Y. Drug Delivery Systems for Wound Healing. *Curr. Pharm. Biotechnol.* **2015**, *16* (7), 621–629. https://doi.org/10.2174/1389201016666150206113720.

(15) Wang, W.; Lu, K. J.; Yu, C. H.; Huang, Q. L.; Du, Y. Z. Nano-Drug Delivery Systems in Wound Treatment and Skin Regeneration. *J. Nanobiotechnology* **2019**, *17* (1), 1–15. https://doi.org/10.1186/s12951-019-0514-y.

(16) Nurkesh, A.; Jaguparov, A.; Jimi, S.; Saparov, A. Recent Advances in the Controlled Release of Growth Factors and Cytokines for Improving Cutaneous Wound Healing. *Front. Cell Dev. Biol.* **2020**, *8* (July), 1–7. https://doi.org/10.3389/fcell.2020.00638.

(17) Heydari, P.; Zargar Kharazi, A.; Asgary, S.; Parham, S. Comparing the Wound Healing Effect of a Controlled Release Wound Dressing Containing Curcumin/Ciprofloxacin and Simvastatin/Ciprofloxacin in a Rat Model: A Preclinical Study. *J. Biomed. Mater. Res. - Part A* **2022**, *110* (2), 341–352. https://doi.org/10.1002/jbm.a.37292.

(18) Blanco-Fernandez, B.; Castaño, O.; Mateos-Timoneda, M. Á.; Engel, E.; Pérez-Amodio, S. Nanotechnology Approaches in Chronic Wound Healing. *Adv. Wound Care* **2021**, *10* (5), 234–256. https://doi.org/10.1089/wound.2019.1094.

(19) Lin, C. C.; Metters, A. T. Hydrogels in Controlled Release Formulations: Network Design and Mathematical Modeling. *Adv. Drug Deliv. Rev.* **2006**, *58* (12–13), 1379–1408. https://doi.org/10.1016/j.addr.2006.09.004.

(20) Wang, J.; Kaplan, J. A.; Colson, Y. L.; Grinstaff, M. W. Mechanoresponsive Materials for Drug Delivery: Harnessing Forces for Controlled Release. *Adv. Drug Deliv. Rev.* **2017**, *108* (4), 68–82. https://doi.org/10.1016/j.addr.2016.11.001.

(21) Brandl, F.; Kastner, F.; Gschwind, R. M.; Blunk, T.; Teßmar, J.; Göpferich, A.

Hydrogel-Based Drug Delivery Systems: Comparison of Drug Diffusivity and Release Kinetics. *J. Control. Release* **2010**, *142* (2), 221–228. https://doi.org/10.1016/j.jconrel.2009.10.030.

(22) Higuchi, T. Rate of Release of Medicaments from Ointment Bases Containing Drugs in Suspension. *J. Pharm. Sci.* **1961**, *50* (10), 874–875. https://doi.org/10.1002/jps.2600501018.

(23) Hoare, T. R.; Kohane, D. S. Hydrogels in Drug Delivery: Progress and Challenges. *Polymer (Guildf).* **2008**, *49* (8), 1993–2007. https://doi.org/10.1016/j.polymer.2008.01.027.

(24) Wang, H.; Wei, J.; Simon, G. P. Response to Osmotic Pressure versus Swelling Pressure: Comment on “Bifunctional Polymer Hydrogel Layers as Forward Osmosis Draw Agents for Continuous Production of Fresh Water Using Solar Energy.” *Environ. Sci. Technol.* **2014**, *48* (7), 4214–4215. https://doi.org/10.1021/es5011016.

(25) Duran-Mota, J. A.; Oliva, N.; Almquist, B. D. Chapter 19. Nanobiomaterials for Smart Delivery. In *Soft Matter for Biomedical Applications*; 2021; pp 475–498. https://doi.org/10.1039/9781839161124-00475.

(26) Oliva, N.; Conde, J.; Wang, K.; Artzi, N. Designing Hydrogels for On-Demand Therapy. *Acc. Chem. Res.* **2017**, *50* (4), 669–679. https://doi.org/10.1021/acs.accounts.6b00536.

(27) Ashley, G. W.; Henise, J.; Reid, R.; Santi, D. V. Hydrogel Drug Delivery System with Predictable and Tunable Drug Release and Degradation Rates. *Proc. Natl. Acad. Sci. U. S. A.* **2013**, *110* (6), 2318–2323. https://doi.org/10.1073/pnas.1215498110.

(28) Ejaz, M.; Yu, H.; Yan, Y.; Blake, D. A.; Ayyala, R. S.; Grayson, S. M. Evaluation of Redox-Responsive Disulfide Cross-Linked Poly(Hydroxyethyl Methacrylate) Hydrogels. *Polymer (Guildf).* **2011**, *52* (23), 5262–5270. https://doi.org/10.1016/j.polymer.2011.09.018.

(29) Lakes, A. L.; Jordan, C. T.; Gupta, P.; Puleo, D. A.; Hilt, J. Z.; Dziubla, T. D. Reducible Disulfide Poly(Beta-Amino Ester) Hydrogels for Antioxidant Delivery. *Acta Biomater.* **2018**, *68*, 178–189. https://doi.org/10.1016/j.actbio.2017.12.030.

(30) Liu, J.; Chen, Z.; Wang, J.; Li, R.; Li, T.; Chang, M.; Yan, F.; Wang, Y. Encapsulation of Curcumin Nanoparticles with MMP9-Responsive and Thermos-Sensitive Hydrogel Improves Diabetic Wound Healing. *ACS Appl. Mater. Interfaces* **2018**, *10* (19), 16315–16326. https://doi.org/10.1021/acsami.8b03868.

(31) Ariga, K.; Mori, T.; Hill, J. P. Mechanical Control of Nanomaterials and Nanosystems. *Adv. Mater.* **2012**, *24* (2), 158–176. https://doi.org/10.1002/adma.201102617.

(32) Chen, J.; Peng, Q.; Peng, X.; Han, L.; Wang, X.; Wang, J.; Zeng, H. Recent Advances in Mechano-Responsive Hydrogels for Biomedical Applications. *ACS Appl. Polym. Mater.* **2020**, *2* (3), 1092–1107. https://doi.org/10.1021/acsapm.0c00019.

(33) Ashwini Kumar, G.; Bhat, A.; Prasanna Lakshmi, A.; Reddy, K. An Overview of Stimuli-Induced Pulsatile Drug Delivery Systems. *Int. J. PharmTech Res.* **2010**, *2* (4), 2364–2378.

(34) Li, J.; Mooney, D. J. Designing Hydrogels for Controlled Drug Delivery. *Nat. Rev. Mater.* **2016**, *1* (12), 16071. https://doi.org/10.1038/natrevmats.2016.71.

(35) Tezuka, Y. Topological Polymer Chemistry by Electrostatic Self-Assembly. *Kobunshi* **2004**, *53* (8), 575–578. https://doi.org/10.1295/kobunshi.53.575.

(36) Oliva, N.; Almquist, B. D. Spatiotemporal Delivery of Bioactive Molecules for Wound Healing Using Stimuli-Responsive Biomaterials. *Adv. Drug Deliv. Rev.* **2020**, *161–162*, 22–41. https://doi.org/10.1016/j.addr.2020.07.021.

(37) Gao, W.; Zhang, Y.; Zhang, Q.; Zhang, L. Nanoparticle-Hydrogel: A Hybrid Biomaterial System for Localized Drug Delivery. *Ann. Biomed. Eng.* **2016**, *44* (6), 2049–2061. https://doi.org/10.1007/s10439-016-1583-9.

(38) Gaharwar, A. K.; Peppas, N. A.; Khademhosseini, A. Nanocomposite Hydrogels for Biomedical Applications. *Biotechnol. Bioeng.* **2014**, *111* (3), 441–453. https://doi.org/10.1002/bit.25160.

(39) Khan, S.; Ranjha, N. M. Effect of Degree of Cross-Linking on Swelling and on Drug Release of Low Viscous Chitosan/Poly(Vinyl Alcohol) Hydrogels. *Polym. Bull.* **2014**, *71* (8), 2133–2158. https://doi.org/10.1007/s00289-014-1178-2.

(40) Adler, J.; Parmryd, I. Quantifying Colocalization by Correlation: The Pearson Correlation Coefficient Is Superior to the Mander's Overlap Coefficient. *Cytom. Part A* **2010**, *77* (8), 733–742. https://doi.org/10.1002/cyto.a.20896.

(41) Pike, J. A.; Styles, I. B.; Rappoport, J. Z.; Heath, J. K. Quantifying Receptor Trafficking and Colocalization with Confocal Microscopy. *Methods* **2017**, *115*, 42–54. https://doi.org/10.1016/j.ymeth.2017.01.005.

(42) Reiser, A.; Woschée, D.; Mehrotra, N.; Krzysztoń, R.; Strey, H. H.; Rädler, J. O. Correlation of MRNA Delivery Timing and Protein Expression in Lipid-Based Transfection. *Integr. Biol.* **2019**, *11* (9), 362–371. https://doi.org/10.1093/intbio/zyz030.

Chapter 5: Conclusions

This page is intentionally left blank

Conclusions

In the present thesis, a general hydrogel-based platform for the delivery of genetic material to human dermal fibroblasts has been developed for its further application as a wound dressing in diabetic foot ulcers. The matrix of the platform consists of a hydrogel formed by PEG and PBAE, crosslinked *via* disulphide bonding. The nucleic active component is encapsulated in PBAE polyplexes that are released in a sustained manner over time as the matrix degrades. The therapeutic aspect is achieved by delivering inhibitors of miRNAs whose overexpression in diabetic fibroblasts isolated from patients' ulcers have been linked to impaired healing.

In order to secure the protection and the significant arrival of the therapeutic genetic material inside the human fibroblasts, the optimization of the carrier was performed first.

- The formulation C6RH showed unprecedented high transfection efficiency in human dermal fibroblasts compared to the controls and other PBAE formulations, without compromising their viability. This is a meaningful initial step towards clinical translation and it opens the possibility to expand the use of this formulation to other applications.

The biocompatible, injectable, and degradable hydrogel matrix was prepared next crosslinking thiolated 4-arm PEG molecules with thiol-reactive hydrophilic PBAEs. Different hydrogel formulations were prepared tuning the number of thiol-reactive moieties of the PBAE and the PEG/PBAE ratio.

- It was demonstrated that two SPDP groups per PBAE chain was the minimum number of thiol-reactive moieties per chain needed to obtain an injectable, chemically crosslinked hydrogel. For further studies, the C32T_2CR3 family of formulations was used.

- Formulations HG11 and HG14 were prepared by tuning the PEG/PBAE molecule ratio. Crosslinking with a higher PBAE proportion resulted in an increase in brittleness. However, the presence of more available bonds to be broken (higher crosslinking) slowed the degradation kinetics.

- The cytotoxicity assay showed that the concentration of the PBAE reaches a level above which this polymer compromises cell viability. Hence, only the degradation products of HG11 were non-cytotoxic.

Once the polyplexes and the hydrogel matrix were optimized, we proceeded to prepare the hydrogels doped with PBAE nanoparticles and study the release kinetics, cytotoxicity and transfection efficiency.

- It was demonstrated that polyplexes maintain the stability during the hydrogel preparation. Additionally, the polyplexes were distributed in a uniform manner throughout the three-dimensional hydrogel structure.

- The incorporation of the PBAE polyplexes was shown to affect the microstructure of both formulations. The saturation of PBAEs from both the hydrogel and the particles in the formulation HG14-NP could be the reason for a critical weakening of the structure, leading to an accelerating of its degradation kinetics. The release of the polyplexes occurred mostly *via* bonds cleavage, matching the degradation profiles. HG11-NP showed an initial burst release of polyplexes followed by a sustained stage. In contrast, the stability of the particles in HG14-NP appeared to be disrupted few hours after the start of the experiments, as suggested by PBAEs and nucleic acids having different release kinetics.

- It was demonstrated that HG11-NP could transfect fibroblasts, reaching levels of transfection that are comparable to the levels expected after the first hours of release. Contrarily, HG14-NP did not show any transfection, mostly due to a combination of the cytotoxicity and the disruption of the polyplexes released.

The platform developed throughout this thesis has shown promising results *in vitro* for its eventual use as a treatment for diabetic foot ulcers. The immediate next steps include the optimization of *ex vivo* models, histology and wound healing studies in animal models to demonstrate that the efficacy and the safety of the wound dressing is suitable for a clinical translation.

All in all, the platform herein designed can be used to locally deliver any RNA combination to primary human fibroblasts to tackle complex dermal impaired healing, such as diabetic foot

ulcers. This platform can potentially be used for other cell types, increasing its impact across medical problems with one generalizable approach.